RES | THE SCHOOL for RENEWABLE ENERGY SCIENCE

# SOFC SINGLE CELL TESTING WITH MIXTURE OF GASES SIMULATING BIOGAS, SYNGAS AND PYROLYSIS-REFORMED GASES

Solid Oxide Fuel Cell, hydrogen energy pathways, starting from laboratory experimental activity

Marcin Kalinowski

.

---

UNIVERSITY OF ICELAND

University of Akureyri

PROJEKT PL0460

The Master Thesis was supported by a grant from Iceland, Liechtenstein and Norway through the EEA Financial Mechanism - Project PL0460

# SOFC SINGLE CELL TESTING WITH MIXTURE OF GASES SIMULATING BIOGAS, SYNGAS AND PYROLYSIS-REFORMED GASES

Solid Oxide Fuel Cell, hydrogen energy pathways, starting from laboratory experimental activity.

Marcin Kalinowski

A 30 ECTS credit units Master´s thesis

Supervisors
Prof. Umberto Desideri
Dr. David Dvorak
Prof. Thorsteinn I. Sigfusson

Advisor
Phd. Student Giovanni Cinti

A Master´s thesis done at
RES | The School for Renewable Energy Science
in affiliation with
University of Iceland &
University of Akureyri

Akureyri, February 2011

SOFC single cell testing with mixture of gases simulating biogas, syngas and pyrolysis-reformed gases

Solid Oxide Fuel Cell, hydrogen energy pathways, starting from laboratory experimental activity

A 30 ECTS credit units Master´s thesis



RES | The School for Renewable Energy Science

Solborg at Nordurslod

IS600 Akureyri, Iceland

Telephone + 354 464 0100

www.res.is

Printed in (date)

at Stell Printing in Akureyri, Iceland

## ABSTRACT

The study is focused on testing and evaluation of the performances of the SOFC fuel cells in a several conditions (gas quality, gas quantity and thermal conditions) using ASR and OCV.

The aim of the project is to build methodology for performance evaluating of the single solid oxide cells, fueled by different gases, like also evaluation of this performances.

Additional goal is to evaluate possibility of using investigated gases in SOFC systems in Poland.

# TABLE OF CONTENTS


1 History of the fuel cell ..... 9
1.1 Types of the fuel cells and their applications ..... 10
2.1 SOFC ..... 13
1.1.1 Materials for SOFC ..... 14
1.1.2 SOFC geometry ..... 17
2 SOFC Fuel flexibility ..... 20
2.1 Fuels for SOFC ..... 20
2.1.1 Hydrogen ..... 21
2.1.2 Syngas ..... 25
2.1.3 Biogas ..... 26
2.1.4 Pyrolysis reformed gas ..... 28
2.2 Fuels for SOFC - actual status and perspectives in Poland ..... 29
2.2.1 Actual biogas status and perspectives ..... 29
2.2.2 Actual syngas status and perspectives ..... 31
2.2.3 Actual pyrolysis reformed gas status and perspectives ..... 33
2.3 Fuel processing ..... 34
2.3.1 Direct and indirect fuel reforming ..... 36
2.4 Fuels for test activities ..... 37
3 Parameters for the performance assessment ..... 39
3.1 Area Specific Resistance as a performance prediction parameter ..... 40
3.1.1 ASR – definition ..... 40
3.1.2 ASR – analysis ..... 41
3.1.3 ASR – calculations ..... 45
3.2 Open Circuit Voltage – OCV ..... 46
3.3 Current density – j ..... 47
3.4 Power density – P ..... 47
3.5 Efficiency – $\varepsilon$ ..... 47
3.6 Stoichiometric factor – $\lambda$ ..... 48
3.7 Dilution factor – $D_f$ ..... 49
3.8 Fuel utilization coefficient – $U_f$ ..... 49
3.9 Coefficient of oxygen utilization – $U_{ox}$ ..... 50
4 Test system ..... 51

4.1 Tested single SOFC ..... 52
5 Test procedure ..... 55
6 Test activity ..... 56
6.1 Reference state test analysis and conclusions ..... 57
6.2 Reference state variation test analysis and conclusions ..... 60
6.3 New reference state variation test analysis and conclusions ..... 62
7 λ efect on the cell performance ..... 65
8 $D_f$ effect on the cell performance ..... 69
9 Tested cell degradation rate ..... 72
10 Biogas, syngas and pyrogas test activity AND CONCLUSIAONS ..... 75
11 Conclusions ..... 81
References ..... 82
Appendix A ..... 84
Appendix B ..... 85
Flow meters ..... 85
Manifolds ..... 85
Thermocouples ..... 86
Oven ..... 86
Press ..... 86
Humidifying unit ..... 87
Power Supply ..... 87
Electronic Load ..... 88
Data Acquisition Unit ..... 89
Thermo regulator ..... 90
Pipes and instruments design ..... 90
Data acquisition system ..... 92
Appendix C ..... 93
Appendix D ..... 103
Appendix E ..... 108
Reference state test plan ..... 108
Reference state test elaborating ..... 109
Appendix f ..... 115
Reference state variation test plan ..... 115
Reference state variation test elaborating ..... 116
Appendix G ..... 121
New reference state variation test plan ..... 121

New reference state variation test elaborating.....123
Appendix H .....130

## LIST OF FIGURES

Fig. 1-1 A scheme of the Grove's "Gas Battery" (Thomas, S et al.) ..... 9

Fig. 1-2 Solid oxide fuel cell principle (RES606) ..... 13

Fig. 1-3 SEM image of ASC (bottom left), scheme of ASC and MSC (top), and cross-section of MSC (bottom right). (Tucker 2010, Heo 2010) ..... 14

Fig. 1-4 Example of the ion conductivity of YSZ versus temperature. (Sammes 2006) ..... 17

Fig. 1-5 SOFC tubular design. (Kakaç 2007) ..... 18

Fig. 1-6 SOFC planar design (Kakaç 2007) ..... 18

Fig. 1-7 Integrated planar solid oxide fuel cell scheme (Kakaç 2007) ..... 19

Fig. 1-8 Monolithic SOFC design scheme (Kakaç 2007) ..... 19

Fig. 2-1 Potential fuels for SOFC (Sunghal 2003) ..... 20

Fig. 2-2 Primary energy production of biogas in Poland in 2006 (in ktoe). (EurObserv'ER 2008) ..... 29

Fig. 2-3 RES - production and potential for future in Poland. (RE-SHAPING - Renewable Energy Policy Country Profiles - 2009 version) ..... 31

Fig. 2-4 Raw materials for syngas production. (Lubiewa-Wieleżyński, W & Siroka, A 2009) ..... 32

Fig. 2-5 The world syngas market. (van der Drift 2004) ..... 32

Fig.2-6 Schematic of reaction processes in an SOFC internal reforming, with steam and methane as a fuel. (Sunghal 2003) ..... 35

Fig. 2-7 SOFC internal reforming with recirculation of the anode exit gas. (Sunghal 2003) .. 35

Fig. 2-8 Scheme of direct internal and indirect internal reforming in an SOFC stack. (Sunghal 2003) ..... 36

Fig. 2-9 Carbon deposition pathway in an SOFC direct internal reforming. (Sunghal 2003) . 36

Fig. 2-10 Scheme of reaction processes in an SOFC direct internal reforming. (Sunghal 2003) ..... 37

Fig. 3-1 Ohmic region in a j-V curve. ..... 40

Fig. 3-2 Ohmic loss as a part of the net fuel cell performance. (O'Hayre, R et al. 2006) ..... 41

Fig. 3-3 Total fuel cell resistance as a sum of resistances coming from interconnect, anode, cathode, electrolyte, and cathode.(ResFC601 Ryan O'Hayre) ..... 41

Fig. 4-1 Scheme of the test system ..... 51

Fig. 4-2 Tested SOFCs – anode from the left side and cathode from the right side ..... 53

Fig. 4-3 Assembled SOFC ..... 54

Fig. 6-1 Reference state test report C ..... 58

Fig. 6-2 Tested SOFC before (top) and after (down) the test activity. ..... 59

Fig. 6-3 Reference state λ variation test report C ..... 60

Fig. 6-4 Reference state DN2 variation test report C ..... 61

Fig. 6-5 New reference state λ variation test report C ..... 63
Fig. 6-6 New reference state DN2 variation test report C ..... 64
Fig. 7-1 λ effect on OCV ..... 66
Fig. 7-2 λ effect on ASR at 0,8V ..... 67
Fig. 7-3 λ effect on ASR at 0,7V ..... 68
Fig. 8-1 $D_f$ effect on OCV ..... 69
Fig. 8-2 $D_f$ effect on ASR at 0,8V ..... 70
Fig. 8-3 $D_f$ effect on ASR at 0,7V ..... 70
Fig. 9-1 Degradation rate report ..... 73
Fig. 10-1 Reference state report B (biogas, syngas and pyrogas test activity) ..... 77
Fig. 10-2Biogas, syngas and pyrogas report C (part 1) ..... 78
Fig. 10-3 Biogas, syngas and pyrogas report C (part 2) ..... 79

# LIST OF TABLES

Table 1-1 Overview of the key characteristics of the main fuel cell types – part 1 (Fuel Cell Handbook n°7 2004, Neef 2009, Fuel Cells Los Alamos) ..... 11

Table 1-2 Overview of the key characteristics of the main fuel cell types - part 2 (Fuel Cell Handbook n°7 2004, Neef 2009, Fuel Cells Los Alamos) ..... 11

Table 2-1 Example of wood gas composition, oxidized with air, oxygen and air. (RES'09) .. 26

Table 2-2 Typical landfill gas composition based on dry volume. ..... 27

Table 2-3 Example of biogas composition based on municipal waste. ..... 27

Table 2-4 Example composition of pyrogas. (University of Perugia) ..... 28

Table 2-5 Influence of the conditions on pyrolysis process.(RES'09) ..... 28

Table 2-6 Primary energy production of biogas (in ktoe), gross electricity production from biogas (in GWh) and gross heat production from biogas (in ktoe ) in Poland in 2006. (EurObserv'ER 2008) ..... 30

Table 2-7 Biogas percentage composition before and after reforming (molar fraction)..... 38

Table 2-8 Syngas percentage composition before and after reforming (molar fraction). ..... 38

Table 2-9 Pyrogas percentage composition before and after reforming (molar fraction)..... 38

Table 7-1 Reference state test plan II ..... 65

Table 7-2 List of reference state II test variation reports A ..... 66

Table 9-1 List of polarizations for degradation rate analysis ..... 72

Table 10-1 Biogas, syngas and pyrogas test plan ..... 75

Table 10-2 Biogas, syngas and pyrogas test reports A ..... 76

# 1 HISTORY OF THE FUEL CELL

Christian Friedrich Schönbein (1799 – 1868) and Sir William Robert Grove (1811 -1896) are considered as inventors of the fuel cell. In 1938, Schonbein discovered, and one year later published the principle of the operation of the fuel cell in *Philosophical Magazine*. Several months after, based on his work, Sir William Robert Grove constructed and published in *Philosophical Magazine and Journal of Science* first fuel cell, which he called a ‘gas battery’ (Figure 1-1).

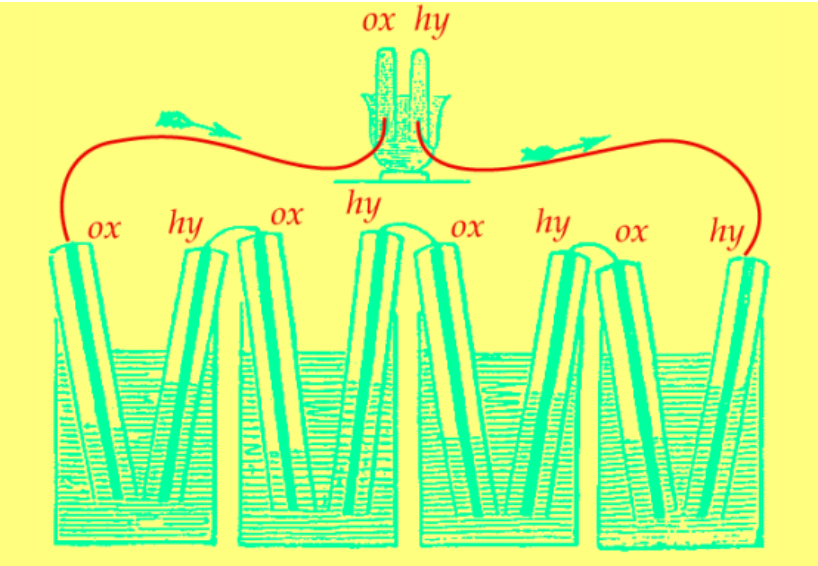


*Fig. 1-1 A scheme of the Grove's "Gas Battery" (Thomas, S et al.)*

Grove‘s 'gas battery' was constructed from two platinum electrodes immersed on one end in a solution of sulphuric acid and the other two ends separately sealed in containers of $O_2$ and $H_2$. In this type of constructed device, a constant current was found to be flowing between the electrodes. The gas containers also contained water. It was noticed by the constructor that the level of $H_2O$ increased in both tubes as the current flowed. In addition, Grove noted that combining pairs of electrodes, connected in series produced higher voltage.

In 1889, Ludwig Mond and Car Langer improved Grove´s cell by making electrodes porous and three-dimensional shaped, thereby the need for a huge area of the cell was significantly reduced.

In 1893, Friedrich Wilhelm Ostwald through his pioneering work related to the physical and chemical reactions, theoretically explained performance of the fuel cell.

After that, many scientists began to study the concept of the fuel cell which resulted in the beginning of the fuel cell technology. Finally, in 1896, Wilhelm W. Jacques developed practical application of the first fuel cell.

Few years later, in 1900, first zirconium solid oxide electrolyte was used by Walther Nernst, which was well known as the developer of the Nernst stress equation, the heat theorem, the concept of entropy, third law of thermodynamics and others.

In twenty century, the development of fuel cell technology was significant. Emil Baur worked on high temperature devices (using molten silver as an electrolyte) and a unit that used a solid electrolyte of clay and metal oxides. Finally, in 1921, he constructed the first molten carbonate fuel cell.

Year 1933 was very important for the development of the fuel cell technology.For the development of the fuel cell technology year 1933 was very important. At first, Thomas Francis Bacon invented the first fuel cell made of hydrogen and oxygen, with practical use. The fuel cells processed air and hydrogen directly into electricity through electrochemical reactions. Then, Bacon worked on alkaline type of fuel cells, and in 1939, he constructed first high pressure (200 bar) cell with nickel electrodes.

In 1950, the teflon material (PTFE - polytetrafluoroethylene) began to be commercially available and was used in the fuel cells with platinum electrodes, acid electrolyte, and also with carbon electrodes and alkaline electrolyte. In 1955 and 1958, chemic scientists, Thomas Grubb and Leonard Niedrach who worked for General Electric Company (GE), developed aqueous electrolyte fuel cell using PTFE material. Grubb used a membrane made of ion-exchange polystyrene sulphated as an electrolyte, while Niedrach elaborated a way of depositing platinum (which acted as a catalyst for oxidation reactions of hydrogen and oxygen reduction) on the membrane.

In 1961, G. V. Elmore and H. A. Tanner published their work entitled *Intermediate Temperature Fuel Cells*, on phosphoric acid fuel cell. Their device could work on air instead of pure oxygen.

In 1990, direct methanol fuel cell was invented by Jet Propulsion Laboratory and University of Southern of California. (Andujar & Segura 2009)

During the last twenty years, a lot of researches were made in the field of fuel cell technology. There are many commercially available fuel cells devices now. In the next section, there are presented types of the fuel cells and some of their applications.

## 1.1 Types of the fuel cells and their applications

At the present time, many types of fuel cells are available on the market. These fuel cells are continuously developing and/or upgrading. The most common way to classify the fuel cells is by the type of electrolyte used in such devices as:

- PEFC - polymer electrolyte fuel cell,
- AFC - alkaline fuel cell,
- PAFC - phosphoric acid fuel cell,
- MCFC - molten carbonate fuel cell.

The second most common classification of the fuel cells is by the range of operating temperatures:

- low temperature (ca. 100 °C),
- intermediate temperature (ca. 250 °C),
- high temperature fuel cells (ca. > 500 °C).

This dependence is also dictated by the type of electrolyte. Temperature has also influence on physicochemical and thermo-mechanical properties of materials used in the cell components like, electrodes, electrolyte, interconnect, current collector, etc. The fuel cells which contain aqueous types of electrolyte, have limited range of operating to about 200 °C or less - because of high vapor pressure and fast degradation at such conditions.

*Table 1-1 Overview of the key characteristics of the main fuel cell types – part 1 (Fuel Cell Handbook n°7 2004, Neef 2009, Fuel Cells Los Alamos)*

| | **PEFC** | **AFC** | **PAFC** | **MCFC** |
|---|---|---|---|---|
| **Electrolyte** | Hydrated Polymeric Ion Exchange Membranes | Mobilized or Immobilized Potassium Hydroxide in asbestos matrix | Immobilized Liquid Phosphoric Acid in SiC | Immobilized Liquid Molten Carbonate in $LiAlO_2$ |
| **Electrodes** | Carbon | Transition metals | Carbon | Nickel and Nickel Oxide |
| **Catalyst** | Platinum | Platinum | Platinum | Electrode material |
| **Interconnect** | Carbon or metal | Metal | Graphite Nickel, | Stainless steel or Nickel |
| **Operating Temperature** | 60 – 80 °C | 65 – 220 °C | 175 - 205 °C | 600 - 1000 °C |
| **Fuel** | hydrogen | hydrogen | hydrogen | Natural gas, coal gas, biogas |
| **Power Range** | W / kW | W / kW | kW | kW / MW |
| **Application (examples)** | Transportation, Portables, Electric utility, | Military Space, Electric utility | CHP, Electric utility, Transportation | Electric utility – Power plants |

*Table 1-2 Overview of the key characteristics of the main fuel cell types - part 2 (Fuel Cell Handbook n°7 2004, Neef 2009, Fuel Cells Los Alamos)*

| | **Electrochemical Reactions** | **Main advantages and disadvantages** | |
|---|---|---|---|
| **PEFC** | anode: $H_2 \rightarrow 2H^+ + 2e^-$<br>cathode: $\frac{1}{2}O_2 + 2H^+ + 2e^- \rightarrow H_2O$<br>overall: $H_2 + \frac{1}{2}O_2 \rightarrow H_2O$ | Solid electrolyte reduces corrosion & management problems<br>Low temperature<br>Quick start-up | Low temperature requires expensive catalysts<br>High sensitivity to fuel impurities |
| **AFC** | anode: $H_2 + 2(OH)^- \rightarrow 2H_2O + 2e^-$<br>cathode: $\frac{1}{2}O_2 + H_2O + 2e^- \rightarrow 2(OH)^-$<br>overall: $H_2 + \frac{1}{2}O_2 \rightarrow H_2O$ | Cathode reaction faster in alkaline electrolyte — so high performance | Expensive removal of $CO_2$ from fuel and air streams required |
| **PAFC** | anode: $H_2 \rightarrow 2H^+ + 2e^-$<br>cathode: $\frac{1}{2}O_2 + 2H^+ + 2e^- \rightarrow H_2O$<br>overall: $H_2 + \frac{1}{2}O_2 \rightarrow H_2O$ | Up to 85 % efficiency in co-generation of electricity and heat<br>Impure H2 as fuel | Pt catalyst<br>Low current and power<br>Large size/weight |
| **MCFC** | anode: $H_2 + CO_3^{2-} \rightarrow 2H_2O + CO_2 + 2e^-$<br>cathode: $\frac{1}{2}O_2 + CO_2 + 2e^- \rightarrow CO_3^{2-}$<br>overall: $H_2 + \frac{1}{2}O_2 + CO_2 \rightarrow H_2O + CO_2$ | Higher efficiency*<br>Fuel flexibility*<br>Inexpensive catalyst*<br>Faster electro-chemical reaction*<br>*(high temperature advantages) | High temperature enhances corrosion and breakdown of cell components |

Moreover, fuels for different kind of fuel cells also depend on operating temperature. In the lower temperature, the fuel cells can only use hydrogen fuel and additionally they are strongly poisoned by CO. On the other hand, the big advantage of the high-temperature fuel cells is that they can use fuels like CO or/and $CH_4$ and convert it/them internally to $H_2$. Brief characteristics of the main fuel cell types are presented in tables 1-1 and 1-2.

In addition, some of the fuel cells are classified by the type of the fuel which they use. One of them is direct methanol fuel cell (DMFC) which refers to PEFC due to the type of electrolyte (Hydrated Polymeric Ion Exchange Membranes). However, an alcohol (methanol) is used as the fuel for DMFC. The operating temperature for DMFCs is in range from 50 to 130 °C, so it shows that this is low-temperature fuel cell. Electrodes and interconnections for this kind of fuel cell are made from carbon and carbon-metal materials, respectively - where the catalyst such as Pt and Ru is used. DMFC´s are mostly used for portable applications, so their power range is in W / kW. It should be noted that DMFC are not in commercial use yet.

The basic reactions which occur in this fuel cell are presented below:

at the anode side: $$CH_3OH + H_2O \rightarrow 6H^+ + 6e^- + CO_2$$

at the cathode side: $$\frac{3}{2}O_2 + 6H^+ + 6e^- \rightarrow 3H_2O$$

overall reaction: $$CH_3OH + \frac{3}{2}O_2 \rightarrow 2H_2O + CO_2$$

The main advantages of the DMFC are:

- fuel is a liquid,
    - size of the fuel tank is less;
    - can use existing infrastructure for refueling;
- do not need any reforming processes,
- proton exchange membrane as an electrolyte,
    - low operating temperature;

The main disadvantages are:

- low efficiency (~40%) compared to the hydrogen types of fuel cells,
- great amount of catalyst (noble metal) needed.

Second type of the fuel cell classified by fuel that they use, is direct carbon fuel cell (DCFC). Only this kind of high temperature fuel cell can use different types of solid carbon fuels like coal, biomass and organic waste. At the same time, DMFCs have theoretically the highest efficiency (80% - based on HHV, direct electrical generation alone without cogeneration) compared to other fuel cells. They are also characterized by high energy density, low CO2 emissions and zero $NO_x$ and/or $SO_x$ emissions. All these advantages make DMFC extremely interesting source of power for power plants and mobile applications. However, this technology is under development and still a lot of researches are needed to fill the hole

between experimental scale setup and commercial application (Muthuvela et al. 2009, Cao et al. 2009 ).

There is one more fuel cell on which current work is focused. Detailed descriptions of solid oxide fuel cell (SOFC) are provided in the next chapter which explains the basic knowledge of SOFCs and more specific issues such as market, targets, and materials for SOFC.

## 2.1 SOFC

Compared to other types of fuel cells, SOFC is also an electrochemical device which converts chemical energy from a fuel into electrical energy. Schematic diagram and basic reactions occurring inside the cell are as follow. (Figure 1-2)

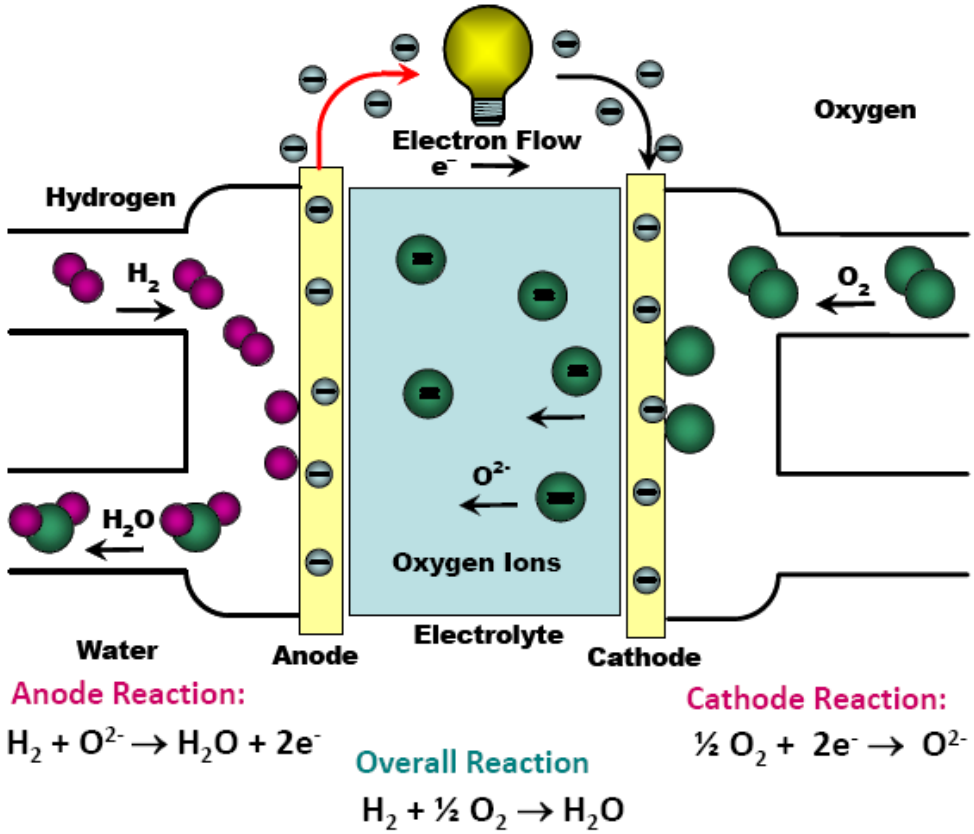


*Fig. 1-2 Solid oxide fuel cell principle (RES606)*

It should be noted, that the charge transport in SOFC electrolyte occurs by ions (O2-) from cathode electrode to anode electrode side where the water is created. The process of conducting ions inside the electrolyte occurs only at high or very high temperatures (usually from 600 to 1000 °C). This fact gives the SOFCs few advantages over the types of the fuel cells from a low and an intermediate temperature. One of the greatest advantages of the SOFCs is the excellent fuel flexibility (more about it in chapter 4) and an inherent chemical resistance to CO poisoning. Moreover, CO can be used as the fuel during chemical reaction with water vapor during the water-gas shift reaction occurring inside the fuel cell, or in external reformer. SOFCs operate at high electrical efficiency (about 55%). However, in case of combined heat and power (CHP) applications, or in combined-cycle gas turbine (CCGT) applications, they can achieve even higher efficiency (70-90%). The power range for SOFCs is from milliwatts to megawatts. All these properties make SOFCs suitable for various

applications, like house energy or power plants. Even though, SOFC has many advantages, there are also disadvantages. Among them are a long start up time and the corrosion of the metal elements. (Bove 2008)

Recently, some of the most important challenges for SOFCs are the development of suitable, not expensive materials and low cost fabrication. Review of the materials of SOFC components, their properties and functions are included in the next chapter. (Tucker 2010)

### 1.1.1 Materials for SOFC

Many types of fuel cells including SOFCs are a membrane-electrolyte-assembly (MEA) and consist of anode, cathode and electrolyte. Presently the most common commercially solid oxide constriction is anode-supported cell (ASC), and the main focus is in metal-supported solid oxide fuel cells (MSC). Example of such constructions is shown below.

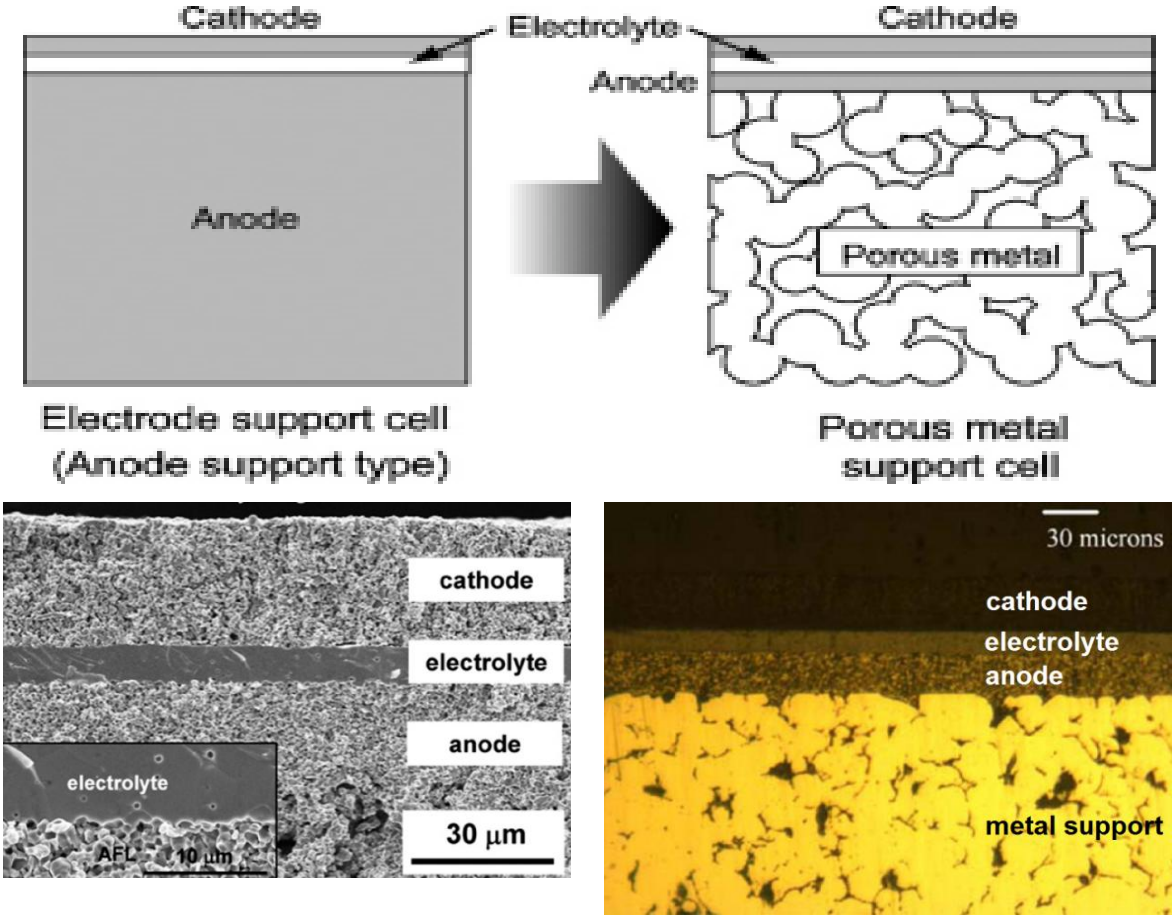


*Fig. 1-3 SEM image of ASC (bottom left), scheme of ASC and MSC (top), and cross-section of MSC (bottom right). (Tucker 2010, Heo 2010)*

The role of the supporting layer is to provide enough mechanical strength for the cells. Currently, there are also fabricated electrolyte-supported cells (ESC) and cathode-supported cells (CSC). In the cases of the ASC, ESC and CSC, the mechanical support is a brittle and costly ceramic, or cermet material. In contrast, the MSC design utilizes ceramic layers only as thick as necessary for electrochemical function. The mechanical support is made from inexpensive and robust porous metal. In the MSC design, the electrochemically active layers are applied directly to the metal support. However, the examinations on SOFC technology

were focused mainly on suitable low cost materials and the low-cost fabrications of the ceramic structures. MSC construction is under demonstrating phase and seems to be promising design to cope these objectives.

In the case of assembling cells in the stack, interconnections are also key elements. All components for SOFC are solid state, and because of the high operating temperature the materials for these elements have straight requirements. One of them is the coefficient of thermal expansion (CTE), which should be as close as possible for each of the material composing the stack to avoid mechanical fracture and material delamination. (Tucker 2010)

In the following part of the thesis, the materials for SOFCs components and their brief characteristics are presented.

### Anode

The function of an anode in SOFC is to provide the sites for the fuel gas to react with the oxide ions supplied by the electrolyte with a structure, which also facilitates the necessary charge neutralization by it electronic conductivity.

Presently, the most common material used for SOFC anodes is composite of Ni/8YSZ (i.e. Ni with 8% mole of YSZ). The positive features of anodes manufactured from Ni/YSZ are:

- high electrical conductivity,
- proper ionic conductivity,
- high activity for the electrochemical reactions and reforming,
- mechanical ability to support the structure of the entire cell.

However, there are several negative characteristics and among them are:

- carbon formation and sulfur formation deposition in the case of using hydrocarbons as a fuel,
    - leads to poor activity for direct oxidation of hydrocarbons,
- oxidation of the Ni to NiO in the case of exposition to air at high temperature,
    - cause a decrease in triple phase boundary as well as disconnection between adjacent Ni particles and concomitant loss of electronic conduction in the anode,
- higher coefficient of thermal expansion (CTE) than the electrolyte and the cathode – in the case of anode-supported cells,
    - can lead to mechanical and dimensional stability problems, especially during thermal cycling,
- in the case of anode supported cells, the possible diffusion of particles between the layers,
    - from anode to support may cause,
        - in reduced oxidation resistance,
        - and increased (CTE) of the support,
    - from support to anode can lead,
        - to reduce of the catalytic activity.

All those problems listed above are the objects of the researches and can be solved by proper stack designs, proper technological processes during manufacturing and also variety of other material investigations. (Fuel Cell Handbook n°7 2004, Tucker 2010)

### Cathode

Materials for cathodes in SOFCs should have similar properties as these for anodes. However, there is the basic difference between them which is the catalytic ability for splitting $O_2$ particles to $O^{2-}$ ions. The cathodes for SOFCs should have the following features:

- chemical stability and low interaction with electrolyte,
- appropriate electronic and ionic conductivity,
- high activity,
- CTE close to YSZ,

Currently, the most cathode popular materials are based on doped lanthanum manganites (LSM). For SOFCs operating at around 1000 °C, strontium-doped $LaMnO_3$ is applied. A composite of LSM-YSZ and alternatively, lanthanum strontium cobalt ferrite (LSCF) or strontium-doped lanthanum ferrite (LSF) are the most conventional composites used in the systems of operating at the temperature around 700 °C to 800°C. All desirable features of SO cathode material can be achieved by adequate fabrication steps. (Fuel Cell Handbook n°7 2004)

### Electrolyte

The performances of SOFCs which operate in the recommended region strongly depend on electrolyte. The main features which SOFC electrolytes should have are:

- high ionic conductivity,
- thick as small as possible,
- good stability under operating conditions,
- low electronic conductivity.

The first two features are extremely important for the overall cell performance. The anode and cathode supported design, allow for reducing thicknesses of the electrolyte layer. Therefore, in the case of ionic conductivity, specific material properties are very significant.

In the past, a lot of materials had been studied for SOFC electrolyte, but still the most common materials are zirconia-based compositions. The YSZ electrolytes in the solid oxide fuel cells have good performances (pure ionic conductor also at low temperatures) and longevity. In addition, it should be mentioned that the ion conductivity of those electrolytes depends on the operating temperature. The example of that dependence for YSZ electrolyte is shown below.

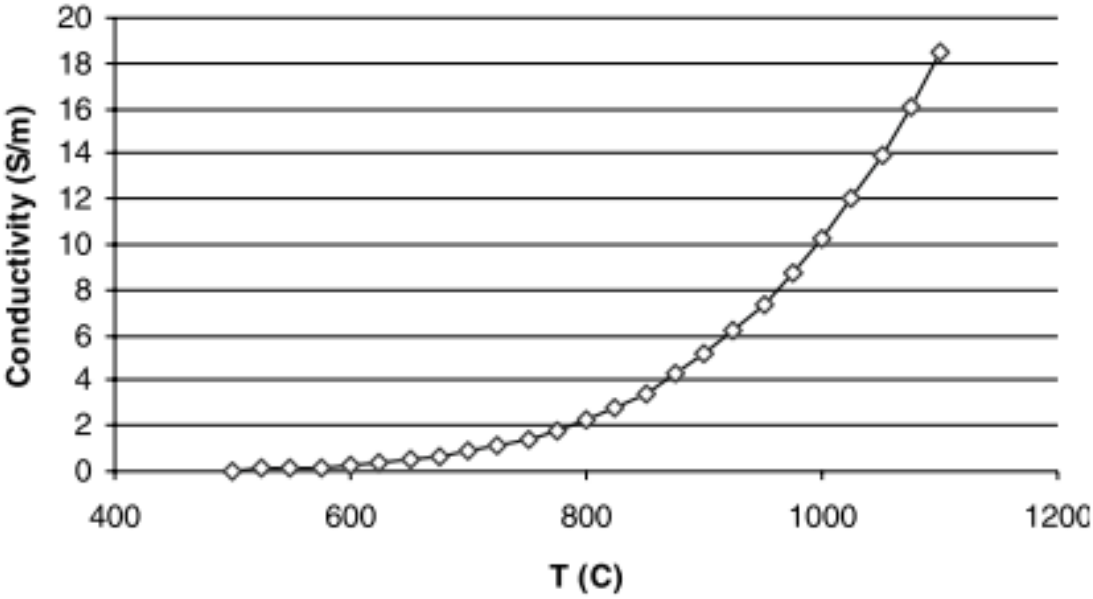


*Fig. 1-4 Example of the ion conductivity of YSZ versus temperature. (Sammes 2006)*

At this point a question arises. Why do not SOFCs usually operate at the higher temperature like 1000 °C? One of the reasons is the high requirement for materials which are unable to operate at such conditions. The next part of the thesis discuses the interconnections for the solid oxide fuel cells. (Fuel Cell Handbook n°7 2004, Sammes 2006)

### Interconnect

The function of interconnect in SOFC systems is to provide high electrical connection between the cells and the gas separation within the cell. Interconnect must be consistent as to thermal conductivity and thermal expansion with all of the cell constituents**.** Moreover, it must be stable with respect to both oxidizing and reducing gases. Not many materials are suitable for operation at such degradable systems. One of them is ceramic, mainly doped lanthanum and yttrium chromites (dopants typically include Mg, Sr, Ca, Ca/Co). Electric conductivity of these materials increases with the temperature, therefore, the temperatures in these types of systems, where ceramics are used, is in range of 900-1000 °C. Those ceramic materials are rigid what make them friable. Moreover, the cost of ceramic materials is high and the process is not easy too, compared to metallic alloys which are applied in lower temperatures of SOFC (~ 800 °C). To illustrate, ferritic stainless steel is good material for SOFC interconnect, mainly because of the high electrical conductivity at lower temperature and thermal expansion, which is similar to the zirconia electrolytes. Most of the time, chromia is used to mitigate the corrosion of interconnects. However then it is common to Cr evaporating, which results in the electrodes poisoning. To avoid this phenomena pervoksites such as lanthanum strontium-doped-manganite or cobaltite are coated on interconnect. The last two features make a major contribution to the degradation of the cell voltage during its operation and still are the main goals for interconnect development (Singhash & Kendall 2003, Sammers 2006, Fuel Cell Handbook n°7 2004, Singhal 2003).

## 1.1.2 SOFC geometry

Tubular and planar designs are the most common construction for SOFCs. Tubular design had been developed by Siemens–Westinghouse during last decades. Discussed design promises

much faster start up times; typically on the range of minutes. The example of that construction is shown on the figure below

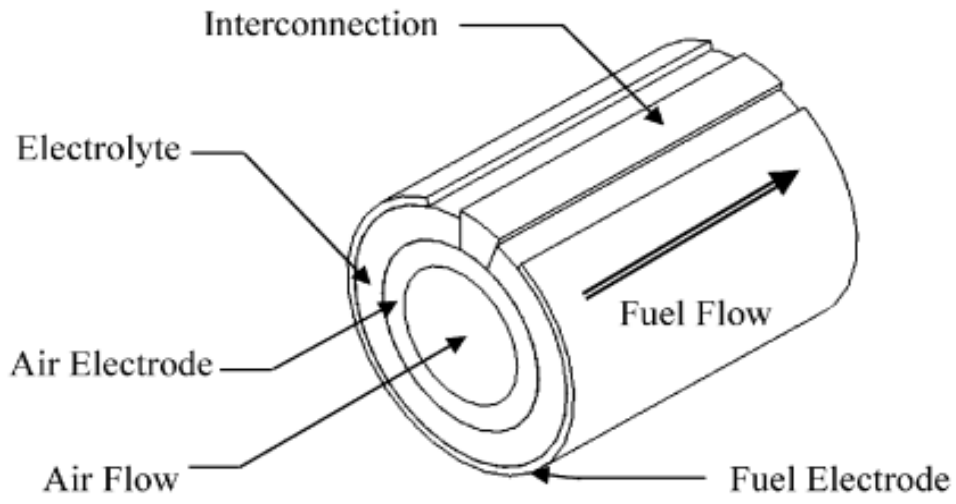


*Fig. 1-5 SOFC tubular design. (Kakaç 2007)*

Planar design offers more compact configuration that results in the higher volume of specific power (W/cm3) compared to tubular design. Anode, electrolyte and cathode are the main constituent parts of the cell and together with the interconnections build the planar design; what is shown on figure 1-6.

SOFCs are generally very thin. To illustrate, in the anode-supported or cathode-supported SOFC, the thickness of electrode-supported cell usually is in the range of 0,3 to 1,5mm and the thickness of the electrolyte is about 20μm. Tubular and planar SOFCs are manufactured in different designs as ASC, ESC, CSC and MSC.

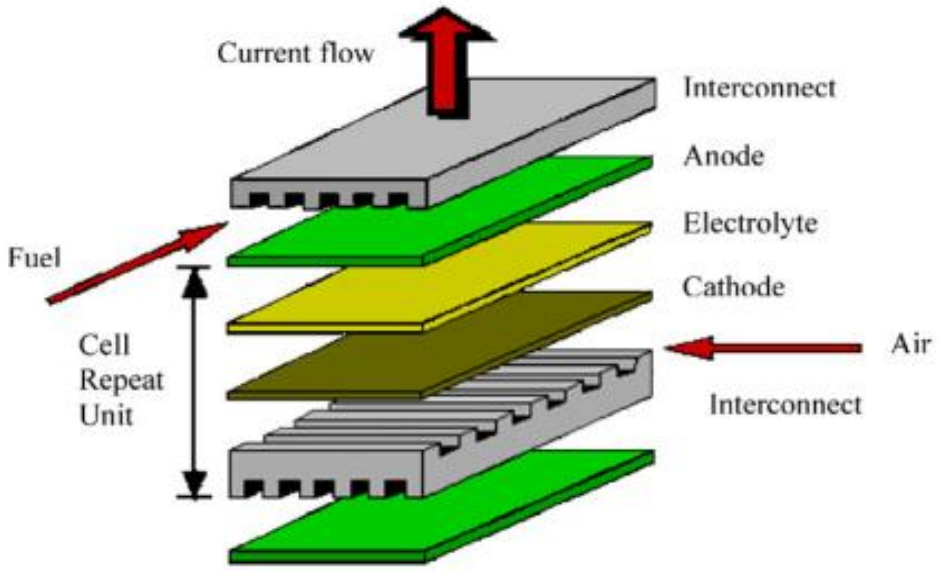


*Fig. 1-6 SOFC planar design (Kakaç 2007)*

There are also known structures such as monolithic, developed by Rolls-Royce integrated planar solid oxide fuel cell (IP-SOFC). The schemes of such designs are shown in figures below.

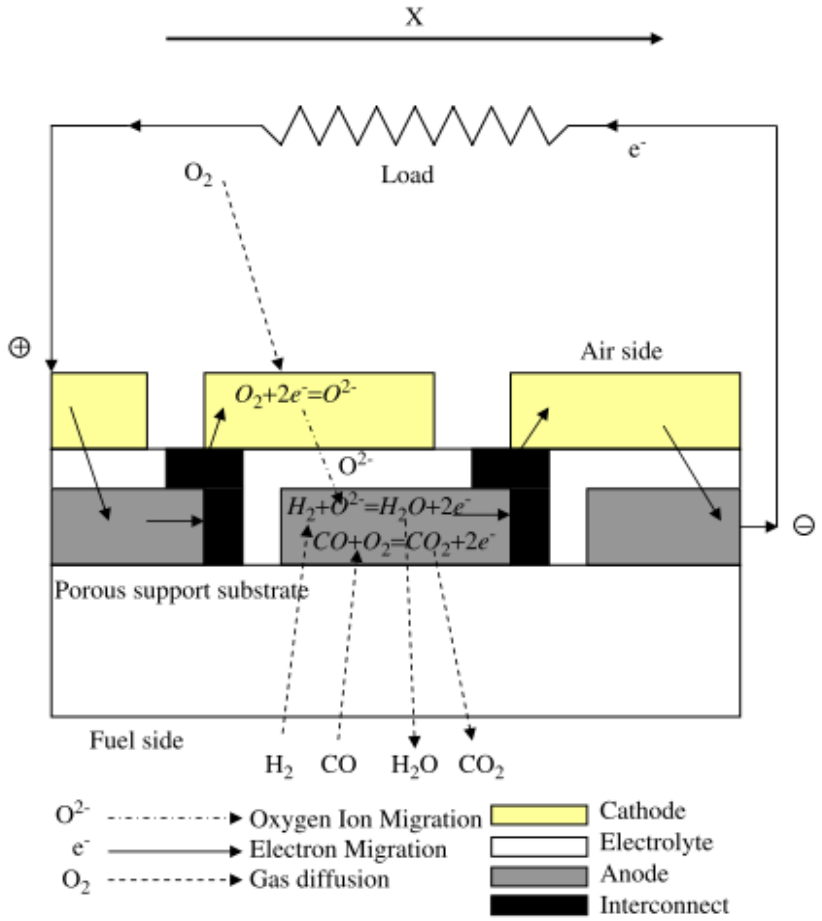


*Fig. 1-7 Integrated planar solid oxide fuel cell scheme (Kakaç 2007)*

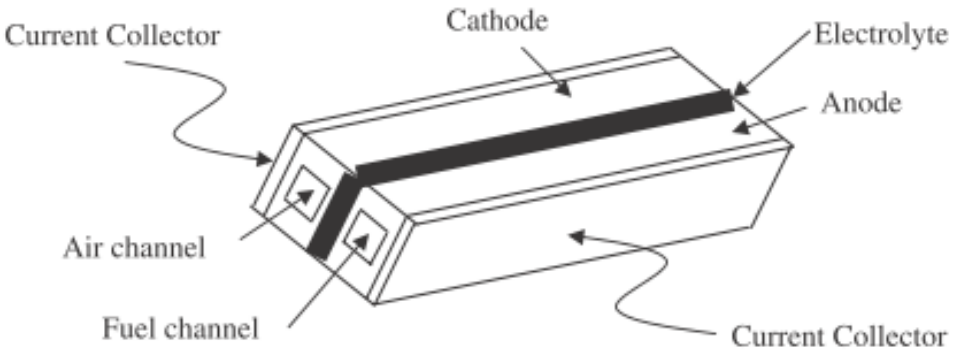


*Fig. 1-8 Monolithic SOFC design scheme (Kakaç 2007)*

In the monolithic configuration anode, electrolyte and cathode are combined in three layers sequence. Corrugated anode and cathode layers form the flow channels for fuel and oxidant gasses. Assembled in such way system is sintered into single block.

The IP-SOFC is a modern design which combines the thermal expansion compliance from the tubular design and low cost component fabrication from the planar design (Kakaç 2007).

# 2 SOFC FUEL FLEXIBILITY

As mentioned in previous chapter, the high operating temperature of SOFCs brings numerous of difficulties, but also significant benefits. One of the most important advantages of this fact is the possibility of running the cells directly on hydrocarbon fuels and CO, instead of on pure hydrogen, like in low and intermediate temperature types of fuel cells. This fact gives SOFCs further advantages:

- significant higher system efficiency,
    - by recuperating waste heat from the stack into the fuel supply;
- not necessarily a complex and expensive external fuel reforming like in case of low temperature fuel cells.

In short, SOFCs can internally reform a wide range of fuels, convert them into power, and also provide high quality of by-product heat for cogeneration (also possibility of use in bottoming cycle). All these facts, with high overall efficiency, negligible air pollutant emissions and slight GHG emissions. (Singhal, Handbook no7)

This chapter focused on the fuels investigated in present thesis. General like also more detailed information about them were presented. What more, actual status of this fuels and their potential in Poland was discused.

## 2.1 Fuels for SOFC

At the present time, the most common fuel for SOFCs is natural gas. It is because of several reasons such as low cost, clean, abundant, easily access, and existing supply infrastructure in many places. The range of potential fuels for SOFCs is presented below.

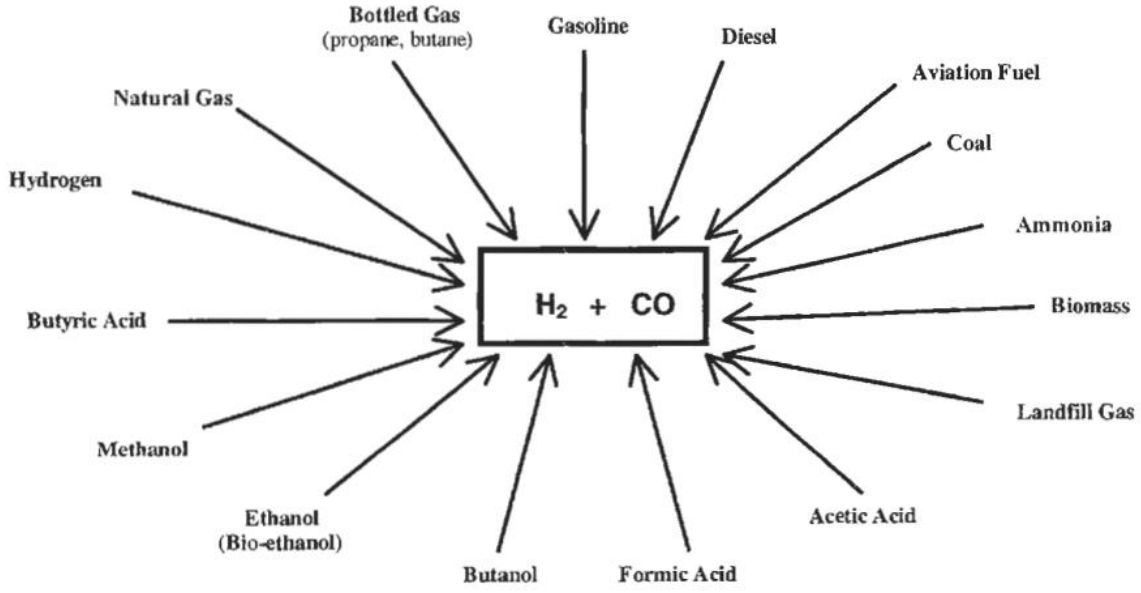


*Fig. 2-1 Potential fuels for SOFC (Sunghal 2003)*

This project is based on the experimental tests of solid oxide fuel, single cells with biogas as well as syngas and pyrolysis-reformed gases. The aim of the study is to compare the performance of the cells, operating under different circumstances and their influences on the performance. However, at first performance of the tested cells, fueled by pure hydrogen have to be evaluated.

### 2.1.1 Hydrogen

Hydrogen is the simplest element on our planet. It can be found as a part of plants or animals, but also in water, alcohols, hydrocarbons and other substances. Moreover, hydrogen is the most abundant element of the universe. The atom of hydrogen (H) has one proton and one electron. Hydrogen molecule consists of two atoms of hydrogen (H2) and in the standard conditions (20°C/ 1 atm) is a gas. It must be produced from compounds that contain it. It also means that hydrogen is an energy carrier, not an energy source. In short, it only stores and delivers energy in a usable form.

Hydrogen can be produced from different resources like fossil fuels, nuclear, biomass, wind, solar, geothermal and hydroelectric power using variety of process technologies.

The main technologies producing hydrogen can be divided into three group processes:

- thermal processes,
- electrolytic processes,
- and photolytic processes.

These processes and connected with them technologies are presented in the following thesis parts.

#### Thermal technologies for hydrogen production

Thermal processes use energy from sources such as natural gas, coal, or biomass, to release hydrogen from their molecular structure. Thermo-chemical processes use heat in combination with closed-chemical cycles to produce hydrogen from feedstock – water in most cases.

Currently, the most popular and efficient pathway for production of hydrogen is steam-methane reforming in large central plants (in most cases). Petroleum refining and ammonia production (for fertilizer) industries, are the main hydrogen consumers. In addition, the main challenge for hydrogen production by natural gas reforming is to make hydrogen cost competitive with available fuels by:

- better designs for lower equipment manufacturing and maintenance cost reduction,
- improvement in process energy efficiency (better catalysts and better heat integration).

Thermal processes and related chemical equations for hydrogen production are presented below.

1. Reforming of natural gas (steam-methane reforming)

- the use of natural gas and high-temperature steam (700-1000 °C) is reacted under high pressure (3 to 25 bar) and in presence of a catalysts (metal based – nickel);
- syngas is produced (also small amounts of carbon dioxide);

$$CH_4 + H_2O\ (+heat) \rightarrow 3CO + 3H_2$$

- carbon monoxide is reacted with water to produce more hydrogen;

$$CO + H_2O \rightarrow CO_2 + H_2 + (small\ amount\ of\ heat)$$

- finally, carbon dioxide and other impurities are removed in a pressure-swing absorption process, leaving pure hydrogen;
    - can occur with other than natural gas fuels, examples are shown below;

*propane* $C_3H_8 + 3H_2O\ (+heat) \rightarrow 3CO + 7H_2$

*ethanol* $C_2H_5OH + H_2O\ (+heat) \rightarrow 2CO + 4H_2$

*gasoline* $C_2H_{18}OH + 8H_2O\ (+heat) \rightarrow 8CO + 17H_2$

2. Partial oxidation processes

- there are two main partial oxidation processes types:
    - thermal partial oxidation (TPOX) reaction,
        - dependent on the air-fuel ratio;
        - proceed at the temperatures 1200 °C and above;
    - catalytic partial oxidation (CPOX),
        - use catalyst in order to reduce temperature requirements;
        - proceed at temperature range of 800 to 900°C;

- the choice of partial oxidation type is connected with the content of sulfur in a reformed fuel:
    - below 50 ppm, CPOX technique is used because higher sulfur content would poison the catalyst;
    - above 50 ppm, TPOX technique is used;

- fuel (such as methane) is reacted with limited amount of air at appropriate temperature;
- syngas is produced (also small amounts of carbon dioxide and nitrogen - if reaction occurs with air),

$$CH_4 + \frac{1}{2}O_2 \rightarrow CO + 2H_2(+heat)$$

- next step is the same as in the case presented above (water gas-shift reaction);
    - in contrast to the previous one process, partial oxidation is exothermic process and occurs much faster;
    - partial oxidation is less efficient compared to steam-methane reforming process (less hydrogen per unit of the input is received);

3. Gasification of coal

- coal is reacted with controlled amount of oxygen (air) and high temperature steam under high pressure;

- produces syngas and carbon dioxide (also small amounts of other impurities like hydrogen sulfide, mercury and particulates);

$$CH_{0,8} + O_2 + H_2O \rightarrow CO + CO_2 + H_2 + \ other\ species$$

**unbalanced reaction*

- syngas is purified;
- water gas-shift reaction occurs;
- hydrogen is removed by a separation of the system;
    - carbon dioxide can be captured and sequestered;

4. Gasification of biomass.

- the process is very similar to the gasification of coal process (high pressure and high temperature reaction) where instead of coal, biomass is reacted with air (gasifier);

$$C_6H_{12}O_6 + O_2 + H_2O \rightarrow CO + CO_2 + H_2 + \ other\ species$$

**simplified example reaction*

    - during biomass oxidation process, additional hydrocarbons are usually produced with syngas;
        - in this case, mentioned hydrocarbons must be reformed with a catalyst to get pure syngas;
- water gas-shift reaction;

5. Pyrolysis

- pyrolysis is a special type of biomass gasification process, which occurs in the absence of oxygen;
    - absence of oxygen results in that undesirable additional hydrocarbons are not generated in the process;
        - water content of the feedstock material is also important in order to reduce this effect;
    - pyrolysis process takes place inside the pyrolyzer at high temperature (600 - 1000°C) and in the presence of a catalyst;
    - biomass fuel is converted into carbon char, carbon dioxide, carbon monoxide, water, hydrogen, methane and other hydrocarbons, and tars,

$$C_aH_bO_c\ (+heat) \rightarrow C + CO_2 + CO + H_2O + H_2 + CH_4 + C_2H_6 + CH_3OH + \cdots + tars$$

**schematic reaction*

    - carbon char and tars are removed;
    - next, to reform typically hydrocarbons, additional process with a catalyst takes place – similar process to steam-methane reforming process;

- steam shifts reaction step;
- produced hydrogen is then separated and purified;

6. Reforming of renewable liquid fuels

- renewable liquid fuels reforming process is proceeded exactly in the same way as reforming of natural gas process, with one difference – as an input, the liquid fuels are used (such as ethanol, and bio-oils);

7. High-temperature water splitting

- very high temperature process (1000 to 2000 °C)
  - the heat is derived from nuclear reactors or from concentrated solar light, respectively;

- consisted of the series of chemical reactions that produce hydrogen and oxygen, only with water as an input;
- each cycle in a process, uses the same chemicals which creates closed loops;
  - actually, this process is in developing stage;

### Electrolytic technologies for hydrogen production

Electrolytic processes use electricity and water as an input, to produce hydrogen. Hydrogen production occurs in an electrolyzer where water is splited into hydrogen and oxygen. Most often, the power for such process comes from renewable energy sources or nuclear (high-temperature electrolysis). Moreover, the pathways of hydrogen production are zero or near to zero of GHG emissions – that make them even more attractive. Another advantage of the electrolytic processes is that, they are very well scalable.

PEM electrolyzers offer low and high differential hydrogen and oxygen pressures. Alkaline electrolyzers are the most common type among the electrolytic types use today. They offer low or no differential hydrogen and oxygen pressures. The main possible advantage of SO electrolyzers over PEM and alkaline electrolyzers is the use of heat from other sources (like nuclear energy) to decrease the amount of electricity used to produce hydrogen from water. However, seals materials and thermal cycling are challenges.

Main types of electrolyzers are listed and briefly described below.

1. Polymer electrolyte membrane electrolyzer

- as in PEM fuel cell, the PEM electrolyzer uses a special plastic material (solid polymer material) for membrane;
- the feedstock (water) reacts at the anode side to form oxygen and positively charged hydrogen ions ($H^+$);
- direct current flows through an external circuit, while the hydrogen ions move across the membrane to the cathode;
- at the cathode side, hydrogen protons combined with electrons (from external circuit) form hydrogen gas;

2. Alkaline electrolyzer

- this kind of electrolyzer is very similar to PEM electrolyzer; the difference is only in the form of electrolyte used – (sodium or potassium hydroxide - liquid electrolyte in porous matrix)

3. Solid oxide electrolyzer

- as an electrolyte, ceramics materials are used which usually operate properly at 500 °C to 800 °C;
- water at the cathode side, reacts with the electrons from the external circuit to form hydrogen and oxygen ions ($O^-$);
- negatively charged oxygen ions move across the membrane, and react at the anode side to create oxygen gas and give up the electrons to the external circuit;

### Photolytic technologies for hydrogen production

Photolytic processes like electrolytic processes, split water into hydrogen and oxygen. The main difference between these two hydrogen production technologies is that the photolytic processes use light energy.

Photobiological and photoelectrochemical water splitting processes are in early and very early stages of research, respectively. However, both of these processes offer long-term potential for hydrogen production. (DOE, RES603)

Two main kinds of photolytic processes for hydrogen production are briefly presented below.

1. Photobiological water splitting processes

- use sunlight and specialized microorganism (like green algae and cyanobacteria);
- mentioned microorganisms in their natural metabolic processes, produce hydrogen (and oxygen as a byproduct) from water in the presence of the sunlight;
    - presently, these processes are too slow to be used commercially;

2. Photoelectrochemical water splitting processes.

- specialized semiconductors called photoelectrochemical materials, produce hydrogen and oxygen directly from water, using sunlight;
    - different semiconductor materials work at particular wavelengths of light and energies;

## 2.1.2 Syngas

Syngas is a combustible mixture of the hydrogen and carbon monoxide gas, as well as carbon dioxide. In principle, synthetic gas can be produced from wide variety of hydrocarbon materials like natural gas, naphtha, residual oil, biomass, petroleum coke or coal, in several thermal processes:

- steam reforming of natural gas - or other liquid fossil fuels like propane, gasoline, or liquid bio fuels like ethanol and bio-oils to produce hydrogen,
- partial oxidation of hydrocarbon fuels,

- gasification of coal and/or biomass,

These processes were discussed in the previous chapter. It should be also noted, that syngas produced by listed technologies has different composition. The highest H2/CO ratio syngas is produced by steam-methane reforming process, which gives obvious advantage for this process in hydrogen production application. In addition, it has a big importance for overall dominance for this technique in syngas production technologies.

Syngas can be used as an intermediate in producing:

- synthetic natural gas,
- ammonia,
- methanol,
- synthetic petroleum (Fisher-Tropsch process and methanol to gasoline process),
- and other chemicals.

First of all discussed gas mixture, can be used as a fuel for power production in solid oxide fuel cells - on what (inter alia) the present work is focused.

Gas mixture called wood gas (primarily consists of nitrogen, hydrogen, carbon monoxide and small amounts of methane) is a type of synthetic gas, generated by gasification of biomass like wood chips or sawdust. This gas composition after purification from tars and soot/ash particles, meets the requirements for direct use in solid oxide fuel cells or in engines. Moreover, wood gas composition strongly depends on the gasification process, the gasification medium (air, oxygen or steam) and the fuel moisture. The highest hydrogen share in wood gas mixture is usually yielded by the steam gasification process (oxygen oxidation is not in commercial use). The examples of different wood gas compositions are shown in table below.

*Table 2-1 Example of wood gas composition, oxidized with air, oxygen and air. (RES'09)*

| **Gas component name and chemical formula** | **Oxidizer type** | | |
|---|---|---|---|
| | **Air** | **Oxygen** | **Steam** |
| *nitrogen - $N_2$* | 50 - 60 % | 2 - 5 % | 2 - 5 % |
| *carbon monoxide – CO* | 10 - 15 %, | 28 – 38 % | 30 – 40 % |
| *hydrogen - $H_2$* | 14 % | 28 – 35 % | 22 – 28 % |
| *carbon dioxide - $CO_2$* | 12 - 20 % | 22 – 30 % | 15 – 20 % |
| *methane - $CH_4$* | 2 - 4 % | 4 – 8% | 10 – 12 % |

### 2.1.3 Biogas

Biogas is a mixture produced from organic matters by biological breakdown during anaerobic digestion process. Feedstock sources for this process are biomass materials such as:

- manure,
- sewage,
- municipal waste,
- green waste,
- and energy crops.

Biogas from these feedstock materials contains primarily methane and carbon dioxide. This kind of mixture is a flammable fuel, which can be combusted with oxygen (air). Energy released during combustion process can be utilized for heating and cooking purposes, or as a fuel for any type of heat engine to generate mechanical and/or electrical energy. Moreover, compressed biogas can be used to power internal combustion engines in vehicles or can be source of biomethane production.

Landfill gas is a type of biogas produced from chemical reactions with waste - putrescible materials, in a presence of microbes in the landfill. The composition and the rate of production depend on the waste composition, landfill geometry and the age of the landfill. The typical landfill gas composition based on dry volume, is presented in table 2-2.

The composition of manure or swage based on biogas, depends on several parameters, such as the biodigestor employed, the type of organic material and the constancy of the feeding process of the biodigestor. This type of biogas consists higher concentration of methane and lower composition of carbon dioxide. Detailed example of such gas mixture is shown in table 2-3.

*Table 2-2 Typical landfill gas composition based on dry volume. (http://en.wikipedia.org/wiki/Landfill_gas_monitoring)*

| **Gas component name and chemical formula** | **Percentage share** |
|---|---|
| *methane - CH4* | 45 - 60 % |
| *carbon dioxide - CO2* | 40 - 60 % |
| *nitrogen - N2* | 2 - 5 % |
| *oxygen - O2* | 0,1 – 1,0 % |
| *sulphides, disulphides, mercaptans etc.* | 0 – 1,0 % |
| *ammonia - NH3* | 0,1 – 1,0 % |
| *hydrogen - H2* | 0 – 0,2 % |
| *carbon monoxide - CO* | 0 – 0,2 % |
| *trace constituents* | 0,01 – 0, 6 % |

*Table 2-3 Example of biogas composition based on municipal waste. (http://www.energia-odnawialna.net/biomasa.html)*

| **Gas component name and chemical formula** | **Percentage share** |
|---|---|
| *methane - $CH_4$* | 52 - 85 % |
| *carbon dioxide - $CO_2$* | 14 - 18 % |
| *nitrogen - $N_2$* | 0,6 - 7,5 % |
| *oxygen - $O_2$* | 0 - 1 %. |
| *hydrogen - $H_2$* | 0 - 5 % |
| *carbon monoxide – CO* | 0 - 2,1 %, |
| *sulfate hydrogen - $H_2S$* | 0,08 - 5,5 % |

### 2.1.4 Pyrolysis reformed gas

Plant materials like green waste, sawdust, waste wood, woody weeds are the feed stocks for the pyrolysis process. Moreover, agricultural sources like: nut shells, straw, cotton trash, rice hulls, switch grass and poultry litter, dairy and potentially other manures, are suitable for pyrolysis process. However, it should be noted that in this process the humidity of the feedstock material cannot exceed 10%.

Pyrolysis reformed gas is produced during pyrolysis process (described in chapter 2.1.1.1) which mainly contain carbon dioxide, carbon monoxide, methane, hydrogen and nitrogen. Detailed composition of the pyrogas obtained from wood feedstock is presented below in the table. This gas was experimentally obtained by the Faculty of Industrial Engineering in the University of Perugia.

*Table 2-4 Example composition of pyrogas. (University of Perugia)*

| Gas component name and chemical formula | Percentage share |
|---|---|
| *carbon monoxide – CO* | 29 % |
| *hydrogen - $H_2$* | 7 % |
| *methane - $CH_4$* | 21 % |
| *carbon dioxide - $CO_2$* | 38 % |
| *nitrogen - $N_2$* | 5 % |

The product of the pyrolysis process strongly depends on:

- composition related – humidity content, cellulose-hemicellulose-lignin,
- feed-stock related – dimension, density, porosity,
- reactor related - heating rate, temperature and residence time

what is shown in the table below.

*Table 2-5 Influence of the conditions on pyrolysis process.(RES'09)*

| Mode | Conditions | Liquid | Char | Gas |
|---|---|---|---|---|
| *fast pyrolysis* | *moderate temperature, short residence time particularly vapour* | *75%* | *12%* | *13%* |
| *carbonization* | *low temperature, very long residence time* | *30%* | *35%* | *35%* |
| ***gasification*** | ***high temperature, long residence time*** | ***5%*** | ***10%*** | ***85%*** |

Pyrogas is used in the chemical industry, to produce materials such as charcoal, activated carbon, methanol and other chemicals. It is also used to convert ethylene dichloride into vinyl chloride to make PVC, to produce coke from coal, to convert biomass and waste into syngas and safety disposable substances, respectively. Moreover, pyrolysis can be used to transform medium-weight hydrocarbons from oil into lighter ones.

## 2.2 Fuels for SOFC - actual status and perspectives in Poland

The following chapters describe the use of syngas, biogas, and pyrolysis reformed gasses in Poland. These gases can be used directly or indirectly as fuels for power generation in solid oxide fuel cells. Moreover, next chapters present the actual status and the potential production of these gases in Poland.

### 2.2.1 Actual biogas status and perspectives

As it was showed in the previous chapters, biogas can be produced from any kind of biomass or organic waste. The production of biogas in Poland, in 2006 is illustrated on figure 2-2 According to this figure, in Poland, the primary energy production of biomass is 62,6 ktoe. It should be also noted, that the main share in this amount has primary energy of biogas from sewage sludge (43 ktoe), and from landfills (19,1 ktoe). In 2006, biogas from agricultural plants had a minimal share in the primary energy production which reached 6 ktoe.

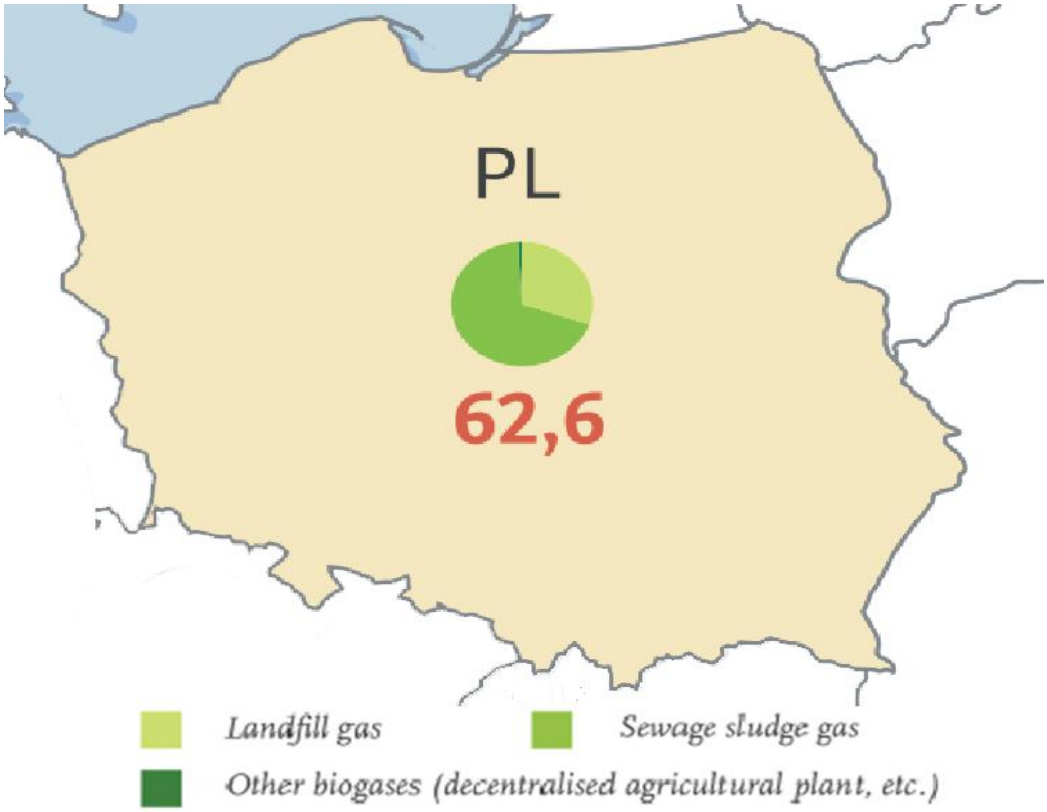


*Fig. 2-2 Primary energy production of biogas in Poland in 2006 (in ktoe). (EurObserv'ER 2008)*

In addition, as *EurObserv'ER 2008* states, gross electricity production from biogas in Poland amounted to 160,1 GWh in 2006. All electricity produced in this period of time, came from CHP plants, which means that in this country did not work any power plant fueled by biogas. Moreover, gross heat production from biogas in this period amounted to 34,2 ktoe where most of it was produced in CHP plants (28,1 ktoe) and only 6 ktoe in heat plants – what is presented in the table below.

*Table 2-6 Primary energy production of biogas (in ktoe), gross electricity production from biogas (in GWh) and gross heat production from biogas (in ktoe ) in Poland in 2006. (EurObserv'ER 2008)*

| **Primary energy production of biogas in Poland in 2006 (in ktoe)** | | | |
|---|---|---|---|
| *landfill gas* | *sewage sludge gas*[1] | *other biogases*[2] | *total* |
| *18,9* | *43,1* | *0,5* | *64,4* |
| **Gross electricity production from biogas in Poland in 2006 (in GWh)** | | | |
| *electricity plants only* | *CHP plants* | *total electricity* | |
| *0* | *160,1* | *160,1* | |
| **Gross heat production from biogas in Poland in 2006 (in ktoe)** | | | |
| *heat plants only* | *CHP plants* | *total heat* | |
| *6* | *28,1* | *32,2* | |

[1] *Urban and industrial.*
[2] *Decentralised agricultural plants, municipal solid waste methanisation plants, centralised codigestion plants.*

Data from 2009 shows that biogas market in Poland developed dynamically. To illustrate, in 2009, biogas from agriculture sector was used in six power plants with total power of 6 MW, compared to zero production in 2006. Also, electricity production from landfill biogas and water waste treatment amounted to 271,5 GWh in 2009 where in 2006 reached 160,1 GWh.

Poland has very high potential for agricultural biogas production because of the huge agricultural land area of 10.7 millions of hectares It is estimated that the potential for agricultural biogas plants and processing facilities of organic waste in Poland is about 90% of the total capacity in Germany (the biggest biogas producer in EU with production of 2,4 Mtoe in 2006). There is also estimated that 12 % of Europe´s biomass potential is available in Poland.

According to the *RE-SHAPING - Renewable Energy Policy Country Profiles - 2009 version* (presented below) in Poland the annual production growth of biogas was 33% between 2005 and 2007. In addition, it shows that for biogas as well as other biomass based fuels, the potential production is much bigger for the future. To illustrate, total realizable potential for biogas by 2020 equals 763 ktoe which is significant amount compared to 17 ktoe of biogas produced in 2007.

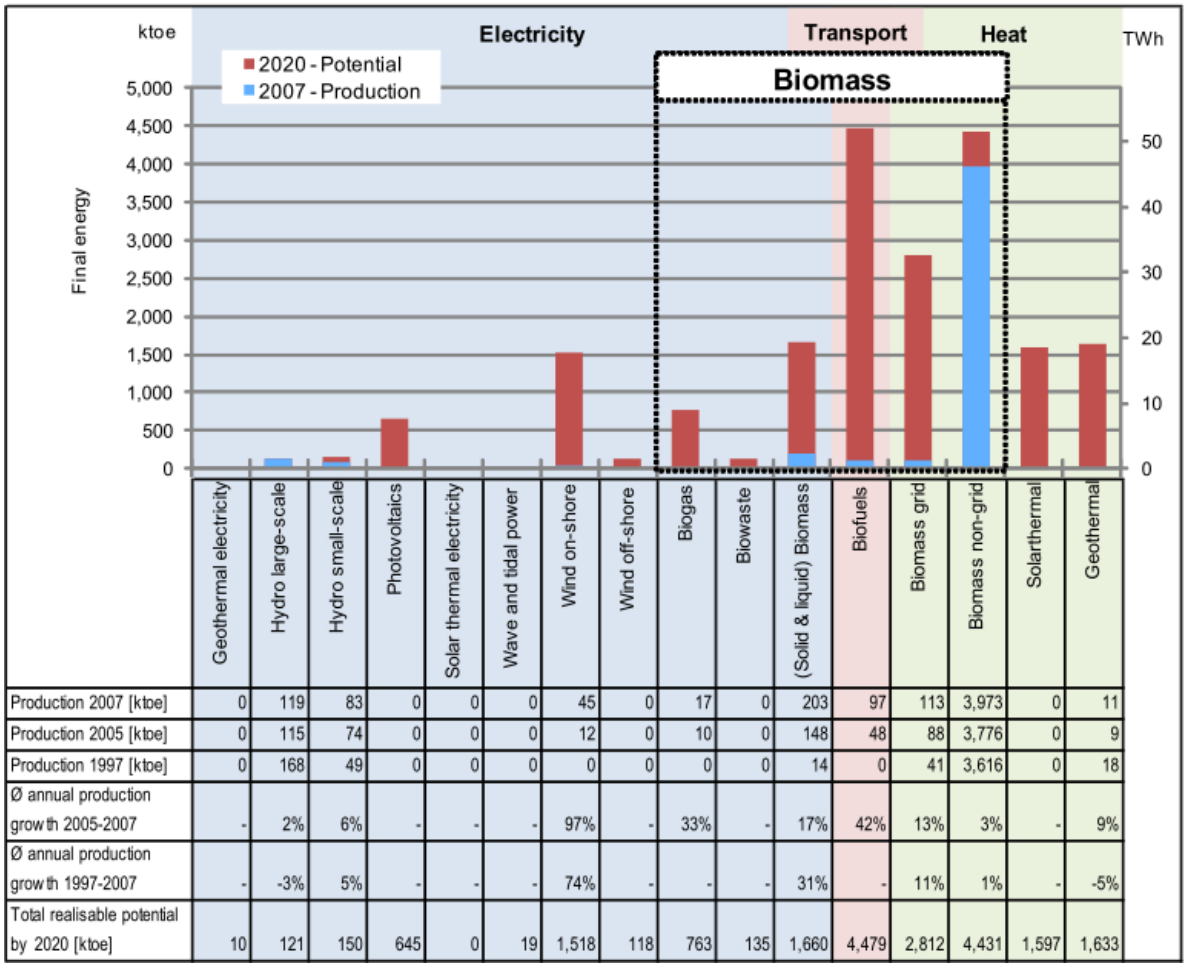


| | Geothermal electricity | Hydro large-scale | Hydro small-scale | Photovoltaics | Solar thermal electricity | Wave and tidal power | Wind on-shore | Wind off-shore | Biogas | Biowaste | (Solid & liquid) Biomass | Biofuels | Biomass grid | Biomass non-grid | Solarthermal | Geothermal |
|---|---|---|---|---|---|---|---|---|---|---|---|---|---|---|---|---|
| Production 2007 [ktoe] | 0 | 119 | 83 | 0 | 0 | 0 | 45 | 0 | 17 | 0 | 203 | 97 | 113 | 3,973 | 0 | 11 |
| Production 2005 [ktoe] | 0 | 115 | 74 | 0 | 0 | 0 | 12 | 0 | 10 | 0 | 148 | 48 | 88 | 3,776 | 0 | 9 |
| Production 1997 [ktoe] | 0 | 168 | 49 | 0 | 0 | 0 | 0 | 0 | 0 | 0 | 14 | 0 | 41 | 3,616 | 0 | 18 |
| Ø annual production growth 2005-2007 | - | 2% | 6% | - | - | - | 97% | - | 33% | - | 17% | 42% | 13% | 3% | - | 9% |
| Ø annual production growth 1997-2007 | - | -3% | 5% | - | - | - | 74% | - | - | - | 31% | - | 11% | 1% | - | -5% |
| Total realisable potential by 2020 [ktoe] | 10 | 121 | 150 | 645 | 0 | 19 | 1,518 | 118 | 763 | 135 | 1,660 | 4,479 | 2,812 | 4,431 | 1,597 | 1,633 |

*Fig. 2-3 RES - production and potential for future in Poland. (RE-SHAPING - Renewable Energy Policy Country Profiles - 2009 version)*

At the present time, there are many investments supported by Polish government and EU, which promote production of energy and heat from biogas. Even though, potential of biogas for such applications is evident. However, there is still lack of using commercial SOFC systems. Today, in Poland, biogas is used for heat and electricity generation – mostly in CHP plants.

### 2.2.2 Actual syngas status and perspectives

The production of the synthesis gas is based mainly on chemical processing of the natural gas (methane). It is estimated that about 80% of the syngas in the word, is produced from natural gas and about 10% from coal. Remainder, 10% of the syngas is obtained through the conversion of the liquefied gas or gasification of heavy residue (asphaltenes, coke) and biomass –what is shown in figure 2-4.

In the IGCC (Integrated Gasification Combined Cycles) syngas is produced from the coal (in small installations biomass or municipal wastes) which is used for electricity generation. This technology is more efficient (45 – 55 %) than conventional power plans (25-35%). It is also more ecological because of lower water requirements and lower emissions of sulfur dioxide, particulates and mercury.

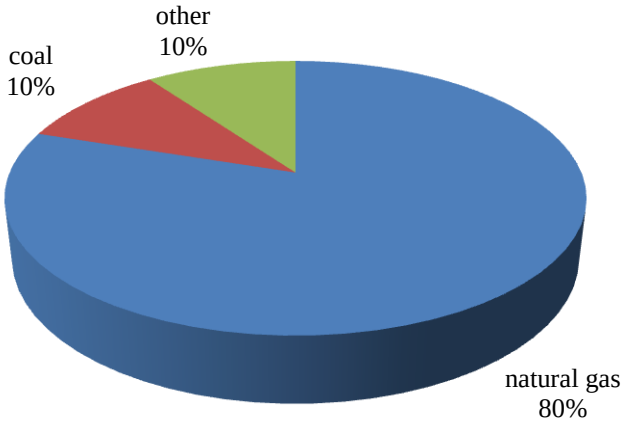


*Fig. 2-4 Raw materials for syngas production. (Lubiewa-Wieleżyński, W & Siroka, A 2009)*

In most cases, syngas is produced from natural gas and is used for almost all world production of methanol and its derivatives, synthesis of oxo-alcohols, ammonia and also for the synthesis of hydrocarbons and hydrogen production. Moreover, almost entire world production of ammonia and nitrogen compounds industry is based on hydrogen obtained from syngas.

Hydrogen obtained from syngas is also used for refining of petroleum products and foodstuffs. In addition, syngas is basic product for liquid fuels production in the Fischer–Tropsch synthesis. During this process, synthesis gas is turned – run over a catalyst and then made into Fischer-Tropsch liquid which is a mixture of hydrocarbons that can be upgraded into a compatible fuel. Now, in the world as well as in Poland, there is increased interest in this technology as a method for producing motor fuels from coal, natural gas and/or biomass. However, in Poland there is no acting factory utilizing this technology.

The world syngas market is approximately 6 EJ/yr. Figure below illustrates the world syngas market with distinction in the use.

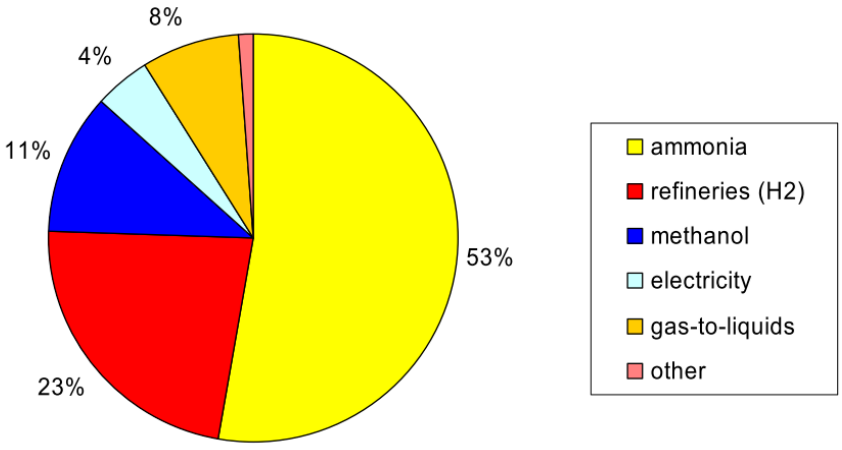


*Fig. 2-5 The world syngas market. (van der Drift 2004)*

In Poland, syngas is produced mainly from natural gas by it conversion, and is used for hydrogen generation. In 2008, it was produced 7mld $m^3$ of hydrogen, which was used for

ammonia and methanol production, and also for refining of petroleum products and foodstuffs.

Syngas can be also used as a direct fuel for SOFC. However, in Poland there in no fuel cell systems in commercial use, so there is no syngas production for such purposes.

Currently, the technology for syngas production is based on natural gas. In 2009, domestic resources of natural gas covered about 30% of the Polish demand – 13,3 mld $m^3$. The rest of the demand (10,6 mld $m^3$) was covered by natural gas imported mainly from Russia (7,4 mld $m^3$). Natural gas consumption by sector in Poland in 2009, was as follow:

- 58,2 % - big industrial users (nitrogen plants, refineries and petrochemical companies),
- 28 % - individual consumers (households, small producers).

However, it should be marked that Polish potential for syngas production is much higher, especially if other potential sources like coal and biomass are taken into account. The technology for syngas production from these feedstock materials is known, and actually, a few plants are in use in Poland .

The potential of biomass production in Poland is significant - what was also presented in the previous chapter. The estimated area for energy crops in Poland amounts to 2 millions of hectares. That gives the theoretical possibility of producing 16 billion $m^3$ of bio-methane in a year - which is about 160 TWh of primary energy (estimated for average yield of maize).

In Poland, the proved reserves of coal are amounted to about 17 mld t. They are significant; however these reserves are available only in 20% (so called operative resources). The increase in operative reserves requires new major investment projects. It should be also noted, that the process of coal gasification for syngas production has some difficulties. One of them is relatively high level of investment and is unavoidable $CO^2$ emissions or the need for its sequestration.

Summing up, currently, in Poland, there is no syngas production for fuel cell systems using in commercial. Moreover, the potential for syngas production is much higher than the actual production level. However, in the case of using other feedstock materials, like biomass and coal (available in the country), new significant investments in the production and conversion are needed. (Lubiewa-Wieleżyński, W & Siroka, A 2009)

### 2.2.3 Actual pyrolysis reformed gas status and perspectives

Both as in the case of biogas and the pyrolysis reformed gas production as a raw material all kind of biomass material is used. However, pyrolysis is much more complex and costly process than biogas production technologies. There are many parameters which influence the product of pyrolysis process. Among them are temperature, processing time, water content, the features of the feedstock materials and oxygen presence. To control all these parameters precisely, it makes the process very advanced technology. Currently, in Poland as well as in the world, there is no commercial scale of plants for biomass processing by the pyrolysis. However, this technology is considered as a very promising for the future generation of the fuel.

The base material in form of biomass for the pyrogas production in Poland is prominent - what was shown in chapter 2.2.1. Moreover, in the recent time, this process is used to process different industrial waste like tires or municipal wastes. However, the technology for

pyrolysis reformed gas production is advanced, complex, and at the same time costly. Because of all these factors, the pyrolysis should be regarded as a complementary technology in relation to other thermo chemical processes for different feedstock fuel processing. It is also very good advantage for future development too.

## 2.3 Fuel processing

Besides of the obvious benefits, internal reforming has also some difficulties. One of them is carbon deposition (especially on the nickel cermet anode) and subsequent build-up of deactivating carbon and rapid deactivation of the cell. It happens when especially higher hydrocarbons are used as fuels. The reactions for this situation are as follow:

| | |
|---|---|
| for methane | $CH_4 \rightarrow C + 2H_2$ |
| general for higher hydrocarbons | $\mathrm{C_nH_{2n+2}} \rightarrow \mathrm{nC} + (\mathrm{n}+1)\mathrm{H_2}$ |

In practice, these reactions are inhibited by adding steam to the fuel, usually with ratio of 2,5 to 3. In such process, $H_2$ production is maximized, and at the same time, carbon deposition through hydrocarbon pyrolysis is minimized:

| | |
|---|---|
| fast strongly endothermic reforming reactions | $CH_4 + H_2O \rightarrow CO + 3H_2$ |
| | $C_nH_{2n+2} + nH_2O \rightarrow nCO + (2n+1)H_2$ |
| slow exothermic fuel cell reactions | $H_2 + O^{2-} \rightarrow H_2O + 2e^-$ |
| | $CO + O^{2-} \rightarrow CO_2 + 2e^-$ |

Moreover, at high operating temperature, CO can be oxidized with $H_2O$ to create $CO_2$ and $H_2$ in the water-gas shift reaction presented below:

$$CO + H_2O \rightarrow CO_2 + H_2$$

Figure below shows described internal reforming SOFC process with methane as a fuel and steam.

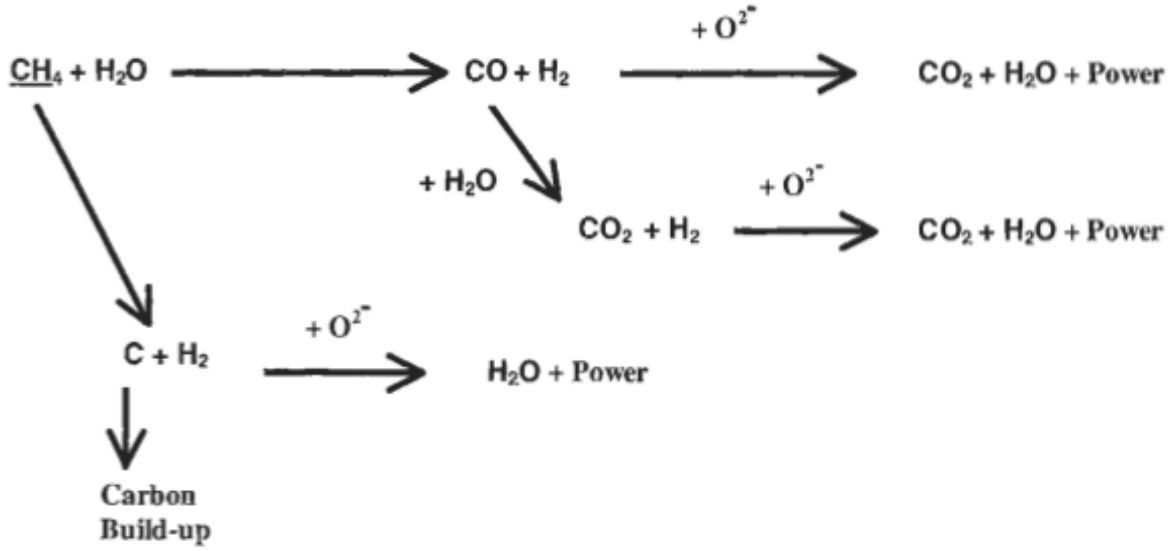


*Fig.2-6 Schematic of reaction processes in an SOFC internal reforming, with steam and methane as a fuel. (Sunghal 2003)*

The diagram of SOFC internal reforming with heat management between fuel cell anode exhaust gas and integrated internal reformer is presentenced below.

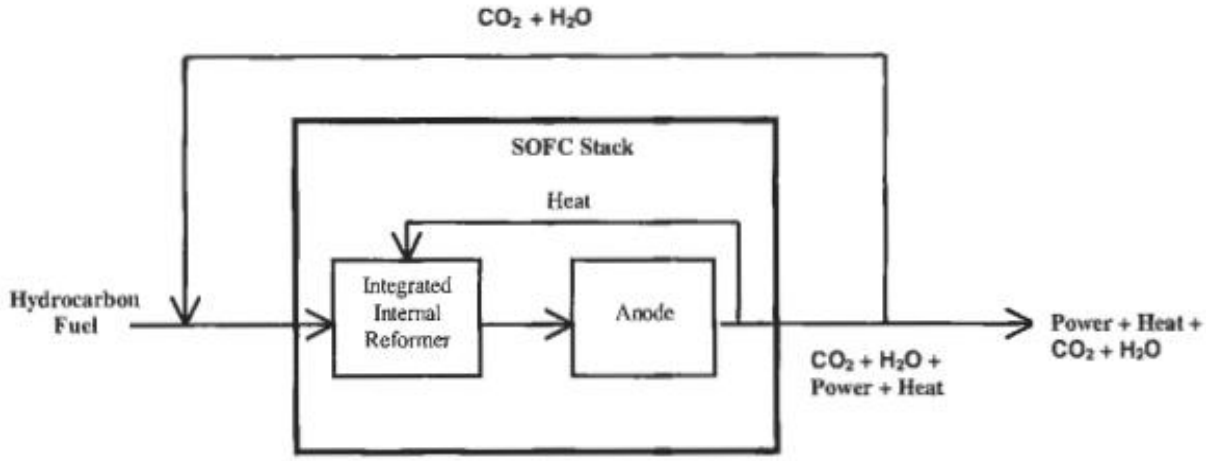


*Fig. 2-7 SOFC internal reforming with recirculation of the anode exit gas. (Sunghal 2003)*

In the following chapter, two main ways of the SOFC internal reforming are presented. General differences and important issues connected with them are also concluded.

### 2.3.1 Direct and indirect fuel reforming

Internal reforming of the fuel in SOFC can occur in two ways, directly and indirectly. The scheme of such reforming processes is presented below.

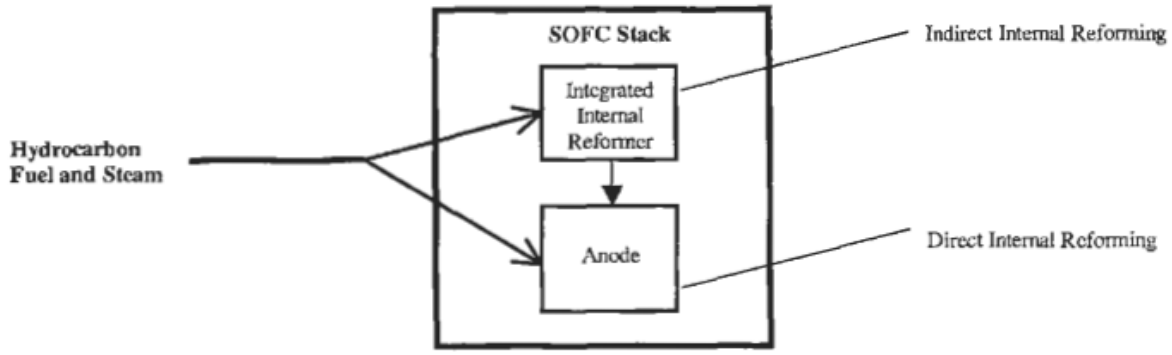


*Fig. 2-8 Scheme of direct internal and indirect internal reforming in an SOFC stack. (Sunghal 2003)*

In the case of direct internal reforming, the anode must fulfill several roles:

- catalyst for reformed hydrocarbon fuels (catalyst for the conversion of hydrocarbons to hydrogen and carbon monoxide),
- electro-catalyst liable for the electrochemical oxidation of hydrogen to water and carbon monoxide to carbon dioxide,
- electrical conductor.

The main challenge for this kind of reforming is the development of proper materials for anode, which fulfill all mentioned criteria.

Another problem concerning direct reforming is deactivating carbon deposition (mentioned in the previous chapter). The diagram illustrating possible reaction pathways of it, is presented below.

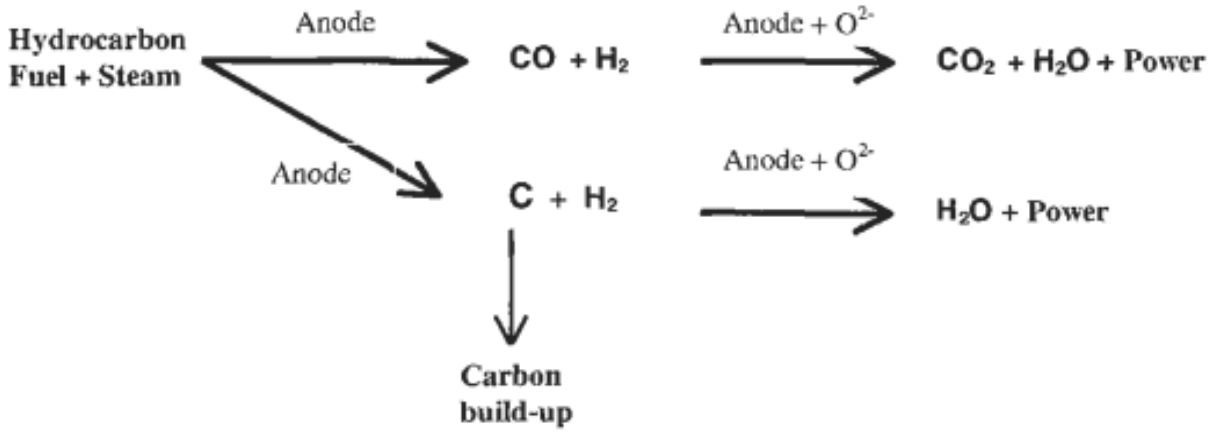


*Fig. 2-9 Carbon deposition pathway in an SOFC direct internal reforming. (Sunghal 2003)*

Another aim for the researchers is to develop nickel-based anode material, which is good enough for hydrocarbon fuel reforming (criteria listed at the beginning of this chapter) and resistant for carbon deposition.

Also, the difficult aspect during direct SOFC fuel reforming is heat management on the length of the anode. In the case of improper heat control, this can lead to cracking of the anode and electrolyte materials.

As the figure 2.3.1.1 shows, indirect internal reforming of hydrocarbons occurs in a separated and integrated reformer with SOFC stack. In this kind of configuration, the reformed fuel (which consists of carbon monoxide and hydrogen) goes to the SOFC anode. The figure 2.3.1.3 shows the reaction scheme of the SOFC indirect internal reforming process.

There are several major disadvantages of indirect over direct reforming. To illustrate, indirect reforming is less efficient, more complex and more costly solution. However, it is still more advantageous than in case of external reformer solution. The big advantage of indirect over direct reforming is that it is thermodynamically easier to control. Moreover, catalyst material for indirect reforming has lower requirements (at the same time it does not have to be electrical conductor) in contrast to martial for the SOFC internal reforming anode.

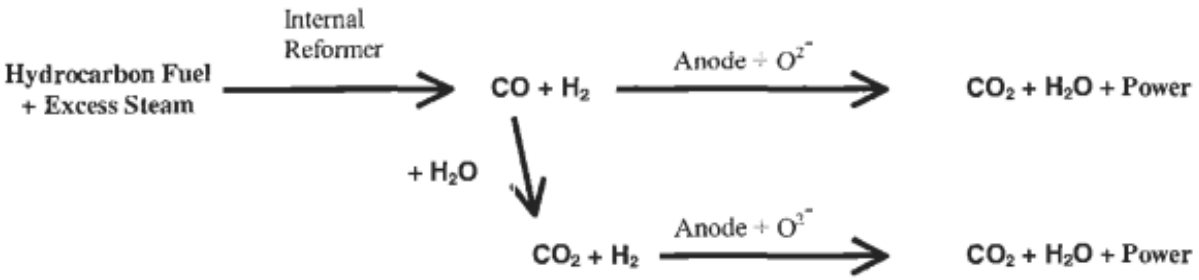


*Fig. 2-10 Scheme of reaction processes in an SOFC direct internal reforming. (Sunghal 2003)*

Concluding, the SOFC direct internal reforming requires the development in the thermodynamic control system and in new no-costly catalyst material for anode, with increased resistance for carbon deposition and sulphur poisoning at the same time. Because of these difficulties, the most popular pattern today is to separate catalyst within the SOFC stack, upstream of the anode. In the most cases, these kinds of designs indirectly reform a large majority of the hydrocarbon fuel and the rest of this fuel is reformed on the anode side. *(Sunghal 2003)*

## 2.4 Fuels for test activities

The present work demonstrates the use of experimental activities on syngas, biogas and pyrogas. Investigated fuels were reformed with steam at 800 °C and 1 bar pressure using *Aspen Plus 2006* software and – *RStoich* reactor model. The tables below show the gasses compositions used as the inputs as well as the gasses compositions after reforming.

*Table 2-7 Biogas percentage composition before and after reforming (molar fraction).*

| **Gas component name and chemical formula** | **Percentage share of the input landfill gas** | **Gas composition after reforming** *(steam, 800°C, 1bar, Aspen – RStoic)* |
|---|---|---|
| *nitrogen – $N_2$* | 5% | 2,1% |
| *carbon monoxide – CO* | – | 19,2% |
| *hydrogen – $H_2$* | – | 57,4% |
| *carbon dioxide – $CO_2$* | 50% | 21,3% |
| *methane – $CH_4$* | 45% | – |

*Table 2-8 Syngas percentage composition before and after reforming (molar fraction).*

| **Gas component name and chemical formula** | **Percentage share of the input wood gas** *(oxidzed by staem)* | **Gas composition after reforming** *(steam, 800°C, 1bar, Aspen – RStoic)* |
|---|---|---|
| *nitrogen - $N_2$* | 3,5% | 2,6% |
| *carbon monoxide – CO* | 40% | 38,2% |
| *hydrogen - $H_2$* | 25% | 44,9% |
| *carbon dioxide - $CO_2$* | 19,5% | 14,3% |
| *methane - $CH_4$* | 12% | – |

*Table 2-9 Pyrogas percentage composition before and after reforming (molar fraction).*

| **Gas component name and chemical formula** | **Percentage share of the input pyrogas** *(wood chip based)* | **Gas composition after reforming** *(steam, 800°C, 1bar, Aspen – RSTorc)* |
|---|---|---|
| *nitrogen - $N_2$* | 5% | 3% |
| *carbon monoxide – CO* | 29% | 31% |
| *hydrogen - $H_2$* | 7% | 43% |
| *carbon dioxide - $CO_2$* | 38% | 23% |
| *methane - $CH_4$* | 21% | – |

It should be noted that in the model as an input were included only the constituent gases with the molar participation of more than one percent in the total gas mixture. Moreover, the output gas mixture consists of only four main gasses $H_2$, CO, $CO_2$ and $N_2$ which means that in this model methane is fully reformed and it is not present in a final gas mixture. Output gases obtained from the simulations are used for the test activity presented at the end of the study.

# 3 PARAMETERS FOR THE PERFORMANCE ASSESSMENT

Present work is focused on SOFC testing, operating at high temperature (700 - 800°C), characterized by greater flexibility in the choice of fuel - with gases simulating biogas, syngas and pyrolysis - reformed gases. The aim of the study is to evaluate the performance of the single cell polarization curves. Tested single cells are not sealed and coated and because of that it is not possible to make absolute evaluation of their performances. The main output of the test is not the absolute value of the voltage range of the parameters, but the trend of that curve. This thesis is focused on how the performance of the SOFC cell changes when the operating parameters are varied: fuel composition, total flow, voltage, power supply and temperature.

In this part of the thesis, the most important parameters used for the purposes of the present thesis are presented. These parameters can be divided into:

- constant parameters,
    - fuel cell active area — A ($cm^2$);
    - pressure — p (bar, atm, Pa);
    - oxygen partial pressure — $p_{ox}$ (bar, atm, Pa);
    - universal gas constant — R = 8,314 (J/mol*K);
    - Faraday constant — F = 96485 (C/mol);
    - lover heating value — LHV (J/mol);

- measured parameters (obtained during the tests),
    - temperature — T (°C, K);
    - current — i (A);
    - voltage — V (V);
    - volumetric gas flows — Q (Nl/h);
    - specific volumetric gas flows — q (Nl/h $cm^2$);

- and finally, computed parameters (obtained based on constant and measured parameters).
    - area specific resistance can — ASR ($\Omega cm^2$);
    - current density — j ($A/cm^2$);
    - power density — P ($W/cm^2$);
    - efficiency — ε (%);
    - stoichiometric factor — λ;
    - dilution factor — $D_f$;
    - fuel utilization — $U_f$;
    - oxygen utilization — $U_{ox}$;

In the following chapters, the listed above parameters are presented. The ASR parameter which is the main factor used for performance assessment is described in detailed analysis below.

## 3.1 Area Specific Resistance as a performance prediction parameter

This study also focuses on Area Specific Resistance (ASR). ASR is a good parameter to evaluate performance of the tested cells, and to make comparison between different cells at various operating conditions. The study on the ohmic region is extremely interesting because it is the operating area for all kinds of the fuel cells.

The following chapters are presented detailed information about the area specific resistance definition, analysis and the method of calculation used in the present work.

### 3.1.1 ASR – definition

As it was mentioned above, ASR is a parameter which can be used for fuel cell performance evaluation. This parameter is connected with the ohmic region - presented below.

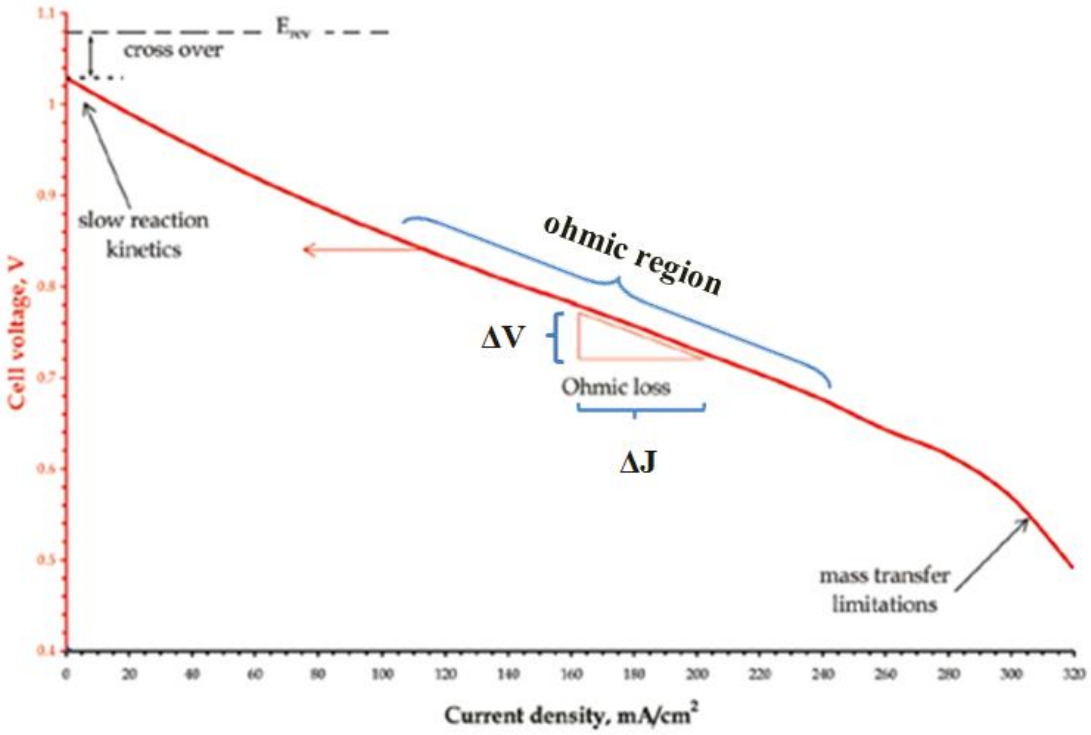


*Fig. 3-1 Ohmic region in a j-V curve.*

The figure above illustrates that ASR is strongly connected with operating area of a fuel cell. Area specific resistance can be calculated based on polarization curve – as the ratio of change in voltage and change in current density:

$$ASR = \frac{\Delta V}{\Delta j} = [\Omega cm^2]$$

Where V is the measured voltage and current density j is calculated as the ratio of cell surface and current.

In general, ASR represents polarization resistance of a fuel cell and depends on the materials. Ohmic region is the typical fuel cell operation area and based on this region, ASR can be estimate and use as a performance indicator for the cell.

### 3.1.2 ASR – analysis

The figures below demonstrate that the charge transport results in a voltage loss. This loss is called an ohmic loss and is a part of a net fuel cell performance indicator.

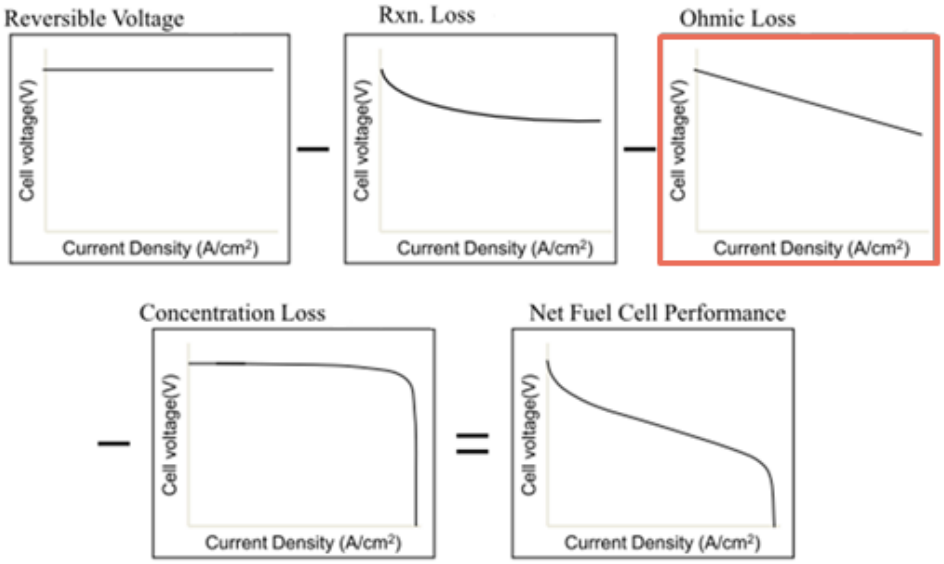


*Fig. 3-2 Ohmic loss as a part of the net fuel cell performance. (O'Hayre, R et al. 2006)*

The total ohmic resistance of a fuel cell is a combination of resistances coming from different components of the device. From the figure below, where it is shown that fuel cell resistance is divided into resistance coming from interconnect, anode electrode components, cathode electrode components, and electrolyte. It is connected with the fact that the current flows serially trough all the components of the fuel cell.

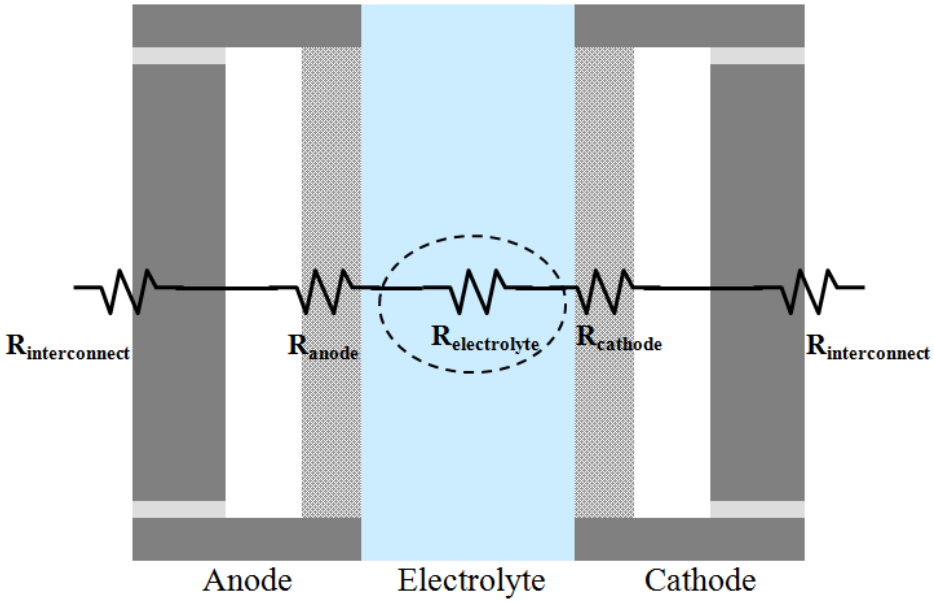


*Fig. 3-3 Total fuel cell resistance as a sum of resistances coming from interconnect, anode, cathode, electrolyte, and cathode.(ResFC601 Ryan O'Hayre)*

The ohmic resistance corresponds to both the electronic ($R_{elec}$) and the ionic ($R_{ionic}$) contributions of the fuel cell resistance what gives

$$\eta_{ohm} = iR_{ohmic} = i(R_{elec} + R_{ionic})$$

where:

$\eta_{ohmic}$ – ohmic loss [V],
i – current [A],
$R_{ohmic}$ – ohmic resistance [Ω],
$R_{elec}$ – electronic resistance [Ω],
$R_{ionic}$ – ionic resistance [Ω].

It is extremely difficult to distinguish all the various sources of resistance loss. To illustrate, the ionic charge transport (represented by $R_{ionic}$) is more difficult than electronic charge transport (represented by $R_{elec}$). It also means that $R_{ionic}$ dominates over $R_{elec}$ - where ion conductivity ($\sigma_{ion}$) and is significantly smaller than metal conductivity ($\sigma_{metal}$). The ohmic resistance corresponds only to ionic resistivity.

In practice, the fuel cells are compared on a per-unit-area basis using the current density instead of the current. As a result, the resistance of the fuel cells is expressed as area-normalized fuel cell resistance when ohmic losses of fuel cell are discussed. Area-normalized fuel cell resistance or in short, area-specific resistance (ASR) is expressed in unit of Ω*cm$^2$. According to that, ohmic losses can be calculated from the current density and $ASR_{ohmic}$,

$$\eta_{ohm} = iR_{ionic} = \frac{i}{A} * AR_{ionic} = j * AR_{ionic} = j * ASR_{ohmic}$$

where $ASR_{ohmic}$ is the ASR of the fuel cell. Therefore, ASR is calculated from ohmic resistance and area of fuel cell – what is shown below:

$$ASR = R_{FC} * A_{FC}$$

Referring to Ohm´s law

$$i = \frac{V}{R}$$

and the fact that resistance of fuel ($R_{FC}$) cell can be expressed as

$$R_{FC} = \frac{L}{A_{FC} * \sigma}$$

where:

L – thickens of fuel cell [cm],
A – area of fuel cell [cm$^2$],
σ - conductivity of fuel cell [Ω/cm],

the ASR can be presented as follow:

$$ASR = A_{FC} * \left(\frac{L}{A_{FC} * \sigma}\right) = \frac{L}{\sigma} = \left[\frac{m}{(\Omega m)^{-1}}\right] = [\Omega m^2]$$

ASR as a part of ohmic loss, is a performance parameter. In practice, the voltage drop connected with an ohmic loss is not desirable and can be minimized by decreasing ASR. To minimize this effect, two ways can be applied. Referring to the equation above, it can be noticed that ASR scales with the thickness of fuel cells. So then, decrease in thickness of an

electrolyte (where charge of ions occurs), results in smaller ASR (and thus better performance of the cell). Moreover, increase in the cell conductivity results in smaller ASR.

To decrease thickness of an electrolyte, anode or cathode supported fuel cell are manufactured.

In the case of conductivity, the issue is more complicated. The conductivity of a fuel cell tells how well material accommodates to move flow of charge. Equation used to express the conductivity of the cell is as follow,

$$\sigma = (nF)cu = \left[\frac{S}{cm}\right] \; or \; \left[\frac{\Omega}{cm}\right]$$

where:

n – number of carriers available to move,

F – Faraday constants [C/mol],

σ - conductivity of fuel cell [S/cm],

c – concentration of carriers (numbers of carriers available to move) [mol/cm$^2$],

u – mobility of carriers (how easy they can move) [cm$^2$/V*s].

Where u is defined as follow:

$$u = \frac{nFD}{RT}$$

where:

D – diffusivity [cm$^2$/s],

R – universal gas constant [J/mol*K],

T – temperature [K],

, and where D is expressed as

$$D = D_0 e^{-\Delta G/(RT)}$$

where:

$D_0$ – constant reflecting the attempt frequency of the hopping process (cm$^2$/s),

$\Delta G_{act}$– activation barier for the difusion process (J/mol),

R – gas constant (J/mol*K).

The complete expression for conductivity combines carrier concentration and carrier mobility can be described as follow

$$\sigma = \left(\frac{(nF)^2 D_0 e^{-\Delta G_{act}/RT}}{RT}\right) * c$$

From the equations above, it can be noticed that in most crystals (ceramic electrolytes), σ is a function of temperature which depends on both, the carrier concentration and the mobility of carriers. However, when using literature data for total fuel cell resistance and area specific resistance, it can be found that there are different than presented above definitions. For example, according to *Fuel Cell Handbook7*, total fuel cell resistance includes electronic, ionic, and contact resistance

$$R = R_{electonic} + R_{ionic} + R_{contact}$$

where $R_{contact}$ corresponds to the contact region between the electrodes and the interconnect. It is also provided that the ASR is a function of the cell design, material choice, manufacturing technique, and operating conditions.

Another formula is provided by *Singhal, SC & Kendall, K.* The authors defined ASR as:

$$ASR(i,t) = \frac{E_{mf} - U}{i}$$

where:

$E_{mf}$ – electromotive force with the inlet fuel and air [V],
U – cell voltage [V],
i – current density [$A/cm^2$].

Next, they divided ASR into ohmic resistance ($R_s$), and electrode polarisation resistance ($R_p$). According to above formula, the ohmic resistance comes from geometric factors such as:

- thickness of the cell components (mainly electrolyte),
- detailed geometry of the contact between current collectors and electrodes,
- geometry between electrodes and electrolyte,
- and also constriction of the current collectors may be important.

And where, the electrode polarisation resistance depends on different contributions from the various rate-limiting steps. Thus, the authors divided ASR into five terms

$$ASR = R_{elyt} + R_{connect} + R_{p,elchem} + R_{p,diff} + R_{p,conver}$$

where:

$R_{elyt}$ – electrolyte resistance calculated from the measured specific conductivity and the thickness [Ω],

$R_{connect} = R_s - R_{elyt}$ – resistance due to non-optimised contact and current collection [Ω],

$R_{p,elchem}$ – electrode polarisation originating from all the limiting chemical and electrochemical processes on the electrode surfaces, in the bulk electrode material and on the electrolyte/electrode interfaces [Ω],

$R_{p,diff}$ – contribution from the gas phase diffusion [Ω],

$R_{p,conver}$ – contribution due to gas conversion, i.e. fuel oxidation and oxygen reduction [Ω].

In addition, as highlighted by the authors, this division of ASR is based on what is possible to measure and calculate reliably, rather than on any physical or electrochemical basis.

*Gemmen, R.S. et al,* also discussed ASR as a performance parameter. They give improved ASR definition, in terms of

$$ASR(i,t) = \frac{E_0(t) - V(i,t)}{i}$$

or,

$$ASR(i,t) = \frac{R_i i + \eta_{aa} + \eta_{ac} + \eta_{ca} + \eta_{cc}}{i}$$

where:

$E_0$ – open circuit voltage (OCV),
V – cell voltage [V],
i – average cell current density [A/cm$^2$],
t – time [s],
$R_i$ – total resistivity of all cell components [Ω],
$\eta_{aa}$ – activation overpotentials for the anode [V],
$\eta_{ac}$ – activation overpotentials for the cathode [V],
$\eta_{ca}$ – concentration overpotentials for the anode [V],
$\eta_{cc}$ – concentration overpotentials for the cathode [V].

This definition can be helpful if focus is in the performance of the cell materials (e.g., modifications in electrode structure). However, if the interest is in the total cell performance (cell material + seal technology), then the reference potential should be the Nernst voltage:

$$ASR(i,t) = \frac{E_N(t) - V(i,t)}{i}$$

or,

$$ASR(i,t) = \frac{\eta_L + R_i i + \eta_{aa} + \eta_{ac} + \eta_{ca} + \eta_{cc}}{i}$$

where:

$E_N$ – ideal Nernst potential [V],
$\eta_L$ - loss due to reactant leakage [V],

This formula includes the loss effect due to reactant leakage. However, as highlighted by the authors - both presented definitions remove loss effects due to variable reactant mixture supply (inherent in any experiment). Presented definitions fully account for all cell losses in an integral sense. It also offers a way to minimize some of the sources of experimental noise. Furthermore, these equations depend on time, and, therefore, they can be also used to evaluate degradation for the cell/stack.

The examples of ASR definition provided above prove that fuel cell science is extremely difficult and the current knowledge is not fully discovered (completed) in this field.

### 3.1.3 ASR – calculations

For the purposes of the present work, the ASR is calculated as is shown in chapter 3.3.1. However, it should be noted, that the definition of ASR does not define the interval (delta) and thus it should be calculated. There are three methods of calculation ASR:

- as the delta of the current step – the value was then calculated for each point (except the first one) of the polarization curve,
    - the result of this, is a new curve defined on the same axis of polarization (see report A);

- ASR at 0,8 V – is determined from the slope of the best fitting line over the measurement data within and including the interval 0,75 – 0,85 V
    - the calculations were made as follow:

$$ASR\ at\ 0{,}8V = \frac{V_{0,85} - V_{0,75}}{j_{0,75} - j_{0,85}}$$

- the subscribes 0,75 and 0,85 indicate the values closer to voltages 0,75 and 0,85, respectively;

- ASR at 0,7 V – the same formula applied as above, but in the neighborhood of 0,75 and 0,65 voltages:

$$ASR\ at\ 0{,}7V = \frac{V_{0,75} - V_{0,65}}{j_{0,65} - j_{0,75}}$$

This work is based on experimental data and preceded in accordance with the FCTESTNET standards (discussed in the following chapters) - which also recommends the same method for ASR calculations.

The use of polarization curve, and more strictly use of ohmic region of polarization curve (where j-V curve is the most linear function) demonstrate the easiest, and as the same time the most accurate way to define the ASR.

## 3.2 Open Circuit Voltage – OCV

The open circuit voltage from the point of thermodynamic is the Nernst potential

$$E = E^0 - \frac{RT}{nF} ln \frac{\prod a_{products}^{\nu_i}}{\prod a_{reactants}^{\nu_i}}$$

where:

$E^0$ – standard-state reversible voltage (V),
R – universal gas constant (J/mol*K),
T – temperature (K),
n – number of electrons transferred in the reaction,
F – Faraday constant (C/mol),
$\prod a_{products}^{\nu_i}$ – products partial pressure,
$\prod a_{reactants}^{\nu_i}$ – reactants partial pressure,

and where $E^0$ is the standard-state reversible voltage expressed as:

$$E^0 = -\frac{\Delta \hat{g}_{rxn}^0}{nF}$$

whereas $\Delta \hat{g}_{rxn}^0$ is the standard-state free-energy change for the reaction expressed in J/mol.

The Nernst equation accounts for the variation of the reversible cell voltage with pressure and chemical activity (chemical composition, concentration, ect.) but does not fully accounts the temperature effects. To fully accounts this temperature effect, in the Nernst equation the standard-state reversible voltage ($E^0$) should be replaced by the temperature-dependent thermodynamic voltage at reference concentration ($E_T$):

$$E_T = E^0 + \frac{\Delta \hat{s}}{nF}(T - T_0)$$

where $\Delta \hat{s}$ is the entropy change of the species participating in the reaction, expressed in (J/mol*K). Thus, the Nernst equation can be given as

$$E = E_T - \frac{RT}{nF} ln \frac{\prod a_{products}^{\nu_i}}{\prod a_{reactants}^{\nu_i}}$$

In summary, presented above equations give ability to predict how the voltage of a fuel cell varies with arbitrary sets of temperature, pressure, and chemical composition.

At the present work, the OCV of the tested cell is presented as a result of the measurements; detected by the acquisition system when the electrical load is not applied to the cell. Then, there is no electrical current flow in a circuit and the maximum value of the cell voltage is reached.

## 3.3 Current density – j

Current density is defined as current (i) per unit of area (A),

$$j = \frac{i}{A}$$

and it is expressed in unit of amperes per square centimeter ($A/cm^2$). This parameter is more fundamental than current because it allows the reactivity of different surface to be compared on a per-unit area basic.

Current density together with voltage is the basic parameter used during test elaboration presented in a present work. Polarization curve (or j-V curve), current density and voltage are the fundamental values for other parameters computation (e.g. ASR).

## 3.4 Power density – P

Power density is defined as the amount of power - the product of current and voltage in unit of watts

$$P = iV = [W]$$

per unit of area (A),

$$P = \frac{iV}{A} = \frac{P}{A}$$

and it is expressed in unit of watts per square centimeter ($A/cm^2$). The function of power density together with j-V curve can be used for presenting the cell performances. In some cases, power density is used for comparison between different fuel cells as well as for presenting the performances of the cells influenced by different circumstances (e.g. temperature or fuel composition).

## 3.5 Efficiency – ε

Efficiency is the indicator which is very import for any energy conversion device. In general, efficiency can be defined as the ratio between the output and input of an energy conversion device. In the case of the fuel cell efficiency, it is calculated as

$$\varepsilon = \frac{P}{\dot{n}_{H2in} LHV_{H2}}$$

where:

P – fuel cell output power (W),

$\dot{n}_{H2,in}$ – molar flow of hydrogen entering the cell (mol/s),

$LHV_{H2}$ – lower heating value of hydrogen.

In the thesis, there are also investigated externally reformed fuels (chapter 2.4) which contain four main gasses: $H_2$, CO, $CO_2$ and $N_2$. In this kind of gas mixture, not only hydrogen but also carbon monoxide, is a fuel for SOFC. Therefore, the equation presented above has to be modified as follow

$$\varepsilon = \frac{\mathrm{P}}{(\dot{\mathrm{n}}_{\mathrm{H2in}} \mathrm{LHV}_{\mathrm{H2}}) + (\dot{\mathrm{n}}_{\mathrm{COin}} \mathrm{LHV}_{\mathrm{CO}})}$$

where $\dot{n}_{COin}$ represents molar flow of carbon monoxide entering the cell (mol/s) and $LHV_{CO}$ stands for lower heating value of hydrogen.

## 3.6 Stoichiometric factor – λ

The stoichiometric air (oxidant) factor (λ) expresses the ratio of the oxidant provided to the cell and the stoichiometric amount of the oxidant, which comes from amount of hydrogen provided to the reaction presented below

$$H_2 + \frac{1}{2} O_2 \rightarrow H_2O$$

In general the λ can be expressed as follow

$$\lambda = \frac{Q_{O_{2in}}}{Q_{O_{2stoic.}}}$$

but in practice and also in this work, when an oxidant air is used, thus the λ can be written as

$$\lambda = \frac{Q_{Air_{in}}}{Q_{Air_{stoic.}}}$$

From the chemical equation, it is known that the $Q_{Air_{stoic}}$ directly depends on the amount of hydrogen provided to the reaction. The hydrogen flow (which is presented as $Q_{H_{2in}}$ ) is known as input parameter (measured value), and thus it can be used instead of $Q_{Air_{stoic}}$. However, the number of hydrogen moles needed per each oxygen mole in the reaction and (2) the partial pressure of oxygen in air (21%), should be taken into account. Thus, the equation above can be written as follow

$$\lambda = \frac{Q_{Air_{in}} * 0{,}21}{\frac{Q_{H_{2in}}}{2}}$$

In the case of using fuel mixtures which contain carbon monoxide, λ can be expressed as

$$\lambda = \frac{Q_{Air_{in}} * 0{,}21}{\frac{Q_{H_{2in}} + Q_{CO_{in}}}{2}}$$

where $Q_{CO_{in}}$ is volumetric flow of carbon monoxide entering the cell (mol/s).

In the present project, this parameter is used for identification of air condition at which fuel cell is operating - determines the amount of air feeding the cathode.

## 3.7 Dilution factor – $D_f$

The dilution factor ($D_{N2}$) is directly concerted to the anode input gas mixture. It is useful when the fuel gas is diluted in an inert gas (such as nitrogen). The effect of such operation is controlled by the dilution factor. The $D_f$ is defined as the ratio between the flow of nitrogen (diluent) and the flow of hydrogen

$$D_f = \frac{Q_{N_{2in}}}{Q_{N_{2in}} + Q_{H_{2in}}}$$

where the denominator represents total flow of the fuel mixture gas (nitrogen and hydrogen, respectively).

In the thesis, there are also investigated externally reformed fuels (chapter 2.4) which contain four main gasses: $H_2$, CO, $CO_2$ and $N_2$. In the case when fuel contains $H_2$, CO, $CO_2$ and $N_2$ gases, the carbon dioxide and nitrogen are treated as diluents and because of that presented above equation is upgraded

$$D_f = \frac{Q_{N_{2in}} + Q_{CO_{2in}}}{Q_{CO_{2in}} + Q_{N_{2in}} + Q_{H_{2in}} + Q_{CO_{in}}}$$

where $Q_{CO_{2in}}$represents volumetric flow of carbon dioxide entering the cell (mol/s).

The $D_{N_2}$ is used for identification of the fuel condition at which fuel cell is operated - express quality of the fuel.

## 3.8 Fuel utilization coefficient – $U_f$

The fuel utilization coefficient ($U_f$) is an indicator which can be defined as a ratio of the spent/consumed fuel flow and the inlet fuel flow. In the thesis, ungraded definition of the $U_f$ is used in terms of

$$U_f = \frac{\dot{n}_{H_{2cons.}}}{\dot{n}_{H_{2in}}}$$

It is also known that $\dot{n}_{H_{2cons.}}$(molar flow of consumed hydrogen) is directly connected with current produced during reaction. Thus, the $U_f$ can be presented as

$$U_f = \frac{i}{nF\dot{n}_{H2in}}$$

where F is the Faraday constant, and where n reflects the number of electrons transferred in the reaction. Presented above definition relates to the ratio of the delivered current to the stoichiometric current equivalent to the fuel flow rate.

In the case of experimental activity, the reformed fuel mixtures contain also CO - which is a fuel for SOFC. In this case, $U_f$ factor can be presented as follow.

$$U_f = \frac{i}{nF(\dot{n}_{H2in} + \dot{n}_{COin})}$$

$U_f$ indicator is used for identification of the fuel share which is consumed in an operated fuel cell.

## 3.9 Coefficient of oxygen utilization – $U_{ox}$

The oxidant utilization coefficient ($U_{ox}$) is based on the oxygen that reacts at the cathode electrode $\dot{n}_{O_{2cons.}}$ and the oxygen which is provided to the reaction $\dot{n}_{O_{2in}}$, can be presented as follow

$$U_{ox} = \frac{Q_{O_{2cons.}}}{Q_{O_{2in}}}$$

However, as it was discussed above instead of oxygen, air is used. Moreover, the amount of oxygen consumed in the reaction can be expressed as the amount of hydrogen provided to the reaction – which is directly connected with current which is produced. Thus, the equation above can be presented in upgraded form,

$$U_{ox} = \frac{\frac{Q_{H_{2cons.}}}{2}}{Q_{Air_{in}} * 0{,}21} = \frac{\frac{i}{nF * 2}}{Q_{Airin} * 0{,}21}$$

Discussed indicator expresses the ratio of the delivered current to the stoichiometric current equivalent to the oxidant (in this case - air). As a result, this parameter is similar to the previous one, with this difference that it is used for expressing the share of oxidant which is used in the reaction.

# 4 TEST SYSTEM

Present project is based on experimental data obtained from the tests which were performed in the Fuel Cell Laboratory, located at the University of Perugia in Italy. In this chapter, the system used for testing is presented. General scheme of the system is shown in figure below.

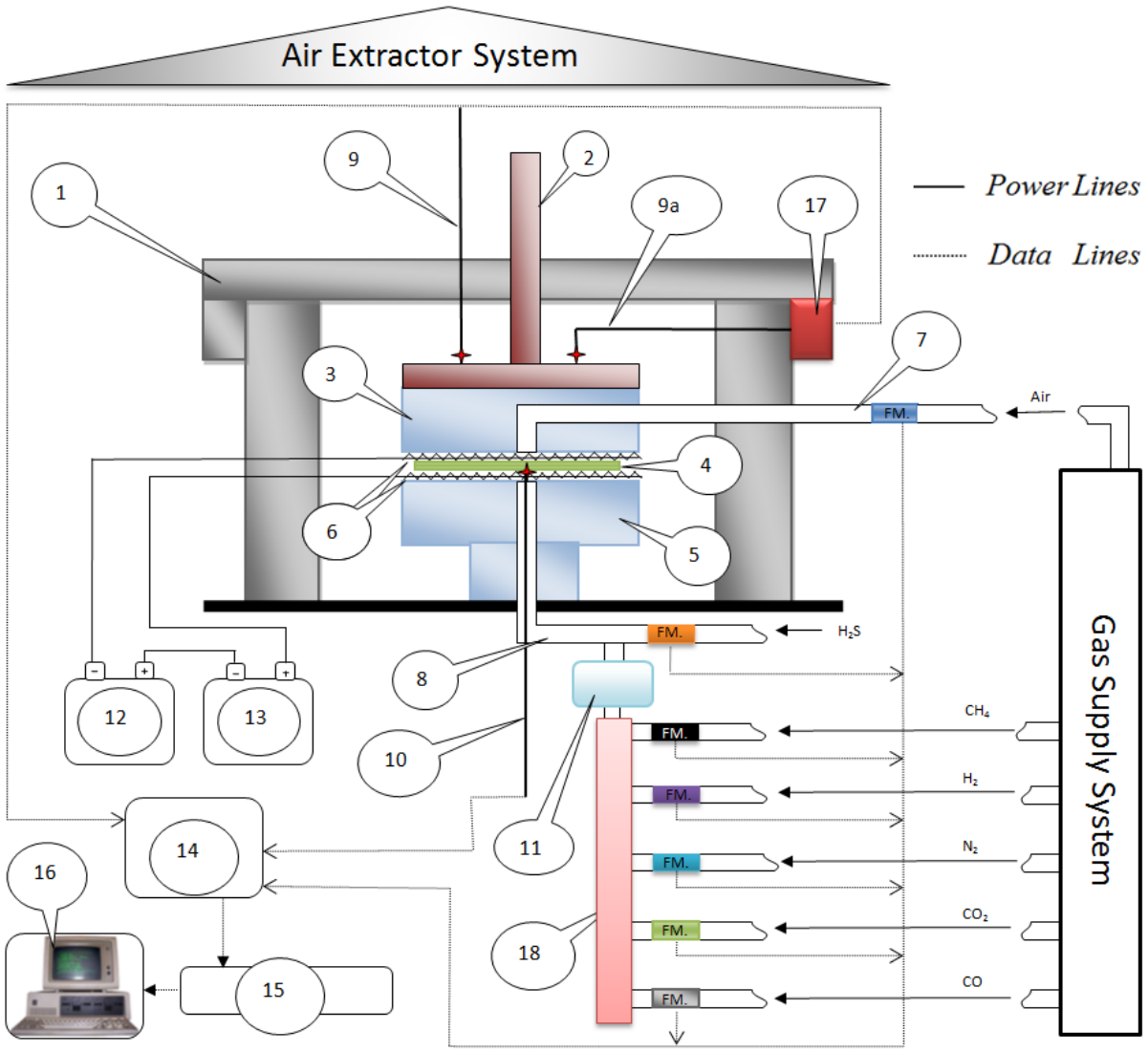


1. *Oven*
2. *Press*
3. *Cathode Manifold*
4. *Solid Oxide Fuel Cell*
5. *Anode Manifold*
6. *Current Collectors*
7. *Cathode feeding pipe*
8. *Anode feeding pipe*
9. *Anode Thermocouple*

9a. *2nd Anode Thermocouple*

10. *Cathode Thermocouple*
11. *Humidifier*
12. *Power supply*
13. *Electronic Load*
14. *Data Acquisition Unit*
15. *Switch*
16. *PC*
17. *Temperature Regulator*
18. *Manifold*

**FM. – Flow Meter*

*Fig. 4-1 Scheme of the test system*

Presented system contains air extractor system, which is safety system in the case of any leakages. The system above is supplied (according to test procedure) with hydrogen, nitrogen, carbon monoxide, carbon dioxide, methane, hydrogen sulfide and air. The system that stores (at pressure from around 200 – 3 bar) and provides gas mix flow is equipped with two pressure reducers (first one to 10 bar and second to 3 bar) and is named gas supply system.

The test rig is equipped in:

- separate for each gas flow meter - which as well as the electronic load is set in real time by the PC,
- the PC central unit with control software – set test inputs and also collect and save the data,
- manifold and humidifier – for $H_2$, $N_2$, $CO_2$ and CO gasses,
- press,
- cell is compressed from above by pneumatic Press working via cathode manifold, ceramic disc and cylinder,
- oven,
- anode and cathode feeding pipes and manifolds;
- three thermocouples – two of them are connected with data acquisition unit and PC, and third thermocouple is connected to temperature regulator and next to data acquisition unit and PC,
- current collectors – which are connected with data acquisition unit,
- tested single SOFC.

The main components of the system like manifolds, thermocouples, oven, press, humidifier, power supply unit, electronic load, data acquisition unit and thermoregulator are described in appendix B. Moreover additional information about the test system construction like the data acquisition system (DAS) and the pipes and instruments design system (P&ID) are also included in the same appendix. This division is used for better understanding how the system works.

To complete description of the main components of the test system, the cells used for testing and the flow meters are presented in following chapters.

## 4.1 Tested single SOFC

The single solid oxide fuel cell used for testing is manufactured by supplier B. The company is specialized in developing and manufacturing high temperature electroceramic devices based on solid oxide fuel cell technology. Investigated cells, in the thesis, has the active area of 50cm$^2$ and is shown in figure below.

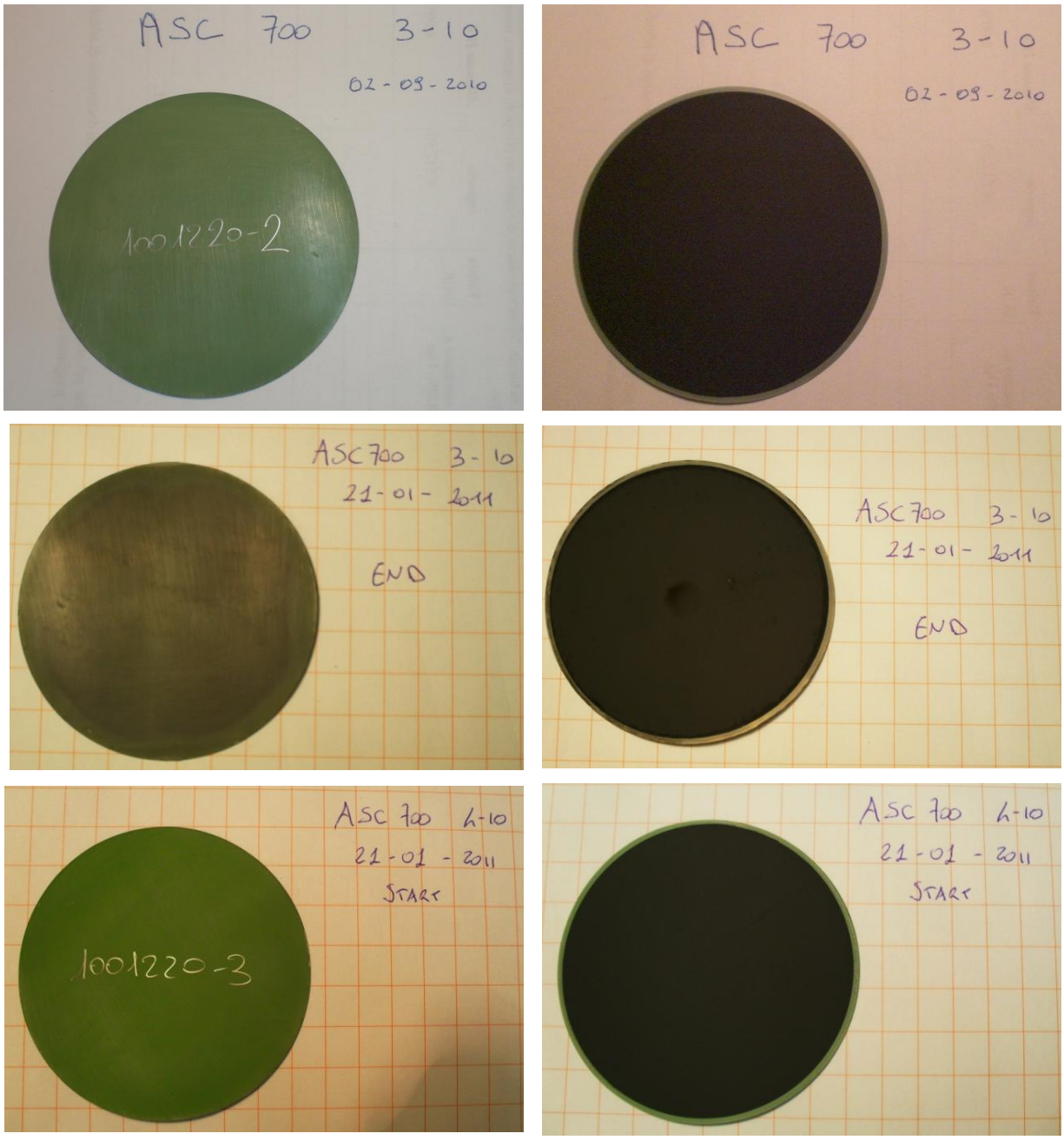


*Fig. 4-2 Tested SOFCs – anode from the left side and cathode from the right side*

As can be noticed from the photos above the anode side of the cell after testing is darker than the anode side of the new cells – before testing. This is because after the start-up procedure the cell anode side is reduced.

Full specification of the cell is provided by the supplier and can be found in the appendix A.

To collect current during the test activity the Ni-Cu mesh and wires are used. While for voltage measurements the platinum wires/sensors are applied (figure below).

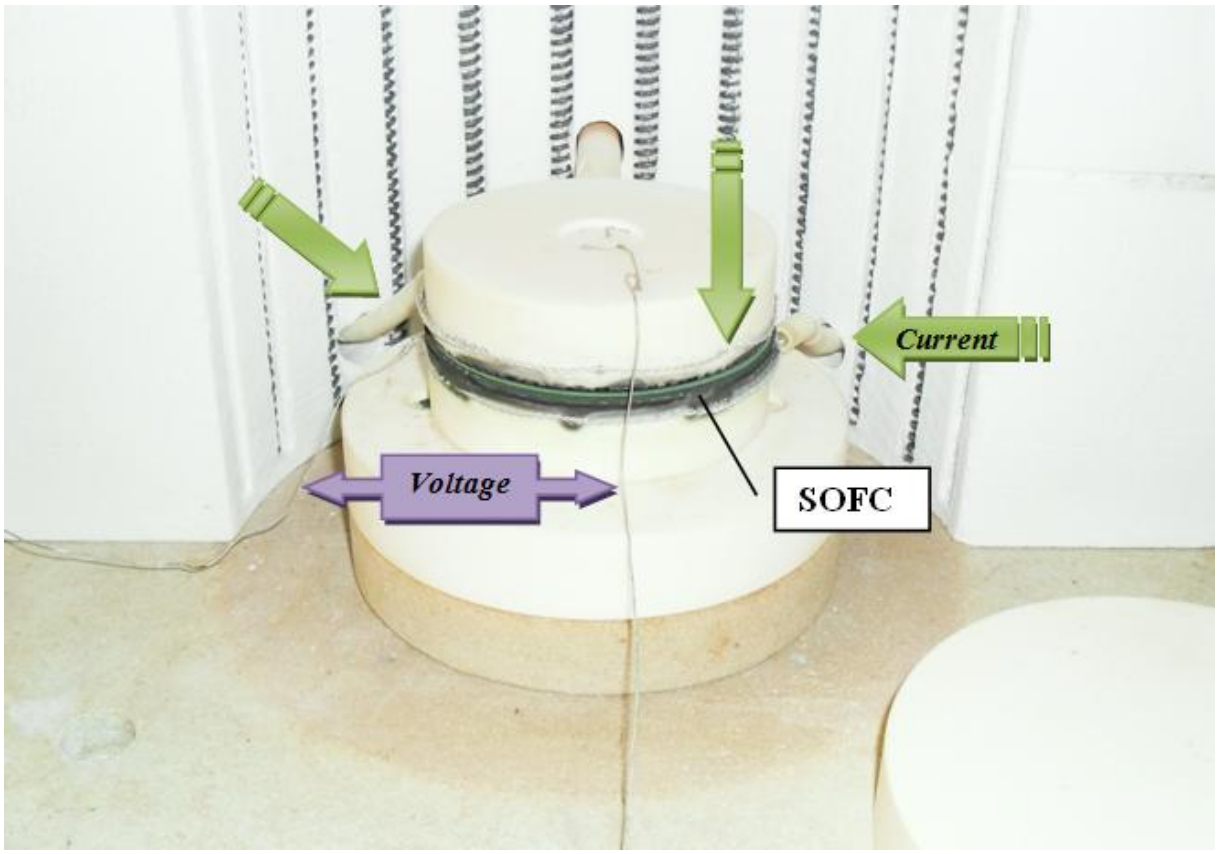


*Fig. 4-3 Assembled SOFC*

Metals for current collectors and voltage measurements are characterized by excellent electrical conductivity properties.

# 5 TEST PROCEDURE

In present work as a reference for experimental testing, the test procedures are used. The cell performance tests are performed in accordance with Safety & Quality Assurance standards ($FCTES^{QA}$). Fuel Cell Testing and Standardisation Network (FCTESTNET) are output of the $FCTES^{QA}$. FCTESTNET are the internationally agreed harmonized test procedures applicable to fuel cells, stacks, and systems. For the purpose of the present work, the procedure for evaluation of performance and endurance at light-duty operating conditions of SOFC single cells operated with hydrogen is used. *SOFC light-duty cell performance and endurance with hydrogen* full procedure is attached in appendix C.

In accordance with *SOFC light-duty cell performance and endurance with hydrogen,* the start-up and shut-down procedure is performed in line with the procedures recommended by the cell supplier (supplier B). These standards are confidential and cannot be used for any publication without manufacturer authorization. However, it should be mentioned that these procedures are necessarily for proper functioning of the cell. The start-up procedure is performed immediately after placement of the tested single cell in the testing device. The main aim of start-up procedure is to bring the cell under working conditions. During the start-up, the temperature is increased in accordance with the procedure in order to avoid thermal stress to the materials before reaching the steady state. The phase activation is very sensitive and important because it determines the functional characteristics and the operational lifetime of the cell. At the end of the start-up, the cell is in steady state and is ready to be subjected to the testing. The purpose of the first start-up, is to reduce the anode.

After the start-up procedure, the stabilization phase takes place. The stabilization and the cell polarisation curves are performed in accordance with the *Test Module M01-SOFC cell polarisation curve* presented in appendix D.

# 6 TEST ACTIVITY

Before starting the tests the test plan was developed. The purpose of this plan is to develop strategy that is used to verify the performance of the tested fuel cell. What more, the test plan is developed in order to check and prove the effect of the chosen parameters on the cell performance. In this work the effect of listed below parameters on the cell performance is discussed.

- T - temperature (°C);
- $\lambda$ - stoichiometric factor;
- $D_f$ - dilution factor;
- $q_{H2}$ – hydrogen specific volumetric flow rate (Nl/h/cm$^2$);

The cell performances are evaluated based on the ASR and the OCV parameters. What more, the plans have to ensured that the system design meets all test demands and other requirements (e.g. gas flow range, temperature). The plans are divided into a several parts in order to check the influence of each of investigated parameters and the fuel type on the cell performance.

First plan is focused on the fuel cell testing in accordance with FCTESTNET procedures (presented in appendix C and appendix D). In this plan are taken into account some modifications concerning specific volumetric fuel flow (q) rates recommended by the FC laboratory (where all presented activities take place) and by the supplier A. Moreover, the influence of the temperature is also included into the plan. Because this plan is based on FCTESTNET procedures and the gasses flow conditions (which are used as reference procedures for the experimental activity), this part of the plan is named reference state plan and in the following chapters reference state results, reference state analysis ect.

The next test plan is based on modifications in the reference state test plan. The changes in this plan concern the $\lambda$ and the $D_f$ indicators. The aim of these modifications is to verify what the influence have these parameters on the performance of the tested cell. Because this test plan is based on FCTESTNET modified procedures, this plan in the following parts of the thesis is named reference state variation plan, reference state variation test results ect.

The third test plan is similar in basic assumptions to the previous one – it is focused on the $\lambda$ and the $D_f$ indicators. However in this case there is also applied to the test conditions a change in the specific volumetric fuel and oxidant flow rates (reduced by half). Because of that this test plan is named new reference state variation test plan.

The next three plans are focused on the evaluating cell performances fueled by syngas, biogas and pyrolysis reformed gas. Parameters for these plans are based on reference state parameters and are detailed discussed in the following chapters. These plans are named from the name of the fuels they are focused on – so then syngas, biogas and pyrogas plans, conditions ect.

All described above plans and the way of its elaborating is presented in appendix E, while the results are presented in the following chapters.

## 6.1 Reference state test analysis and conclusions

The study presented in this part of the thesis is realized on values produced from report A and/or B, depending on the repartitions of the test. There are at least few reasons why these reference tests are prepared. Fist of them is to evaluate the performance of the cell fueled by the different amounts of gases ($q_{H2}$, $D_{N2}$, $\lambda$) in accordance to the three chosen procedures (FCTESTNET, FClab and supplier A). Moreover, each of the standard procedure is examined at three different temperatures (700, 750 and 800 °C). All of that is applied to check the influence of the parameters on the performances.

The second reason is to compare obtained in a present study results with results prepared:

- by other researchers (FCTESTNET),
- in the past, in the laboratory where the experiments took place (FClab),
- and finally, to compare the test results with the results provided by the cell supplier (supplier B).

Is should be also noted that the all points from the list above are not directly connected with the present thesis.

Two parameters in form of ASR and OCV are chosen to evaluate performance of the tested cell. Part of the study is also to evaluate these parameters (and in particular the focus is on the ASR) as are good parameters for the performance assessment. Moreover, the ASR and OCV parameters are used to evaluate the cell degradation level during its operation – discussed in the following chapters.

From the final reference report C (presented below), the main conclusions are:

- the performance parameters are sensitive on different operating temperatures,
    - increase in operating temperature results in decreasing both ASR and OCV values;

- the performance parameters are sensitive on different gas flows conditions,
    - OCV directly depends on $q_{H2}$ and $\lambda$ parameters;
    - ASR depends on $q_{H2}$ and $\lambda$ parameters;
        - when the difference in the $q_{H2}$ and $\lambda$ parameters is significant then this relation is directly proportional to the ASR values (i.e. FClab and supplier A standards);
        - in the case when the amounts of the input gases are only slightly different form each other (FClab and FCTESTNET standards) relation pointed above is not applied anymore;

| | | STANDARD | | | | | |
|---|---|---|---|---|---|---|---|
| | | *FClab* | | *FCtestNET* | | *Supplier A* | |
| $T_{range}$ | °C | 804,5 | 704,5 | 805,4 | 704,8 | 803,8 | 703,6 |
| $T_{step}$ | °C | 50,02 | | 50,30 | | 50,13 | |
| λ | - | 0,98 | | 1,00 | | 1,05 | |
| $D_{N2}$ | - | 0,00 | | 0,00 | | 0,00 | |
| $q_{H2}$ | Nl/hcm$^2$ | 0,97 | | 1,05 | | 0,48 | |

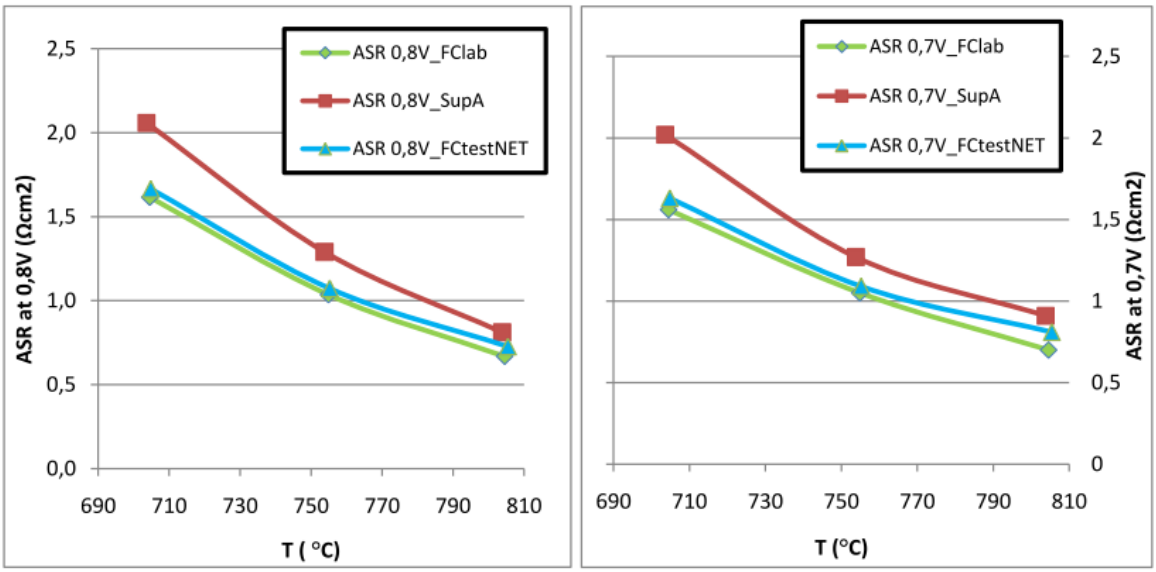


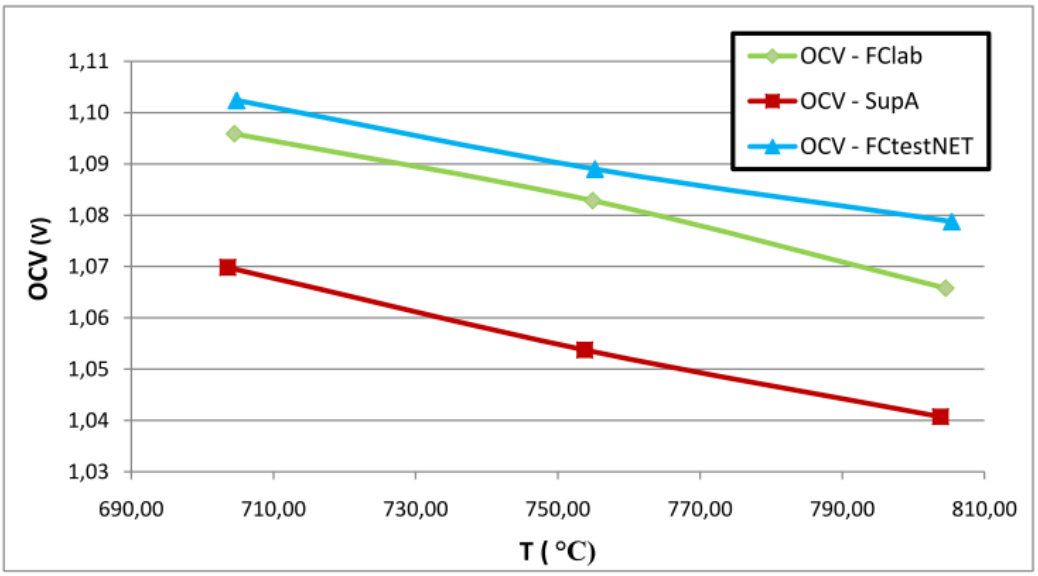


*Fig. 6-1 Reference state test report C*

The last conclusion may be due to the values of λ factor and the test bench construction - where no sealing or coating is used. When air flow (λ) is bigger in the number then hydrogen on the anode side (and more strictly on the edge of the cell) is less concentrated or even some oxygen could react in this cell area. The picture below where SOFC after testing is shown

proves that theory. On the edge of the cell there is dark green ring which most likely is caused by oxidized nickel from the anode electrode. Oxidation effect could occur during test activities where the performances of the cell were investigated with very small hydrogen volumetric flow and constant flow of air (high in comparison with the fuel amount) – which in this case could react on the anode side.

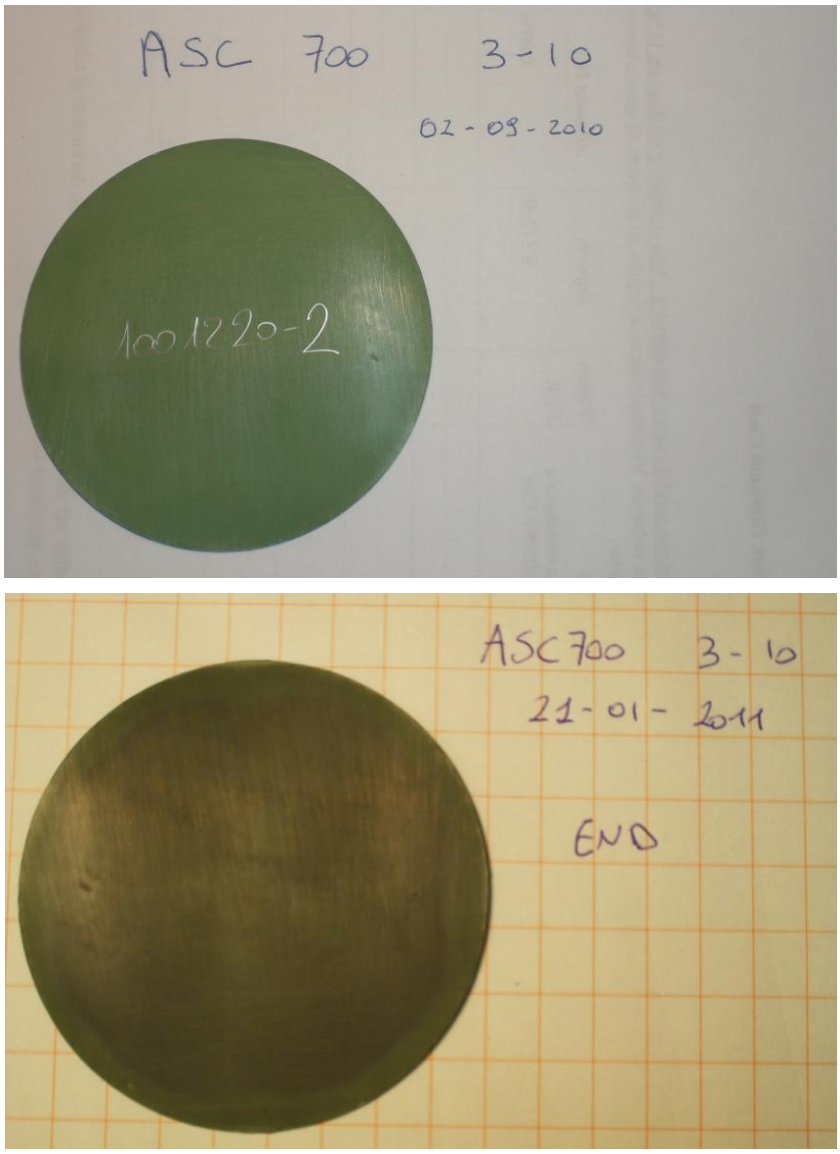


*Fig. 6-2 Tested SOFC before (top) and after (down) the test activity.*

Based on these observations, the next conclusions were made and applied to the following experimental activates:

- temperature of 750 °C was chosen as a reference,
- FCTESTNET procedures were chosen as a reference.

The last presented proposal is chosen not because the cell performances are the best at these conditions – in fact, they are not. It is chosen because it is international standard - what gives a possibility for further analysis/comparison with other results performed according to the same procedures.

## 6.2 Reference state variation test analysis and conclusions

The reference state test results (Example of reference state test report A - appendix E) in comparison with presented in the figure named ´Example of reference state λ variation test report A´ (Reference state variation test elaborating - appendix F) values for decreased volumetric air flow (expressed by λ) results in:

- significant increase in ASR and Uox values,
- decrease in Pmax, jmax, j at 0,8 V and j at 0,7 V, efficiency and also Uf values.

The applied modifications do not have any noticeable influence on the OCV and $U_{ox}$.

The same reference state test results in comparison with the figure named ´Example of reference state $D_f$ variation test report A´ (appendix - F) where change in $D_f$ is applied, effects in:

- increase in ASR values,
- slightly increase in OCV,
- decrease in the Pmax, jmax, j at 0,8 V and j at 0,7 V.

Moreover, any noticeable changes in $U_{ox}$, $U_f$ and efficiency are observed.

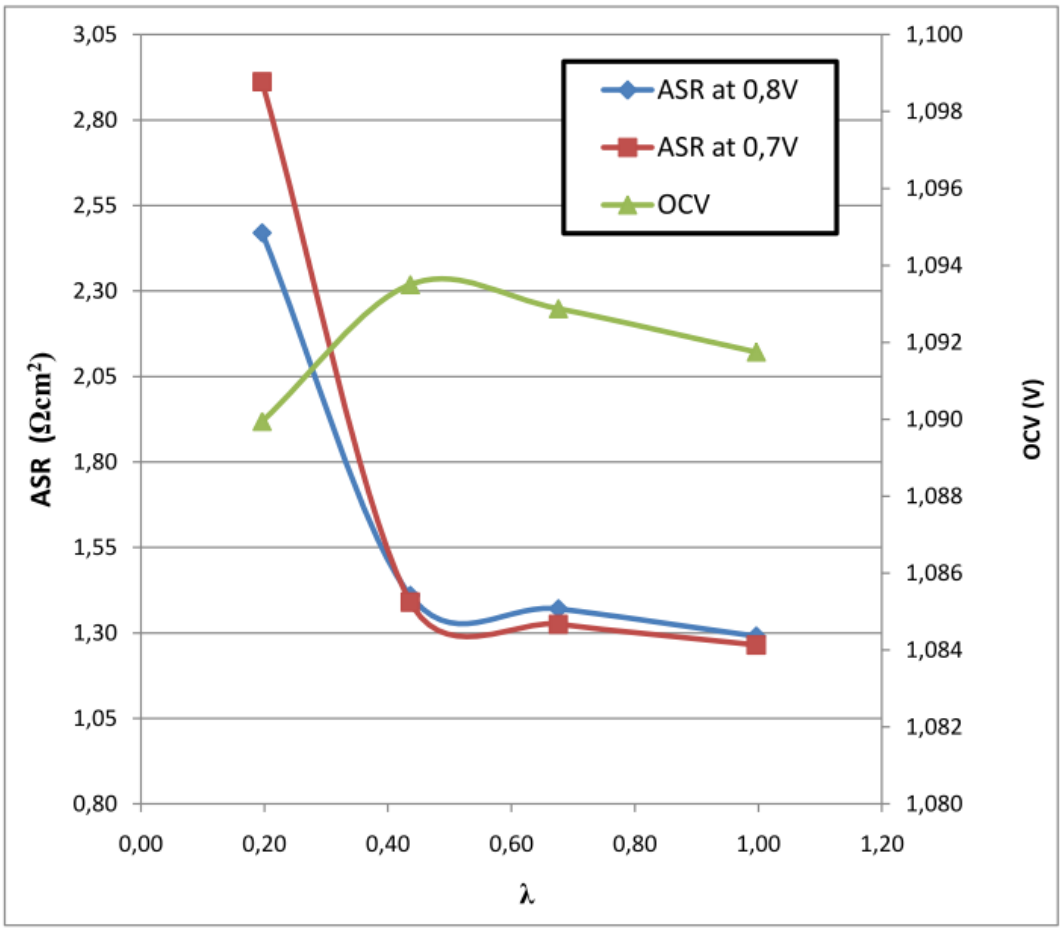


*Fig. 6-3 Reference state λ variation test report C*

According to figure 6-3, it can be noticed that decreasing in λ value results in:

- negligible changes in ASR value in λ range from 1 to around 0,4,
- significant increasing of ARS value in λ range from around 0,4 to 0,2,
- negligible changes in OCV value in λ range from 1 to around 0,4,
- small decrease in OCV value (0,33%) in λ range from around 0,4 to 0,2,

In summary, ASR is sensitive and OCV demonstrate small or negligible changes on λ variations.

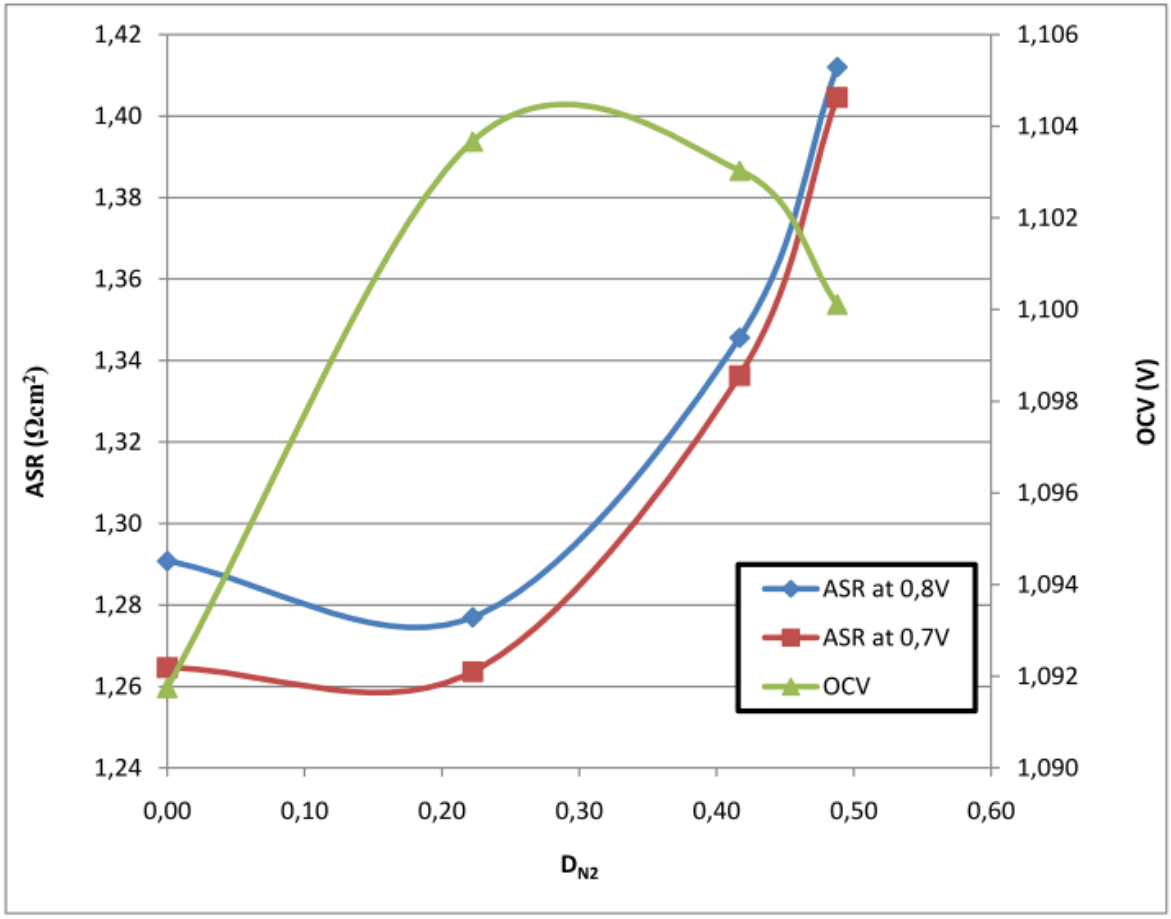


*Fig. 6-4 Reference state DN2 variation test report C*

The main conclusions from report C (figure 6-4) where change in $D_{N2}$ is applied are:

- the performance parameters are sensitive on the investigated parameter,
    - decrease in ASR value for $D_{N2}$ range from 0 to around 0,2,
    - increase in ASR value for $D_{N2}$ range from around 0,2 to 0,5,
    - increase in OCV value for $D_{N2}$ range from 0 to around 0,2,
    - decrease in OCV value for $D_{N2}$ range from around 0,2 to 0,5,

OCV as well as ASR are both, respectively positively and negatively dependent on $D_{N2}$ variations.

## 6.3 New reference state variation test analysis and conclusions

The new reference state variation test results (Example of new reference state variation test report A – appendix G) in comparison with reference state test result (Example of reference state test report A - appendix E), effects in:

- significant increase in ASR values,
- decrease in OCV, $P_{max}$, $j_{max}$, j at 0,8 V and j at 0,7 V, efficiency, $U_{ox}$ and also $U_f$ values.

It proves that the reduced gas flows have negative effects on all parameters presented in the reports.

Next analysis concern the same report (Example of new reference state variation test report A – appendix G) and test results where decreasing in λ value is applied (Example of new reference state λ variation test report A – appendix G). The main conclusions from this comparison are:

- significant increase in ASR and $U_{ox}$ values ,
- significant decrease in $P_{max}$, $j_{max}$, j at 0,8 V and j at 0,7 V,
- not significant decrease in efficiency,

and $U_f$ values do not show any changes.

Next comparison is developed for the same report (Example of new reference state variation test report A – appendix G) and results for report where increasing in $D_f$ is applied (Example of new reference state $D_f$ variation test report A – appendix G). The main conclusions from this analysis are:

- significant increase in ASR values,
- increase in OCV,
- decrease in the Pmax, jmax, j at 0,8 V and j at 0,7 V,

Moreover, any noticeable changes in $U_{ox}$, $U_f$ and efficiency are observed.

The analysis of new reference state variation test results (Example of new reference state variation test report A – appendix G) with λ and $D_f$ effect on the cell performances (Example of new reference state λ and $D_f$ variation test report A – appendix G), shows:

- significant increase in ASR, OCV and Uox values,
- significant decrease in Pmax, jmax, j at 0,8 V and j at 0,7 V,

Moreover, any significant changes in $U_f$ and efficiency are noted.

In the summary, the presented above analysis shows the cumulative effect of λ and $D_f$ factors on the all test output parameters. Moreover, this effect is so significant that a lot of results are not reliable (or even impossible to calculate). Because of that the further analysis of the cumulative effect of λ and $D_f$ factors in not performed.

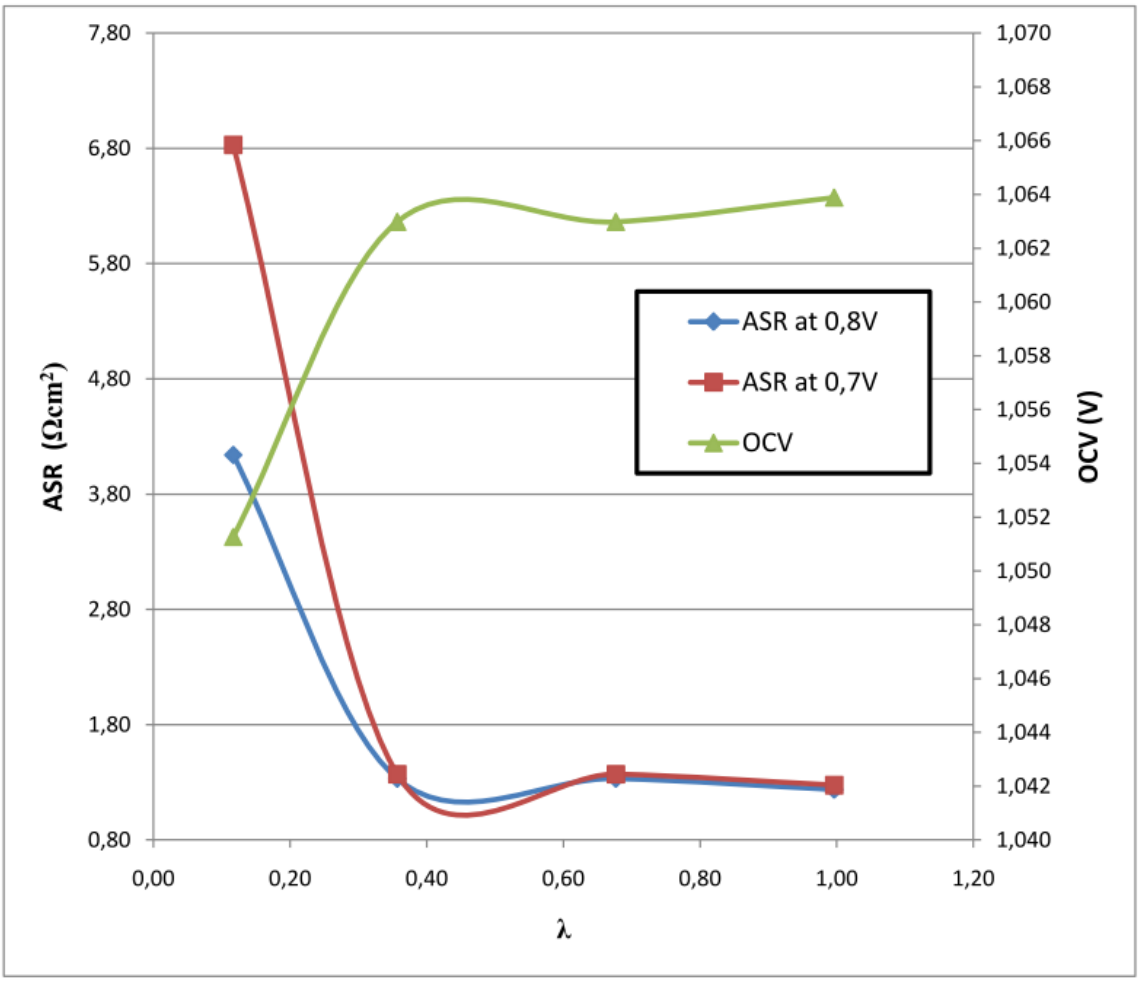


*Fig. 6-5 New reference state λ variation test report C*

From analysis figure 6-5 where the relation between λ value and the performance parameters is shown, the main conclusions are:

- negligible changes in ASR value in λ range from 1 to around 0,4,
- significant increasing of ARS value in λ range from around 0,4 to 0,12,
- negligible changes in OCV value in λ range from 1 to around 0,4,
- decrease in OCV value (around 1,2%) in λ range from around 0,4 to 0,12,

To conclude, ASR is sensitive and OCV demonstrates small or negligible changes on λ variations.

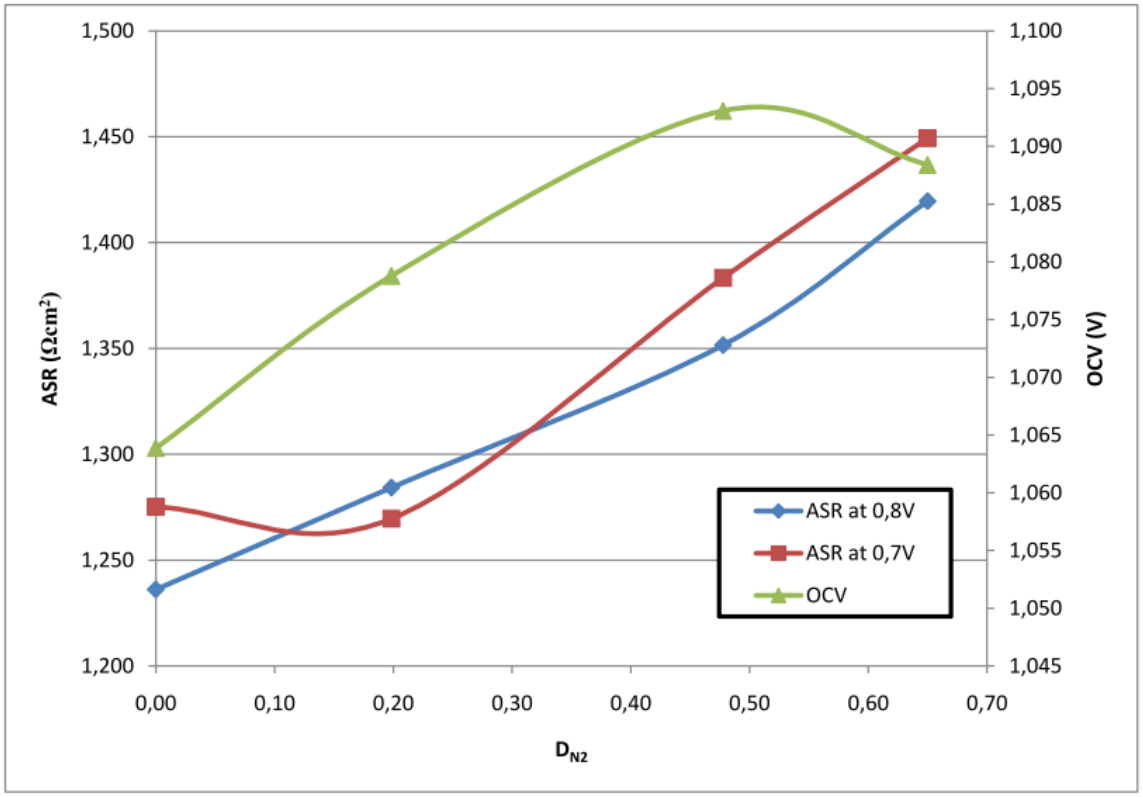


*Fig. 6-6 New reference state DN2 variation test report C*

The same comparison is developed for the report presented in figure 6-6 where change in $D_f$ is applied:

- the performance parameters are sensitive on the investigated parameter,
    - increase in ASR value for the whole $D_{N2}$ range,
    - increase in OCV value for $D_{N2}$ range from 0 to around 0,5,
    - decrease in OCV value for $D_{N2}$ range from around 0,5 to 0,65,

The analysis shows that ASR negatively depends on $D_f$ variations while OCV positively and negatively depends on the same factor.

# 7 λ EFECT ON THE CELL PERFORMANCE

This chapter focuses only on λ indicator and its effect on the cell performance. On the charts presented in this chapter, there are data from the previous chapters and new ones; theoretically, calculated or obtained from further test activity.

Theoretical OCV values as a function of λ (presented in the chart below) are calculated according to the formula presented at the very end of chapter 3.2. The calculations are prepared by using M.S. excel and are included in appendix H.

In fact, after test activity presented so far in the study, the tested cell is replaced by the new one in the same type and all other parameters (presented at the bottom of the figure 4-2). The aim of test activity with replaced SOFC single cell is to verify previously obtained test results. Based on reference state test activity the new test plan is developed. This plan is upgraded based on observations and experience from the last test activity. First, the assumption applied in this plan (named reference state test plan II) is to prepare more steps in λ for the same reference standards (FCTESTNET) while the second one is to prepare one instead of three polarizations for each step. This assumption arises from the fact that all prepared so far tests (for the same input gas conditions) are characterized by very high precision - what can be noted from the reports B.

Reference state test plan II and its results obtained from this plan are presented in the tables below. Moreover, all prepared reports A for these polarizations are included in appendix E.

*Table 7-1 Reference state test plan II*

| **ASC 700 4-10** | | | **Cell acive area** | | | | | | **50** | | **cm²** | |
|---|---|---|---|---|---|---|---|---|---|---|---|---|
| **Name** | | **T** | **$H_2$** | | **$N_2$** | | **Air** | | **$H_2$** | **$D_{N2}$** | **λ** | **T** |
| **std.** | **Pn** | **°C** | **Nl/h** | **Nl/h cm²** | **Nl/h** | **Nl/h cm²** | **Nl/h** | **Nl/h cm²** | **Nl/h cm²** | **-** | **-** | **°C** |
| ref. | **a1** | 750 | 52,5 | 1,05 | 0 | 0 | 124,5 | 2,49 | 1,05 | 0,0 | 1,0 | 750 |
| **λ variations** | **a2** | 750 | 52,5 | 1,05 | 0 | 0 | 112 | 2,24 | 1,05 | 0,0 | 0,9 | 750 |
| | **a3** | 750 | 52,5 | 1,05 | 0 | 0 | 100 | 2,00 | 1,05 | 0,0 | 0,8 | 750 |
| | **a4** | 750 | 52,5 | 1,05 | 0 | 0 | 88 | 1,76 | 1,05 | 0,0 | 0,7 | 750 |
| | **a5** | 750 | 52,5 | 1,05 | 0 | 0 | 75 | 1,50 | 1,05 | 0,0 | 0,6 | 750 |
| | **a6** | 750 | 52,5 | 1,05 | 0 | 0 | 62 | 1,24 | 1,05 | 0,0 | 0,5 | 750 |
| | **a7** | 750 | 52,5 | 1,05 | 0 | 0 | 50 | 1,00 | 1,05 | 0,0 | 0,4 | 750 |
| | **a8** | 750 | 52,5 | 1,05 | 0 | 0 | 38 | 0,76 | 1,05 | 0,0 | 0,3 | 750 |
| | **a9** | 750 | 52,5 | 1,05 | 0 | 0 | 25 | 0,50 | 1,05 | 0,0 | 0,2 | 750 |
| | | | anode | | | | cathode | | anode | | cathode | |

*Table 7-2 List of reference state II test variation reports A*

| ASC700 4-10 | | | | Cell active area: | | | | | | 50 $cm^2$ | | |
|---|---|---|---|---|---|---|---|---|---|---|---|---|
| **Name** | | **Date** | **T** | **$H_2$** | **$N_2$** | **Air** | **$H_2O$** | **λ** | **$D_{N2}$** | **ASR at 0,8 V** | **ASR at 0,7 V** | **OCV** |
| **std.** | **Pn** | **-** | **°C** | **Nl/hcm²** | **Nl/hcm²** | **Nl/hcm²** | **Nl/h** | **-** | **-** | **Ωcm²** | **Ωcm²** | **V** |
| **ref.** | **a1** | 27.1.2011 | 747,05 | 1,05 | 0,00 | 2,49 | RT | 1,0 | 0,0 | 0,95 | 0,94 | 1,095 |
| **λ variations** | **a2** | 27.1.2011 | 746,51 | 1,05 | 0,0 | 2,24 | RT | 0,9 | 0,0 | 0,91 | 0,9 | 1,094 |
| | **a3** | 27.1.2011 | 746,44 | 1,05 | 0,0 | 2,0 | RT | 0,8 | 0,0 | 0,91 | 0,91 | 1,095 |
| | **a4** | 27.1.2011 | 746,16 | 1,05 | 0,0 | 1,76 | RT | 0,7 | 0,0 | 0,91 | 0,90 | 1,095 |
| | **a5** | 27.1.2011 | 746,01 | 1,05 | 0,0 | 1,50 | RT | 0,6 | 0,0 | 0,92 | 0,91 | 1,096 |
| | **a6** | 27.1.2011 | 745,85 | 1,05 | 0,0 | 1,24 | RT | 0,5 | 0,0 | 0,94 | 0,95 | 1,097 |
| | **a7** | 27.1.2011 | 745,80 | 1,05 | 0,0 | 1,0 | RT | 0,4 | 0,0 | 1,00 | 1,08 | 1,097 |
| | **a8** | 27.1.2011 | 746,02 | 1,05 | 0,0 | 0,76 | RT | 0,3 | 0,0 | 1,16 | 1,5 | 1,096 |
| | **a9** | 27.1.2011 | 746,24 | 1,05 | 0,0 | 0,50 | RT | 0,2 | 0,0 | 1,94 | 2,93 | 1,090 |

Based on all presented so far data, the chart below is prepared where OCV as a function of λ is shown.

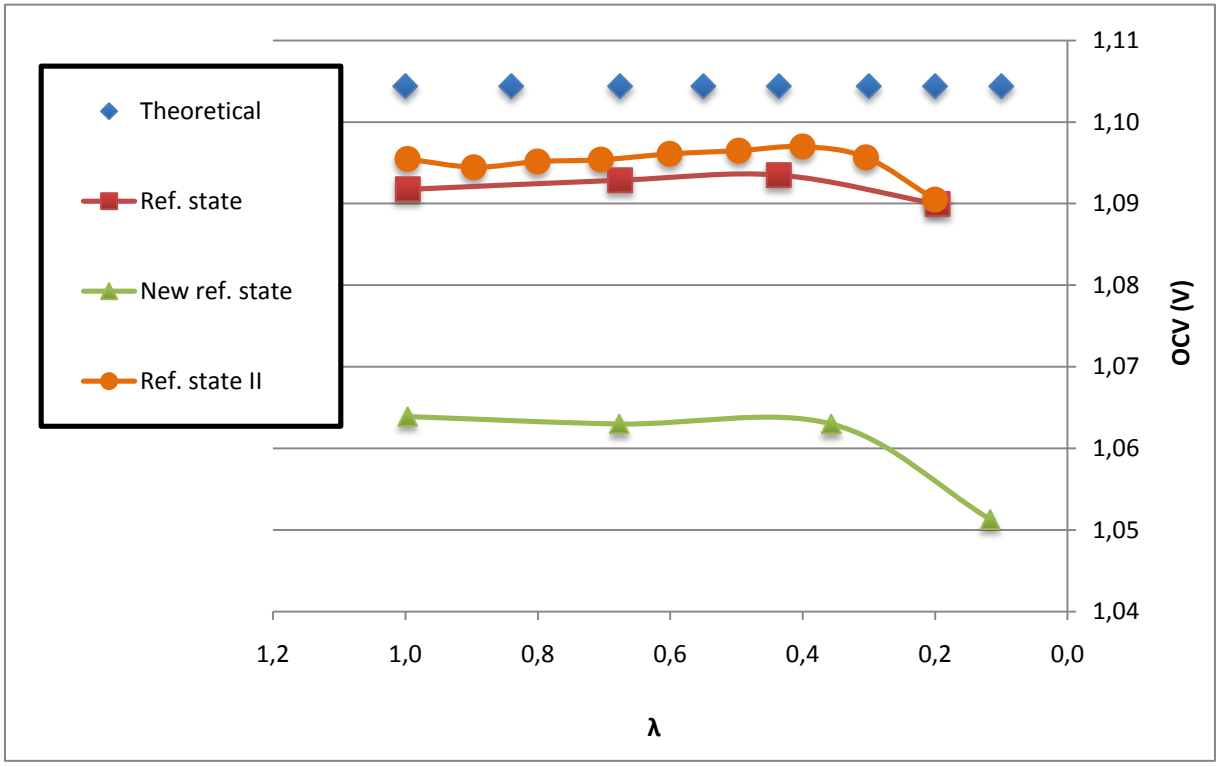


*Fig. 7-1 λ effect on OCV*

Points obtained during the theoretical simulation show that OCV does not depend on the gas quantity - total volumetric flow. The same trend shows the data for all standards in λ range from 1 to around 0,4.

However, insignificantly OCV drop for λ range from around 0,4 to 0,1 can be noticed. This effect can be caused by the crossover at very poor air conditions compared to the constant and high at these points fuel flow. To explain this theory the construction of the test bench should be mentioned – no sealing or coating material is used. All these factors could cause hydrogen absence on the edge of the cell cathode side (oxidation/burning) what results in decreasing of the cell active area and as the same time drop in OCV. Concluding, in this case low oxidant flow results in increased fuel oxidation at the cathode side what in turn effects in OCV decrease.

Moreover, experimentally obtained points show reduction in OCV value when the gas quantities are reduced (*Reference state* and *New reference state* results). This can be also caused by crossover effect. When the flows are decreased, the oxidant and fuel can react with each other in a bigger cell edge area - what results in OCV drop.

This effect can be understood by an analogy. Pretend that we have a combustible gas in a pressurized tank with pipeline connected. When we cause ignition of that gas at the end of pipeline, the oxidation reaction (burning) will occur only in this area (at the end of pipeline). However, when we close valve near to the gas tank, the pressure inside the pipeline will fall down and the reaction will occur inside the pipeline. This analogy is not perfect but may help in understanding discussed effect.

The figure presented below shows ASR at 0,8V as a function of λ.

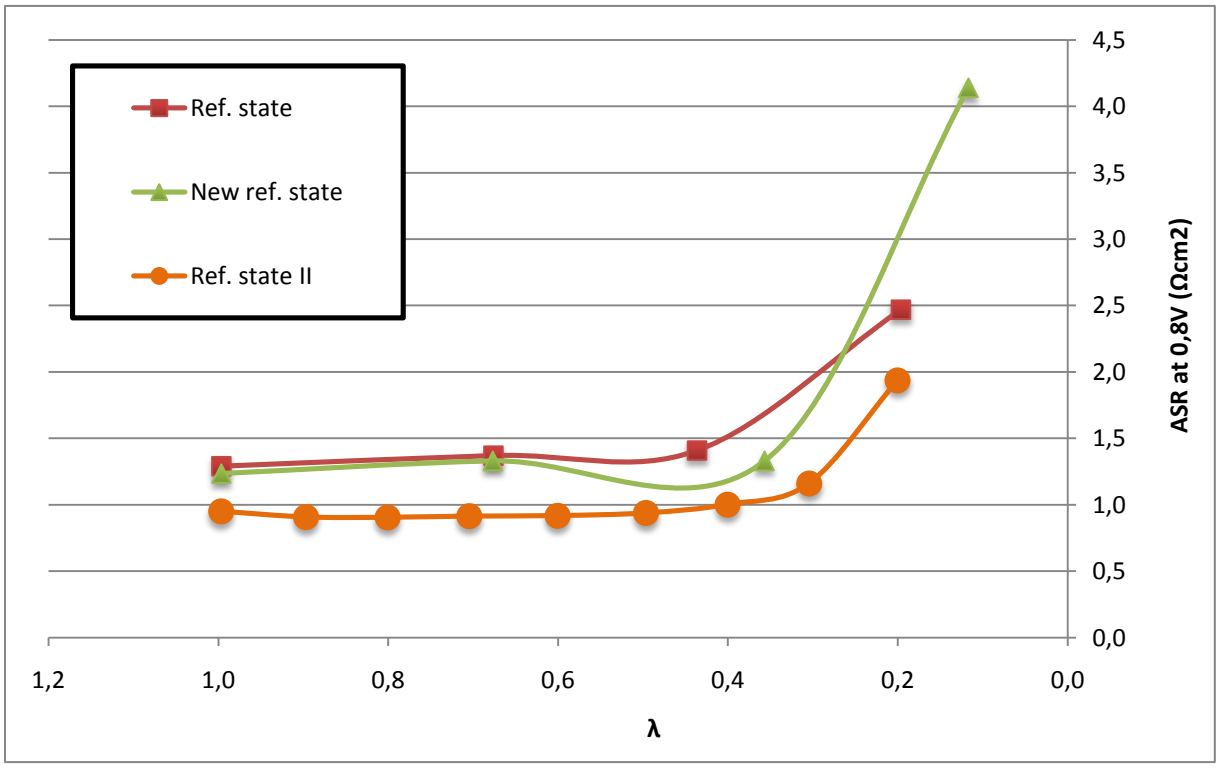


*Fig. 7-2 λ effect on ASR at 0,8V*

From this chart, it can be noticed that the ASR doesn't depend on the air gas quantity - total volumetric flow (*Reference state; Reference state II* and *New reference state*). Moreover, the

points for each standard have the same trend what means that the measurements are highly precise. The reference state II results in the comparison with the reference state and the new reference state results, shows better (lower) ASR value. This effect most likely is caused by the ASC700 3-10 cell degradation (operation time from 2.IX.2010 to 21.I.2011). Moreover, the trends of the points for each of the standards show that they are the same in order to ASR axis:

- relatively constant values for λ range from 1 to around 0,4 and
- ASR significantly increase for λ range from around 0,4 to 0,1.

Figure below shows the same relation as in the previous figure but with the difference in ASR at 0,7V which is used instead of 0,8V. According to this chart, the conclusions are exactly the same as to the presented above. That also leads to the conclusion that in this area of 0,65V and 0,85V, the performances of the cell are stable and it is good area for such research.

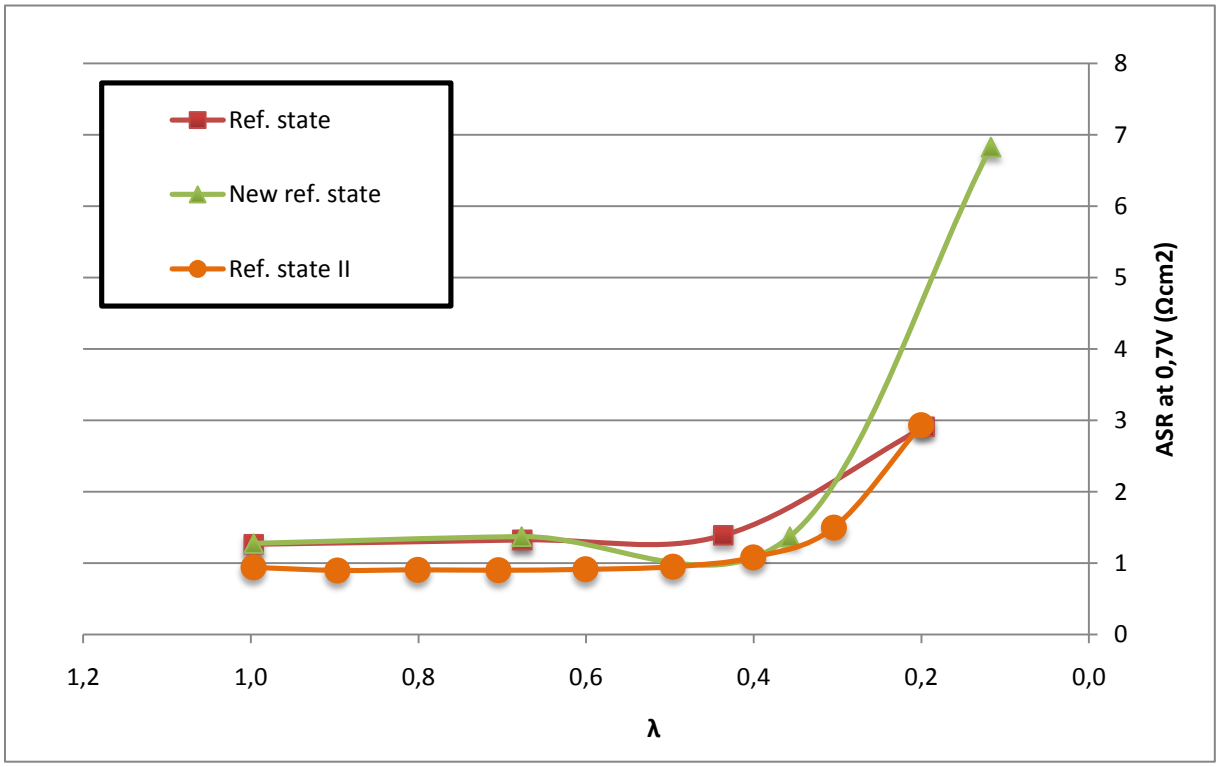


*Fig. 7-3 λ effect on ASR at 0,7V.*

In summary, presented analysis shows that OCV depends on λ factor and the quantity of the input gases. ASR is not sensitive on changes in the input gas flows while it depends on λ variations.

Moreover, the lack of sealing in the test bench construction has significant effect on the investigated performance parameters at low gas flows.

# 8 $D_f$ EFFECT ON THE CELL PERFORMANCE

In this chapter, the influence of $D_f$ factor on the cell performance parameters is discussed. Presented in the study results are used to illustrate how OCV and ASR depend on variations in dilution factor value. This relation is shown in figures below.

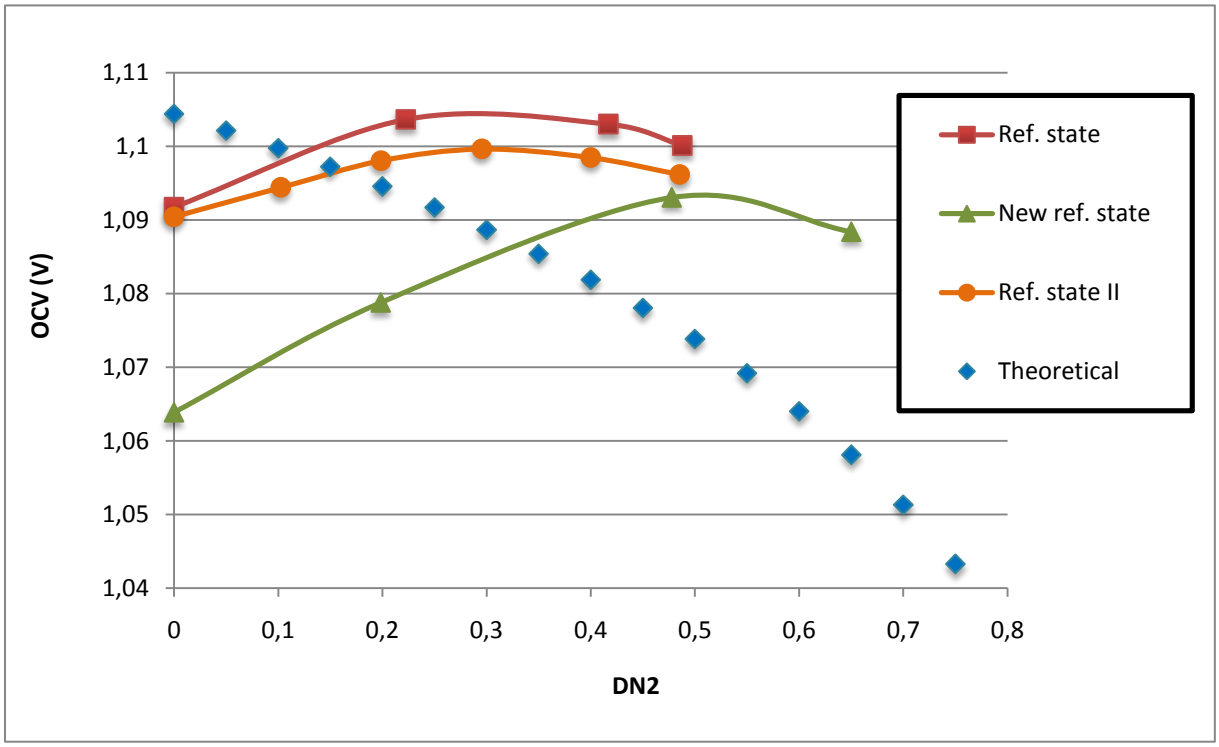


*Fig. 8-1 $D_f$ effect on OCV*

It can be noticed from the chart above that theoretical simulation of this dependence where increase in $D_{N2}$ value is applied, results in OCV drop (computations included in appendix E). This phenomenon is connected with partial pressure of the reactant (Nernst equation – chapter 3-2) which is decreased by adding nitrogen to the fuel.

However, from obtained experimentally data, the conclusion arises that this phenomenon is only in part correct. OCV for reference state and reference state II increases in $D_f$ range from 0 to around 0,3 and decreases in range of around 0,3 to 0,5. For new reference state polarizations (where total input gas flows are reduced by half) can be observed similar trend - in $D_f$ range from 0 to around 0,5 OCV increases and next is decreases in range of around 0,5 to 0,7. This phenomenon also can be explained by the test rig construction and crossover effect. When the total fuel mixture flow increases, the influence of the air on the oxidant reaction side is minimized what at the same time results in increasing the cell active area and OCV value. However, after certain value, the OCV trend becomes similar to the theoretical. At this point, OCV drops due to the lowering reactant partial pressure. Is should be also noted that the difference in OCV variation for the same flow conditions is very small and amounts to around 0,9%.

On the figures below, the influence of $D_f$ factor on ASR at 0,8V and ASR at 0,7V is presented. The relations between investigated indicators are very similar to each other. In both cases, there is significant difference between the points obtained from ASC700 3-10 cell

(reference state and new reference state) and replaced ASC700 4-10 cell (reference state II). That leads to the same as highlighted in the previous chapter conclusion about degradation of the cell during its test activity.

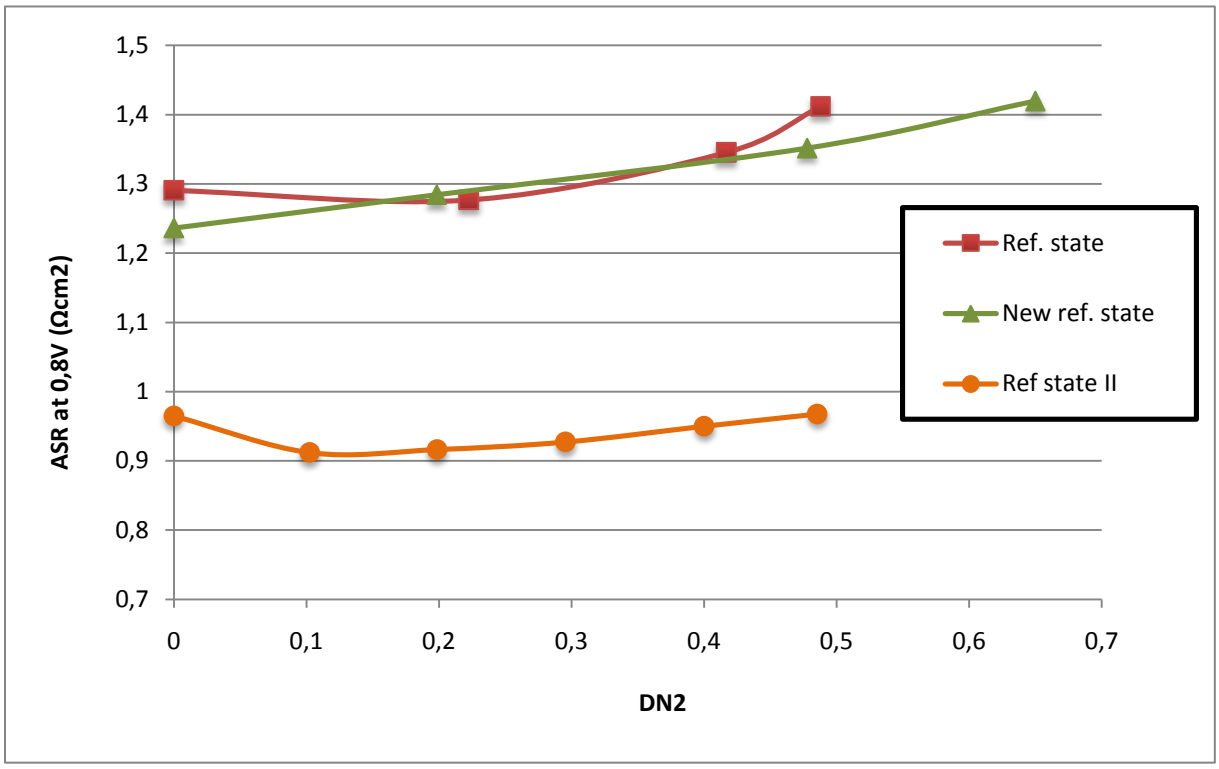


*Fig. 8-2 $D_f$ effect on ASR at 0,8V*

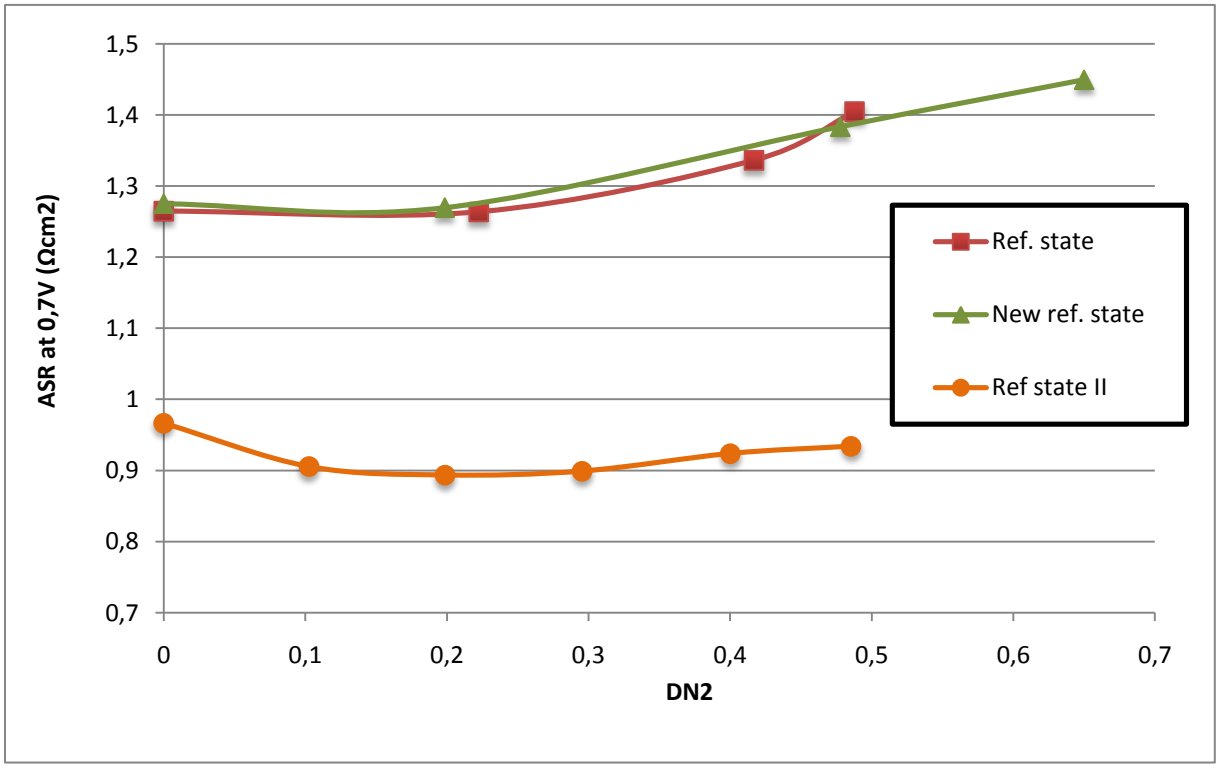


*Fig. 8-3 $D_f$ effect on ASR at 0,7V*

In addition, all results show the same trend what leads to the following conclusions:

- ASR doesn't depend on the total fuel mixture flow (reference state and new reference state),
- small amount of nitrogen in the fuel mixture positively influences on the ASR,
    - to the $D_{N2}$ value of around 0,1 – 0,2;
- highly diluted fuel results in increasing ASR value.
    - $D_{N2}$ range from 0,1 -0,2 to 0,5 -0,7;

The last pointed above conclusion is caused by the lower concentration of reactant at the anode side. The decrease in ASR value by adding small amount of nitrogen to the fuel can be caused by:

- better gas distribution on the cell reacting surface,
- minimize air effect on the edge of the cell (reduction of the crossover effect).

However, this effect does not take place in the case of new reference state tests where the total gas flows are reduced by half. This effect can be explained by reduced air influence on the anode fuel gas. It means that the fuel mixture flow is too small to reduce the oxidant gas influence on the anode side.

In summary, OCV as well as ARS depend on the fuel quality and the total volumetric flows of the input gases have influence only on OCV parameter.

# 9 TESTED CELL DEGRADATION RATE

Based on the selected polarizations presented in the table below, the analysis of the degradation rate of the cells is prepared. For this analysis, there are chosen polarizations prepared according to the same procedure (FCTESTNET). The prepared tests are grouped into four groups.

Group 1 includes four polarizations prepared the same day (29.11.2010) with ASC700 3-10 cell.

Next groups, 2a and 2b contain polarizations prepared at the very beginning and in the middle of tests with λ and $D_{N2}$ variations, respectively. It should be noted that these tests are not used before in the study (one of the additional test activities in the lab.). Moreover, these tests concern the same ASC700 3-10 cell and all of them are prepared on 10.1.2011.

The other groups, 3a and 3b contain polarizations prepared before and after tests with λ and $D_{N2}$ variations, respectively. These tests also concern the same ASC700 3-10 cell and all of them are prepared on 18.1.2010.

The assumption of the analysis is to use test data from the last 4 group which contains three polarizations prepared on 27.1.2011. However, it should be noted that these results comes from new/replaced ASC700 4-10 cell. This assumption makes it possible to show how the investigated ASC700 3-10 cell performance could have been at the beginning of the test activity.

*Table 9-1 List of polarizations for degradation rate analysis*

| Degradation Rate Polarization List | | | | | | | | | | Cell active area: | 50 | $cm^2$ | |
|---|---|---|---|---|---|---|---|---|---|---|---|---|---|
| Name | | Date | T | $H_2$ | $N_2$ | Air | $H_2O$ | λ | $D_{N2}$ | ASR at 0,8 V | ASR at 0,7 V | OCV | Cell |
| n | Pn | - | °C | Nl/hcm$^2$ | Nl/hcm$^2$ | Nl/hcm$^2$ | Nl/h | - | - | Ωcm$^2$ | Ωcm$^2$ | V | - |
| **1** | P10 | 29.11.2010 | 755,3 | 1 | 0 | 2,5 | RT | 1 | 0 | 1,08 | 1,11 | 1,09 | **ASC700 3-10** |
| | P11 | 29.11.2010 | 755,2 | 1 | 0 | 2,5 | RT | 1 | 0 | 1,07 | 1,08 | 1,09 | |
| | P12 | 29.11.2010 | 755,2 | 1 | 0 | 2,5 | RT | 1 | 0 | 1,07 | 1,08 | 1,09 | |
| | P13 | 29.11.2010 | 755,2 | 1 | 0 | 2,5 | RT | 1 | 0 | 1,08 | 1,08 | 1,09 | |
| **2a** | R4 | 10.1.2011 | 746,25 | 1 | 0 | 2,49 | RT | 1 | 0 | 1,25 | 1,26 | 1,09 | |
| **2b** | R8 | 10.1.2011 | 754,33 | 1 | 0 | 2,49 | RT | | 0 | 1,29 | 1,3 | 1,09 | |
| **3a** | p1 | 18.1.2011 | 755,54 | 1 | 0 | 2,5 | RT | 1 | 0 | 1,29 | 1,23 | 1,09 | |
| | p2 | 18.1.2011 | 755,53 | 1 | 0 | 2,5 | RT | 1 | 0 | 1,25 | 1,24 | 1,09 | |
| **3b** | p12 | 18.1.2011 | 755,54 | 1 | 0 | 2,5 | RT | 1 | 0 | 1,34 | 1,32 | 1,09 | |
| | p13 | 18.1.2011 | 755,83 | 1 | 0 | 2,5 | RT | 1 | 0 | 1,29 | 1,27 | 1,09 | |
| **4** | r1 | 27.1.2011 | 752,9 | 1 | 0 | 2,5 | RT | 1 | 0 | 0,9 | 0,9 | 1,1 | **ASC700 4-10** |
| | r2 | 27.1.2011 | 746,0 | 1 | 0 | 2,5 | RT | 1 | 0 | 1,0 | 1,0 | 1,1 | |
| | r3 | 27.1.2011 | 746,1 | 1 | 0 | 2,5 | RT | 1 | 0 | 1,0 | 1,0 | 1,1 | |

**Dedradation Rate Report**

**ASC700 3-10** **Ref. 1 - 2a - 2b - 3a - 3b - 4**

***ASC700 4-10*** ***Ref. 4***

**Cells active area** **50** **$cm^2$**

| Name | Date | T | $H_2$ | $N_2$ | Air | $H_2O$ | λ | $DN_2$ | ASR at 0,8V | ASR at 0,7V | OCV |
|---|---|---|---|---|---|---|---|---|---|---|---|
| - | - | °C | Nl/hcm$^2$ | Nl/hcm$^2$ | Nl/hcm$^2$ | Nl/h | - | - | Ωcm2 | Ωcm2 | V |
| **1** | 29.11.2010 | 755 | 1,05 | 0,0 | 2,5 | RT | 1,0 | 0,0 | 1,07 | 1,09 | 1,09 |
| **2a** | 10.1.2011 | 746 | 1,05 | 0,0 | 2,5 | RT | 1,0 | 0,0 | 1,25 | 1,26 | 1,09 |
| **2b** | 10.1.2011 | 754 | 1,05 | 0,0 | 2,5 | RT | 1,0 | 0,0 | 1,29 | 1,30 | 1,09 |
| **3a** | 18.1.2011 | 756 | 1,05 | 0,0 | 2,5 | RT | 1,0 | 0,0 | 1,27 | 1,23 | 1,09 |
| **3b** | 18.1.2011 | 756 | 1,05 | 0,0 | 2,5 | RT | 1,0 | 0,0 | 1,31 | 1,30 | 1,09 |
| ***4*** | *27.1.2011* | *748* | *1,05* | *0,0* | *2,5* | *RT* | *1,0* | *0,0* | *0,95* | *0,96* | *1,09* |

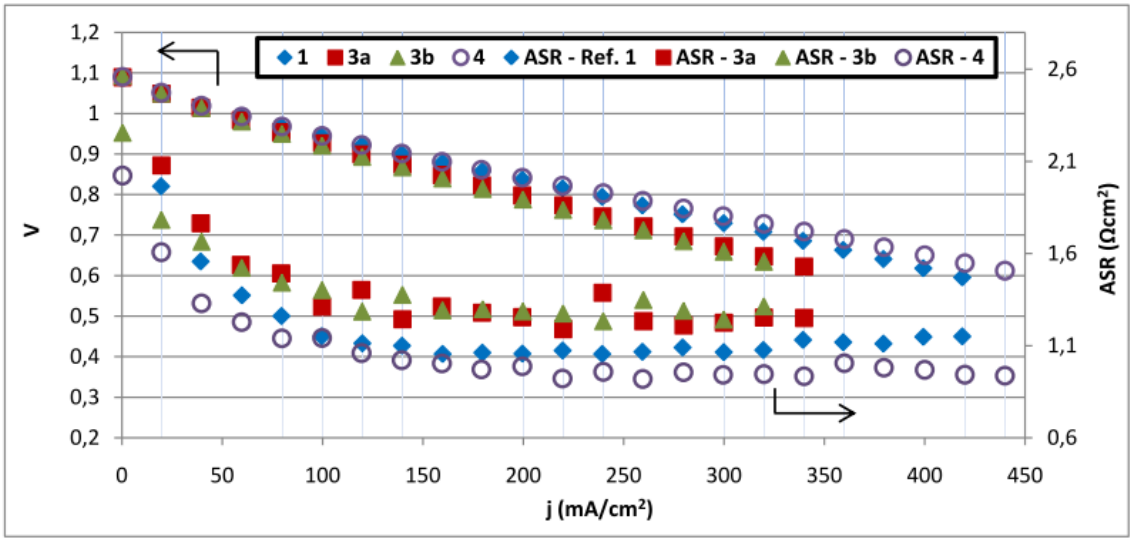


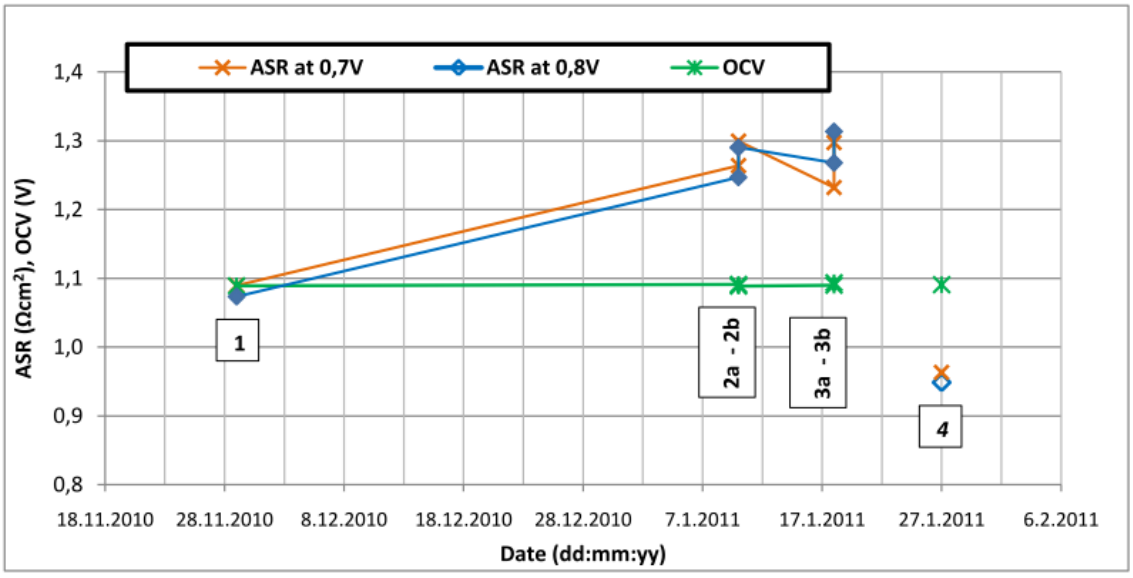


*Fig. 9-1 Degradation rate report*

The average results from grouped polarizations are shown on the top of the report above. From the same report, it can be noticed that during test activity the cell effectives decreased. The drop in the performances is shown on the top chart j vs. V, ASR. The best results which were prepared in six days after the start-up are for new/replaced ASC700 4-10 cell (polarization 4). Moreover, it can be noticed that cell ASC700 3-10 shows decrease in the performances during the test activity – polarizations 1 and 3a which are performed on 29.11.2011 and 18.1.2011, respectively. Also, the tests prepared on the same date (3a and 3b) show decrease in the performances. These polarizations are prepared before and after tests with $\lambda$ and $D_{N2}$ variations, respectively.

The analysis of the performance parameters of the tested cells as a function of time is presented on the bottom of the report. The chart shows the same trend as highlighted above for 3a - 3b and also for 2a - 2b polarizations prepared at the very beginning and in the middle of tests with $\lambda$ and $D_{N2}$ variations, respectively. This fact leads to the conclusion that these test activities are very destructive for the cell performances.

Moreover, on the bottom of the chart, there are presented ASR and OCV values for all polarizations chosen for the analysis. From the plot, it can be noticed that the ASR values increase with time while the OCV values do not change. Polarizations 4 and 3a-3b are prepared in 6 and 138 days after the start-up, respectively. For these measurements, the difference in both, ASR at 0,8V and ASR at 0,7V values reach up to around 35% while the difference in the OCV is 0,091%.

In summary, the same trends of the points presented on j vs. V, ASR and Date vs. ASR, OCV charts lead to the conclusion that ASR is a good parameter for degradation rate assessment while OCV is not.

# 10 BIOGAS, SYNGAS AND PYROGAS TEST ACTIVITY AND CONCLUSIAONS

The gases obtained from the simulation discussed in chapter 2.3 are used as the input for test activity presented in this part. The tables 2-7, 2-8 and 2-9 show the percentage compositions of biogas, syngas and pyrogas after reforming, respectively. However, the exact values of the flows for each of the fuels are calculated based on reference state flows. First, the fuel power ($P_{H2}$) is calculated from the reference state flow ($Q_{H2}$) and LHV of hydrogen. Next, based on:

- the percentage shares of hydrogen and carbon monoxide in the input gas mixture (reactive gases),
- their lower heating values,
- the reference state of $P_{H2}$,

the input power of the fuel for each gas has to be equal to the reference state. The calculations are prepared in excel file and are included in appendix E.

Based on such prepared flows, the test plans for biogas, syngas and pyrogas are developed. In the tables below, there are illustrated test plans for each of the gases.

*Table 10-1 Biogas, syngas and pyrogas test plan*

| **ASC 700 4-10** | | | | | **Cell active area** | | **50** | | **cm²** | | |
|---|---|---|---|---|---|---|---|---|---|---|---|
| **rep A** | **T** | **$H_2$** | **$N_2$** | **CO** | **$C0_2$** | **Air** | **$D_f$** | **λ** | **$H_2$** | **CO** | **T** |
| Pn | °C | Nl/h cm² | Nl/h cm² | Nl/h cm² | Nl/h cm² | Nl/h cm² | - | - | Nl/h cm² | Nl/h cm² | °C |
| **r1** | 750 | 1,05 | 0 | - | - | 2,49 | 0,00 | 1,00 | 1,05 | - | 750 |
| **b1** | 750 | 0,75 | 0,028 | 0,25 | 0,28 | 2,49 | 0,234 | 1,04 | 0,75 | 0,25 | 750 |
| **b2** | 750 | 0,75 | 0,028 | 0,25 | 0,28 | 2,49 | 0,234 | 1,04 | 0,75 | 0,25 | 750 |
| **b3** | 750 | 0,75 | 0,028 | 0,25 | 0,28 | 2,49 | 0,234 | 1,04 | 0,75 | 0,25 | 750 |
| **b4** | 750 | 0,75 | 0,028 | 0,25 | 0,28 | 2,49 | 0,234 | 1,04 | 0,75 | 0,25 | 750 |
| **b5** | 750 | 0,75 | 0,028 | 0,25 | 0,28 | 2,49 | 0,234 | 1,04 | 0,75 | 0,25 | 750 |
| **r2** | 750 | 1,05 | 0 | - | - | 2,49 | 0,00 | 1,00 | 1,05 | - | 750 |
| **s1** | 750 | 0,53 | 0,03 | 0,45 | 0,17 | 2,49 | 0,169 | 1,07 | 0,53 | 0,45 | 750 |
| **s2** | 750 | 0,53 | 0,03 | 0,45 | 0,17 | 2,49 | 0,169 | 1,07 | 0,53 | 0,45 | 750 |
| **s3** | 750 | 0,53 | 0,03 | 0,45 | 0,17 | 2,49 | 0,169 | 1,07 | 0,53 | 0,45 | 750 |
| **s4** | 750 | 0,53 | 0,03 | 0,45 | 0,17 | 2,49 | 0,169 | 1,07 | 0,53 | 0,45 | 750 |
| **s5** | 750 | 0,53 | 0,03 | 0,45 | 0,17 | 2,49 | 0,169 | 1,07 | 0,53 | 0,45 | 750 |
| **r3** | 750 | 1,05 | 0 | - | - | 2,49 | 0,00 | 1,00 | 1,05 | - | 750 |
| **p1** | 750 | 0,57 | 0,04 | 0,41 | 0,30 | 2,49 | 0,262 | 1,07 | 0,57 | 0,41 | 750 |
| **p2** | 750 | 0,57 | 0,04 | 0,41 | 0,30 | 2,49 | 0,262 | 1,07 | 0,57 | 0,41 | 750 |
| **p3** | 750 | 0,57 | 0,04 | 0,41 | 0,30 | 2,49 | 0,262 | 1,07 | 0,57 | 0,41 | 750 |
| **p4** | 750 | 0,57 | 0,04 | 0,41 | 0,30 | 2,49 | 0,262 | 1,07 | 0,57 | 0,41 | 750 |
| **p5** | 750 | 0,57 | 0,04 | 0,41 | 0,30 | 2,49 | 0,262 | 1,07 | 0,57 | 0,41 | 750 |
| **r4** | 750 | 1,05 | 0 | - | - | 2,49 | 0,00 | 1,00 | 1,05 | - | 750 |

**b – biogas; s – syngas; p – pyrogas; r – reference state*

*Table 10-2 Biogas, syngas and pyrogas test reports A*

| Name | Date | T | $H_2$ | $N_2$ | Air | CO | $CO_2$ | H2O | λ | DN2 | ASR at 0,8V | ASR at 0,7 V | OCV |
|---|---|---|---|---|---|---|---|---|---|---|---|---|---|
| PN | - | °C | Nl/hcm$^2$ | Nl/hcm$^2$ | Nl/hcm$^2$ | Nl/hcm$^2$ | Nl/hcm$^2$ | Nl/h | - | - | Ωcm$^2$ | Ωcm$^2$ | V |
| **r1** | 28.1.2011 | 747 | 1,05 | 0,0 | 2,49 | 0,00 | 0,00 | RT | 1,00 | 0,00 | 0,94 | 0,92 | 1,09 |
| **b1** | 28.1.2011 | 747 | 0,75 | 0,03 | 2,49 | 0,25 | 0,28 | RT | 1,04 | 0,23 | 0,92 | 0,89 | 1,08 |
| **b2** | 28.1.2011 | 747 | 0,75 | 0,03 | 2,49 | 0,25 | 0,28 | RT | 1,04 | 0,23 | 0,91 | 0,87 | 1,08 |
| **b3** | 28.1.2011 | 747 | 0,75 | 0,03 | 2,49 | 0,25 | 0,28 | RT | 1,04 | 0,23 | 0,90 | 0,88 | 1,08 |
| **b4** | 28.1.2011 | 747 | 0,75 | 0,03 | 2,49 | 0,25 | 0,28 | RT | 1,04 | 0,23 | 0,90 | 0,88 | 1,08 |
| **b5** | 28.1.2011 | 747 | 0,75 | 0,03 | 2,49 | 0,25 | 0,28 | RT | 1,04 | 0,23 | 0,91 | 0,88 | 1,08 |
| **r2** | 28.1.2011 | 747 | 1,05 | 0,0 | 2,49 | 0,00 | 0,00 | RT | 1,00 | 0,00 | 0,92 | 0,91 | 1,09 |
| **s1** | 28.1.2011 | 747 | 0,53 | 0,03 | 2,49 | 0,45 | 0,17 | RT | 1,08 | 0,17 | 0,90 | 0,87 | 1,08 |
| **s2** | 28.1.2011 | 747 | 0,53 | 0,03 | 2,49 | 0,45 | 0,17 | RT | 1,08 | 0,17 | 0,90 | 0,87 | 1,07 |
| **s3** | 28.1.2011 | 747 | 0,53 | 0,03 | 2,49 | 0,45 | 0,17 | RT | 1,08 | 0,17 | 0,92 | 0,87 | 1,07 |
| **s4** | 28.1.2011 | 747 | 0,53 | 0,03 | 2,49 | 0,45 | 0,17 | RT | 1,08 | 0,17 | 0,93 | 0,89 | 1,07 |
| **s5** | - | - | - | - | - | - | - | - | - | - | - | - | - |
| **r3** | - | - | - | - | - | - | - | - | - | - | - | - | - |
| **p1** | 28.1.2011 | 747 | 0,57 | 0,04 | 2,49 | 0,41 | 0,3 | RT | 1,07 | 0,26 | 0,91 | 0,88 | 1,07 |
| **p2** | 28.1.2011 | 747 | 0,57 | 0,04 | 2,49 | 0,41 | 0,0 | RT | 1,08 | 0,26 | 0,90 | 0,87 | 1,07 |
| **p3** | 28.1.2011 | 747 | 0,57 | 0,04 | 2,49 | 0,41 | 0,3 | RT | 1,07 | 0,26 | 0,89 | 0,88 | 1,07 |
| **p4** | 27.1.2011 | 747 | 0,57 | 0,04 | 2,49 | 0,41 | 0,3 | RT | 1,07 | 0,26 | 0,90 | 0,87 | 1,07 |
| **p5** | 28.1.2011 | 747 | 0,57 | 0,04 | 2,49 | 0,41 | 0,3 | RT | 1,07 | 0,26 | 0,90 | 0,88 | 1,07 |
| **r4** | 29.1.2011 | 747 | 1,05 | 0,0 | 2,49 | 0,00 | 0,0 | RT | 1,00 | 0,00 | 0,90 | 0,89 | 1,10 |

The list of reports B includes some polarizations prepared according to reference state standards. From the report presented below, it can be noticed that reference state tests prepared at the beginning, in the middle and at the end of the test activity, do not show big differences in the results, respectively. That leads to the conclusion that the investigated gases do not have influence on the cell performance.

Moreover, all reports are included in appendix H.

**RREPORT B** **POLARIZATION ref 1, 2, 4**

**ASC700 4-10** **Active area** **50** **$cm^2$**

| # | Date | T | $H_2$ | $N_2$ | Air | CO | $CO_2$ | $H_2O$ | λ | $D_f$ | ASR at 0,8 V | ASR at 0,7 V | OCV |
|---|---|---|---|---|---|---|---|---|---|---|---|---|---|
| n | - | °C | Nl/hcm² | Nl/hcm² | Nl/hcm² | Nl/hcm² | Nl/hcm² | Nl/h | - | - | Ωcm² | Ωcm² | V |
| ref1 | 28.1.2011 | 747 | 1,05 | 0,00 | 2,49 | 0,00 | 0,00 | RT | 1,0 | 0,0 | 0,94 | 0,92 | 1,09 |
| ref2 | 28.1.2011 | 747 | 1,05 | 0,00 | 2,49 | 0,00 | 0,00 | RT | 1,0 | 0,0 | 0,92 | 0,91 | 1,09 |
| ref4 | 29.1.2011 | 747 | 1,05 | 0,00 | 2,49 | 0,00 | 0,00 | RT | 1,0 | 0,0 | 0,90 | 0,89 | 1,10 |

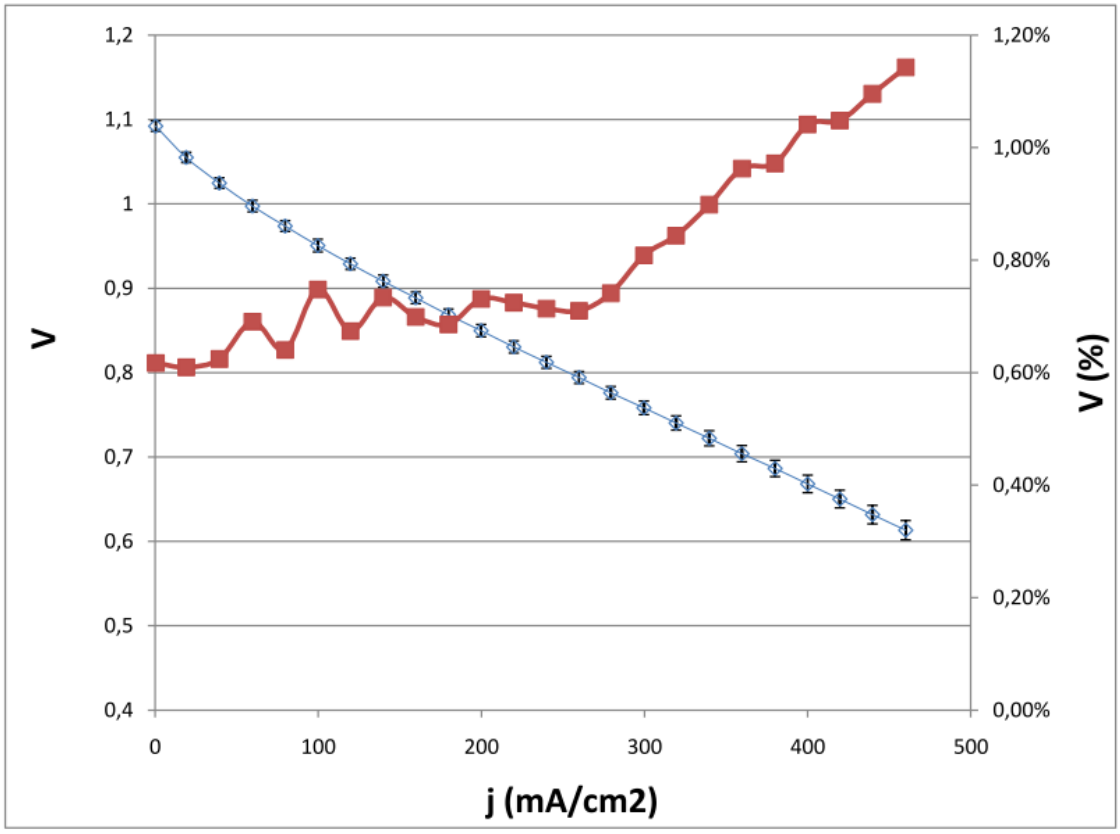


| # | Date | T | $H_2$ | $N_2$ | Air | CO | $CO_2$ | $H_2O$ | λ | $D_f$ | ASR at 0,8 V | ASR at 0,7 V | OCV |
|---|---|---|---|---|---|---|---|---|---|---|---|---|---|
| n | - | °C | Nl/hcm2 | Nl/hcm² | Nl/hcm² | Nl/hcm² | Nl/hcm² | Nl/h | - | - | Ωcm² | Ωcm² | V |
| **ref 1, 2, 4** | **28.1.2011** | **747** | **1,05** | **0,0** | **2,5** | **0,0** | **0,0** | **RT** | **1,0** | **0,0** | **0,9** | **0,9** | **1,1** |

*Fig. 10-1 Reference state report B (biogas, syngas and pyrogas test activity)*

Final report C is presented below. In this report, the cell performance parameters are presented on the charts as function of dilution factor, stoichiometric factor, hydrogen specific flow and carbon monoxide specific flow, respectively.

**RREPORT C**

**ASC700 4-10** **Active area** **50 cm2**

| Parameter | Unit | Biogas | Syngas | Pyrogas | Ref. state |
|---|---|---|---|---|---|
| | | *varied values* | | | |
| $D_f$ | - | 0,23 | 0,17 | 0,26 | 0,00 |
| λ | - | 1,04 | 1,08 | 1,07 | 1,00 |
| $q_{H2}$ | Nl/hcm$^2$ | 0,75 | 0,53 | 0,57 | 1,05 |
| $q_{CO}$ | Nl/hcm$^2$ | 0,25 | 0,45 | 0,41 | - |
| | | *input values* | | | |
| T | °C | 747,1 | 746,9 | 747,3 | 747,0 |
| | | *output values* | | | |
| OCV | V | 1,08 | 1,07 | 1,07 | 1,09 |
| ASR at 0,8V | Ωcm$^2$ | 0,91 | 0,91 | 0,90 | 0,92 |
| ASR at 0,7V | Ωcm$^2$ | 0,88 | 0,88 | 0,88 | 0,91 |

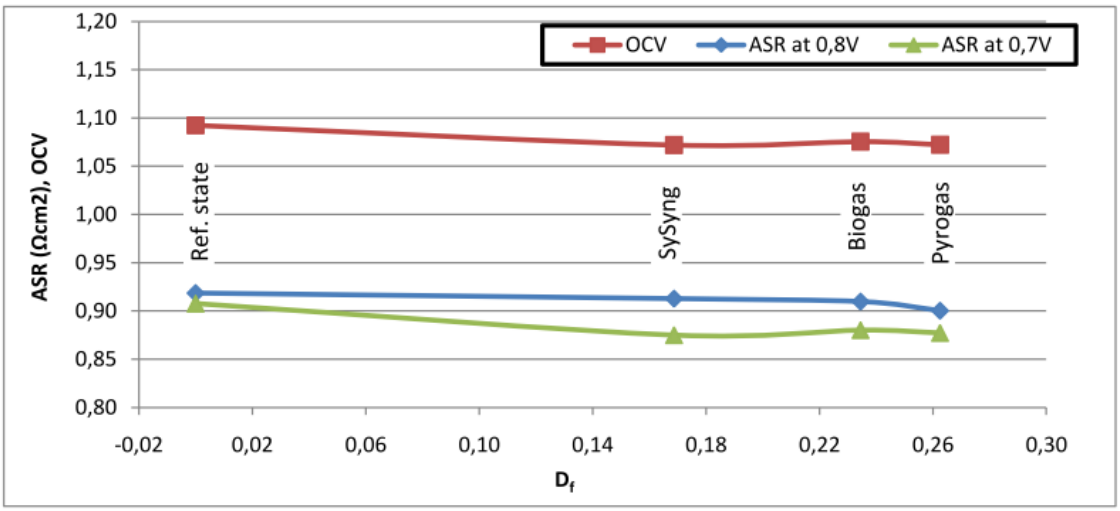


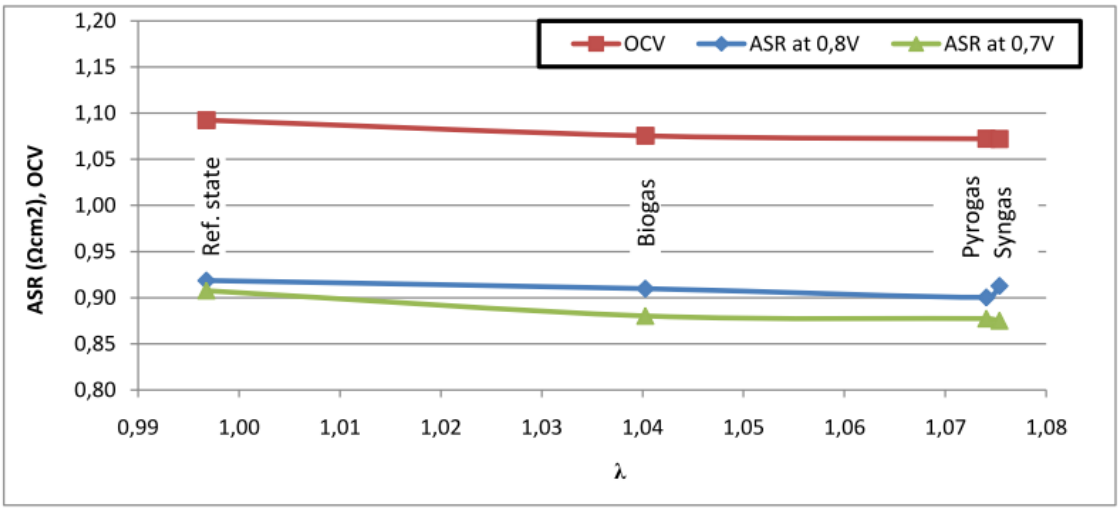


*Fig. 10-2Biogas, syngas and pyrogas report C (part 1)*

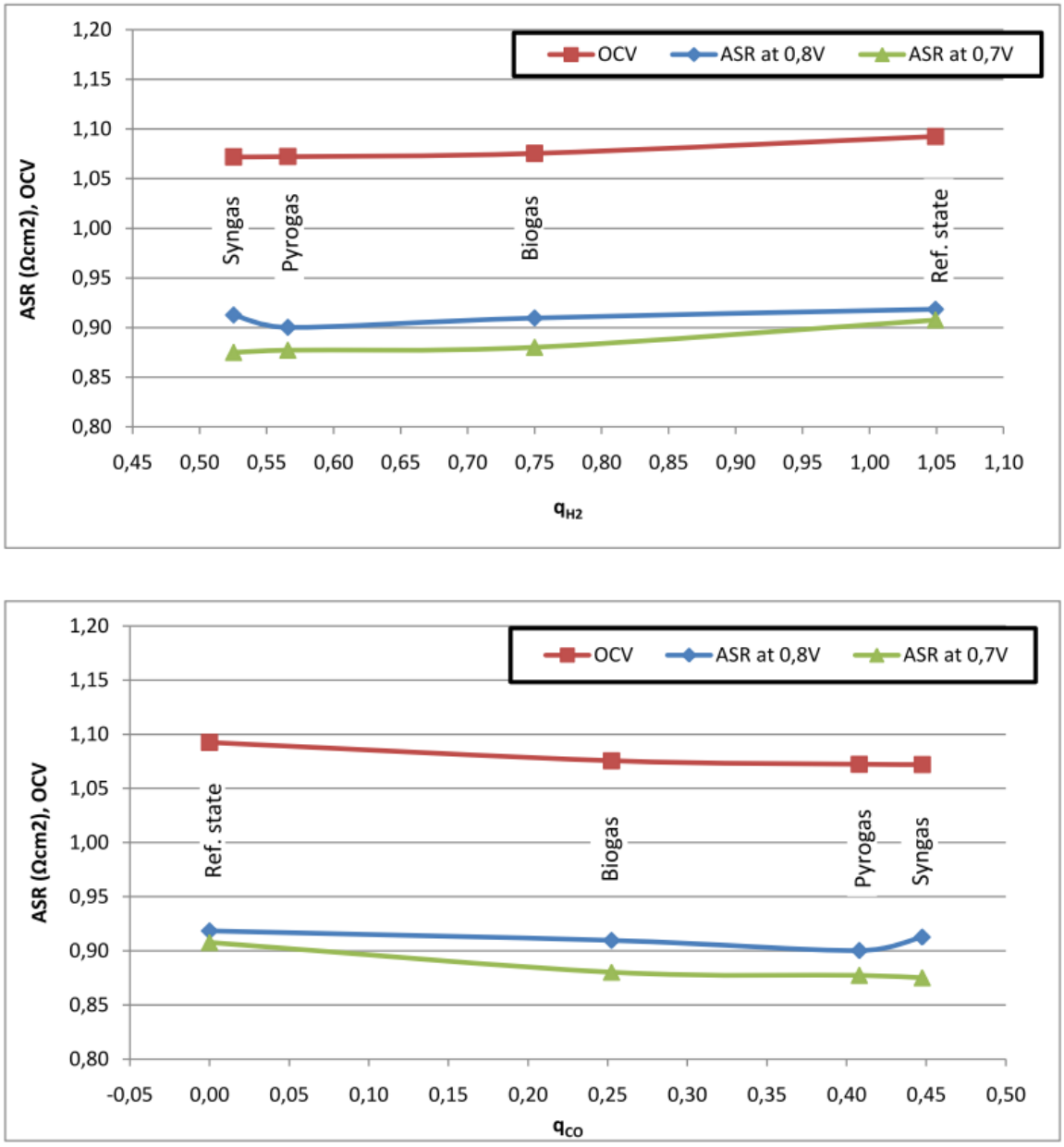


*Fig. 10-3 Biogas, syngas and pyrogas report C (part 2)*

The first graph ($D_f$ vs. ASR at 0,7V and ASR at 0,8V) shows higher OCV and ASR values for reference state measurements in comparison to the same indicators for all investigated gases. Moreover, biogas from all of the gasses is characterized by the highest OCV value and syngas by the lowest. However, the OCV differences between biogas-syngas and syngas-reference state tests show that the values are very insignificant and amount to around 0,33% for both of them. ASR values are also slightly different and equal to around 2% - between the highest for reference state and the lowest for pyrogas. The standard deviations for ASR at 0,8V and ASR at 0,7V are 0,65% and 0,26% for studied gases.

In conclusion, the gases show slightly lower ARS and insignificant lower OCV values than the reference state results. Pyrogas, characterized by the highest $D_f$ value shows the best trend in ASR results.

The second reported chart shows the dependence of the same performance parameters and stoichiometric factor. In this case, the reference states measurements are also insignificant lower in OCV and ASR values than these ones obtained for other gases. The differences between all discussed tests are very similar to these presented in the previous paragraph.

In summary, OCV and ASR parameters directly depend on $D_f$ and $\lambda$ indicators.

Next, on the two report charts, the specific hydrogen and carbon monoxide flows in the fuel mixture are shown as a function on the performance indicator, respectively. As it can be noticed, the values of the reactive gases flows do not have influence on ASR and OCV values. The relations are still the same:

- the highest ASR and OCV results are for reference state tests,
- all gas mixtures present insignificant differences in OCV values,
- pyrogas shows the lowest values for both ASR indicators.

Based on the analysis from the presented test activity, the main conclusion emphasizes that the change in the fuel results in small ASR and insignificant OCV variations. That in result can cause higher cell output power. That leads to another conclusion that biogas, syngas as well as pyrogas can be successfully used instead of hydrogen as the fuel in SOFC.

Moreover, the insignificantly better pyrogas results in comparison to biogas and syngas can be caused by the highest $D_f$ value. The influence of dilution factor on ASR and OCV is presented in the previously presented test analysis.

# 11 CONCLUSIONS

From the analysis presented in this thesis, the conclusion arises that ASR is not only material dependent parameter but also depends on fuel quality. Moreover, because of the fact that ASR is not influenced by the total flows of the input gasses, it is much better parameter for fuel cell performance assessment than OCV.

In addition, the data shows that only very small amount of the oxidant gas has influence on ASR value. In practice, this situation does not have a big importance because the fuel cells are supplied by enough amounts of air - which is the cheapest and the most abundant available oxidant.

Moreover, all discussed fuels can be produced from biomass that, give obvious environmental benefits and also possibility to control compositions during production processes. This fact can be very important because as it is shown in the study, the fuel quality has influence on the cell performance. ASR gives the possibility to investigate the best cell performance given by fuel mixtures examination. Thesis shows that $D_f$ value in rage of around 0,2 – 0,3 can decrease ASR of the cell, while for dilution factor values higher than around 0,35 the cell ARS increase. Moreover, this trend does not change with total volumetric fuel flow.

Next, examined in the thesis biogas, syngas and pyrogas show negligible compared to hydrogen influence on the fuel cell performance parameters. However, it should be noted that small decrease in OCV and slightly better ASR in result can cause higher cell output. This fact leads to the conclusion that use of biogas, syngas as well as pyrogas can be very attractive fuel.

All these facts can be very important because it can make fuel cell technology even more effective and at the same time more economically profitable.

However, it should be mentioned that study presented in this thesis requires future development and research. Few of them could be:

- tests with upgraded (sealed) or new test rig,
- tests on SOFC, provided by different suppliers,
- research with practically obtained and reformed fuels instead of simulated gas mixtures,
- long term durability tests,
- tests with stacks,
- tests on direct and indirect internal fuel reforming systems.

Biogas, syngas and pyrogas can provide low cost and clean fuel for power generating applications. In fact, as it is shown in the thesis, biomass and bio-fuels have big potential in Poland. However, there is still lack of commercial used of fuel cell systems and because of that this technology should be considered as a very promising for the future.

# REFERENCES


Andujar, JM & Segura, F 2009, 'Fuel cells: History and updating. A walk along two centuries', *Renewable and Sustainable Energy Reviews,* vol. 13, no. 9, pp. 2309–2322.

Bove, R & Ubertini, S 2008, *Modeling Solid Oxide Fuel Cells - Methods, Procedures and Techniques*, Springer, Cleveland, USA.

Cao, D et al. 2007, 'Direct carbon fuel cell: Fundamentals and recent developments', *Journal of Power Sources,* vol. 167, no. 2, pp. 250-257.

*Fuel Cell Handbook. Seventh edition,* EG&G Technical Services, Inc., Morgantown, West Virginia, USA: U.S. Department of Energy, 2004.

Gemmen, R.S. et al. 2008, 'Degradation measurements and analysis for cells and stacks', *Journal of Power Sources,* vol. 184, no. 1, pp. 251-259.

Heo, Y-H et al. 2010, 'Redox-induced performance degradation of anode-supported tubular solid oxide fuel cells', *International Journal of Hydrogen Energy.*

Kawalec, M 2010, 'Test activity on SOFC single cell: performance with poisoned mix ($H_2S$)', Master thesis, RES in affiliation with University of Iceland & University of Akureyri, Akureyri

Kolb, G 2008, *Fuel Processing for Fuel Cells,* WILEY-VCH, Mainz, Germany

Lubiewa-Wieleżyński, W & Siroka, A 2009, 'Raw materials for chemical industry. Demand and logistic', *Przemysł Chemiczny*.

Muthuvela, M et al. 2009, 'Fuel Cells - Exploratory Fuel Cells | Direct Carbon Fuel Cells', *Encyclopedia of Electrochemical Power Sources,* pp. 158-171.

Neef, H-J 2009, 'International overview of hydrogen and fuel cell research', *Energy*, vol. 34, no. 3, pp.327–333.

O'Hayre, R, Cha, SW, Colella, W & Prinz, FB 2006, *Fuel Cell Fundamentals*, John Wiley & Sons, New York.

Sammes, N 2006, *Fuel Cell Technology: Reaching Towards Commercialization*, Springer, London.

Singhal, SC & Kendall, K 2003, *High Temperature Solid Oxide Fuel Cells: Fundamentals, Design and Applications*, Elsevier, UK.

Thomas, S & Zalbowitz, M, '*Fuel Cells Green Power',* Los Alamos Los Alamos National Laboratory, New Mexico

Tucker, MC 2010, 'Progress in metal-supported solid oxide fuel cells: A review', *Journal of Power Sources*, vol. 195, no. 15, pp. 4570–4582.

van der Drift, R. et al, 'Bio-syngas: key intermediate for large scale production of green fuels and chemicals' *The 2nd World Conference on Biomass for Energy, Industry, and Climate Protection,* 10-14 May 2004, Rome, Italy, pp. 2155-2157

Zhou, X-D & Singhal, SC 2009, 'Fuel Cells - Solid Oxide Fuel Cells | Overview', *Encyclopedia of Electrochemical Power Sources,* pp.1-16

Polski rynek gazu w 2009 roku (2010), vieved 4 January 2011 <http://weglowodory.pl/polski-rynek-gazu-w-2009-roku/>

U.S. Department of Energy, *Hydrogen production,* viewed 18 November 2011, <http://www1.eere.energy.gov/hydrogenandfuelcells/production/current_technology.html>

Rathmann, M et al. 2009, *Renewable Energy Policy Country Profiles,* viewed 11 December 2010, <http://www.ecofys.com/com/publications/brochures_newsletters/documents/RE-SHAPING_Renewable_Energy_Policy_Country_profiles_2009.pdf>

EurObserv'ER, (2008), *Biogas Barometer*, viewd 16 December 2010, <http://www.eurobserv-er.org/pdf/baro186_a.pdf>

*Energy Generation by a Renewable Source – Sewage Biogas,* USP – Sao Paulo's University, viewd 15 December 2010, <http://cenbio.iee.usp.br/download/projetos/14_RIO6_enrg-biog.pdf>

# APPENDIX A

## General description

[redacted] provides anode-supported, thin-film electrolyte, solid oxide fuel cells produced in its pilot production line in Trento. The cells are composed of an electrolyte (YSZ) sandwiched between two electrodes, a porous perovskite cathode and the anode support structure. For low temperature cells, a ceria barrier layer separates the cathode form the electrolyte. Good mechanical stability is provided by the relatively dense anode structure; the thin anode hardly shows any gas diffusion limitations. Precise wet ceramic processing enables efficient use of raw materials. The cells are produced by anode and electrolyte co-casting and co-sintering followed by screen-printing of the cathode layer.

## Operating range

The cells allow for a high fuel utilisation (>70 %) and demonstrate high power densities (>1 W/cm²)*. Cells can be operated in a temperature range of 600°C to 850°C under humidified hydrogen, reformed hydrocarbons or synthesis gas mixtures.

## Production flexibility and quality

[redacted] cells are produced in different configurations and according to customers' geometrical specifications. The cells have been tested for more than thousand hours in single cell tests and stack operations, showing stable performance. Quality control is one of the company's priorities: production statistics, mechanical and electrochemical tests are used to verify and optimise the quality and reproducibility of all production batches.

## SOFC Anode Supported Cells designed for intermediate temperature application (~700°C)

### Cell Architecture

| layer | composition | thickness |
|---|---|---|
| anode | Ni/8YSZ | 240 ± 20 µm |
| electrolyte | 8YSZ | 8 ± 2 µm |
| bilayer cathode | GDC+LSCF | 50 ± 10 µm |

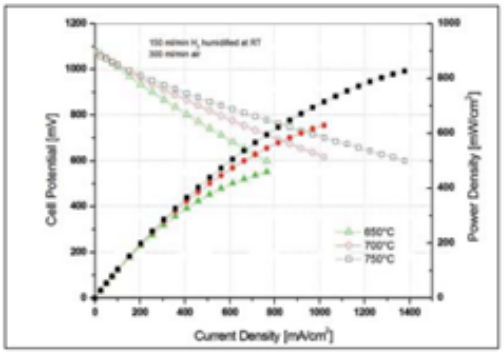


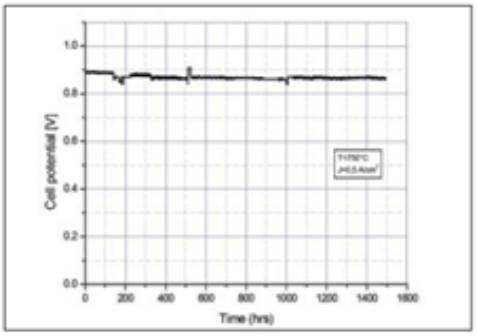


| properties | 650°C | 700° | 750°C |
|---|---|---|---|
| **ASR** @ 0.7 V [Ωcm2]* | 0.57 | 0.39 | 0.28 |
| **j** @ 0.7 V [mA/cm2] | 580 | 800 | 1025 |
| **P** @ 0.7 V [mW/cm2] | 405 | 560 | 715 |

*calculated in the range 0.75-0.65V

# APPENDIX B

## Flow meters

The system is equipped with nine flow meters, seven on anode side and two on cathode side. Discussed devices are supplied with gases under 3 bar pressure. Each one of them is used to supply the system with appropriate (set) amount of gas and register (measure) actual flow. Also, each flow meter has its own flow range what is presented in table below.

*Flow meters parameters*

| Gas | DAS/P&ID number | Flow range [Nl/h] | Model name | Accuracy |
|---|---|---|---|---|
| $H_2$ | 205 | 0-30 | Brooks 5850 S | ± 0,7% of rate and ± 0,2% F.S. |
| | 206 | 0-50 | | |
| $N_2$ | 204 | 0-50 | | |
| $CO_2$ | 201 | 0-80 | | |
| $CO$ | 203 | 0-180 | | |
| $CH_4$ | 202 | 0-50 | | |
| $H_2S$ | 207 | 0-27 | | |
| $Air$ | 101 | 0-50 | | |
| | 102 | 0-80 | | |

## Manifolds

Made of durable ceramic material which can which can endure extreme temperatures above 1000 °C. Its main function is to spread air or fuel evenly on the surface of Fuel Cell during testing, which assures the same performance in every point of Fuel Cell. Without this device calculations regarding current density will be incorrect because of uneven current generation on active area.

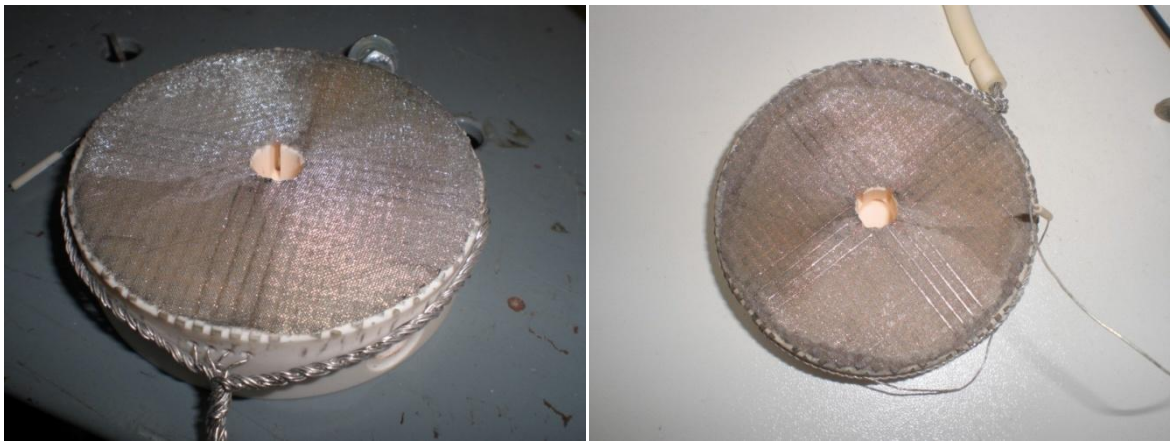

*Anode (right) and cathode (left) manifolds.*

## Thermocouples

Test rig includes three thermocouples type K, which means that they are composed of chromel and alumel materials. Two of thermocouples (marked as 1 and 3 on Figure 4.2.5 below) acquire and sends data (temperature) to Data Acquisition Unit. Third thermocouple (marked as 2 on Figure 4.2.5 below) are connected to thermo regulator and working as feedback device allowing acquiring constant temperature.

Two of thermocouples (marked as 1 and 2) are rigid type and are acquiring data from inside of Oven. Third one (marked as 3) is elastic type which allows it insertion thru anode pipeline and acquiring data directly from surface of SOFC.

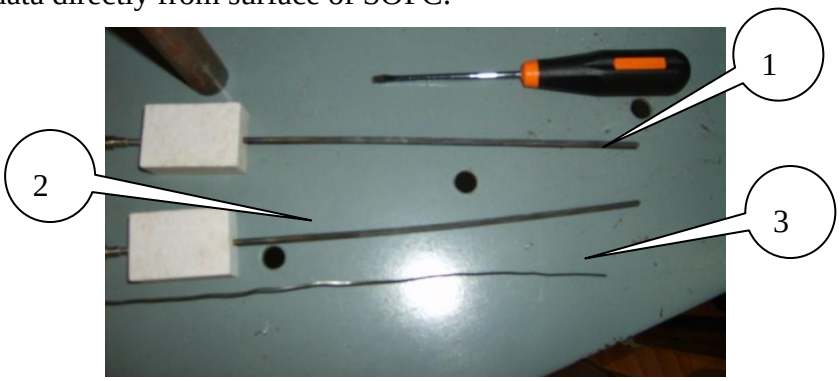


*Thermocouples used in test rig*

## Oven

Main function of the Oven is acquiring and keeping temperature inside. It's composed of three parts made by isolating material. Two parts, which are creating empty inside cylinder, have implemented heating device in form of resistance heating spiral wires. Third part, located on them, have a purely insolating purpose. Heating part of are connected and controlled to Thermo Regulator.

## Press

Pneumatic Press is device located on top of test rig with purpose of applying mechanical pressure to cathode Manifold and by that Manifold to Fuel Cell and anode Manifold. Pressure is applied in two ways. First is purely gravitational and originate ceramic cylinder of weight very close to 1kg which additionally connect actual pneumatic press with cathode Manifold. Second part is actual pneumatic press which is set to work in two modes – 0.5 bar of pressure translates to 4.5 kg of mechanic load and 1.8 bar of pressure – 11 kg of mechanic load.

Press is necessary to acquire condition specified in start-up procedure attached to tested Fuel Cell regarding mechanical load during Start-Up and operating.

## Humidifying unit

Humidifying unit (below) is relatively simple device which forces mixture of Hydrogen and Nitrogen to go thru water to humidify it. As the conditions inside are the same as atmospheric (about 20 °C and 1 atm) there is about 4% of water in mixture after Humidifying unit.

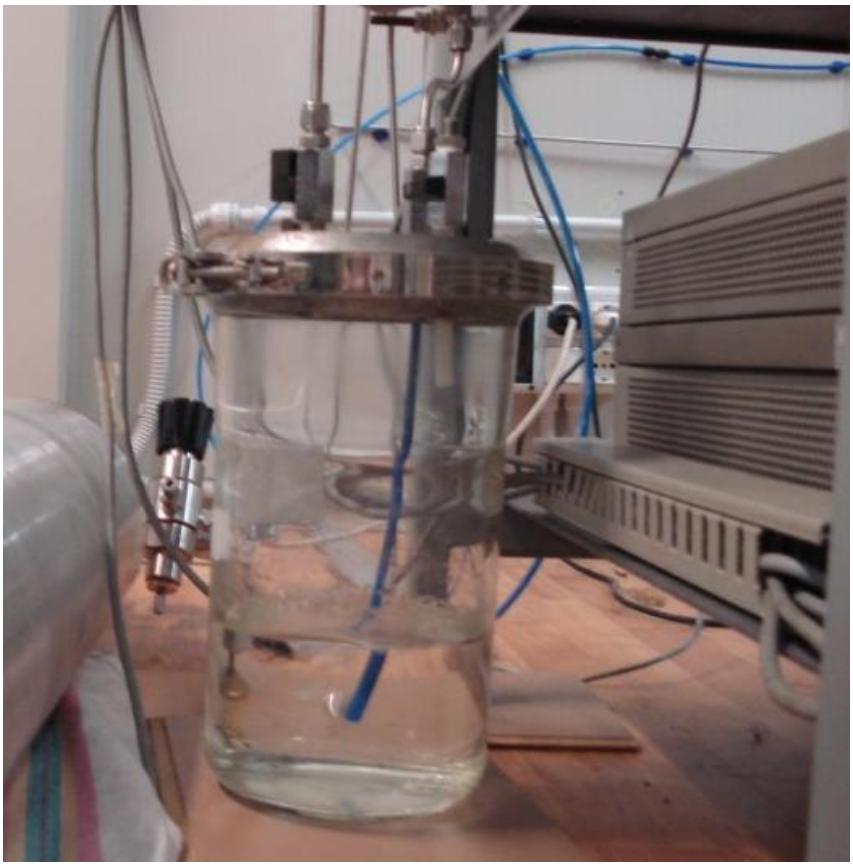

*Humidifying unit*

Humidificator is necessary device to acquire conditions specified in Start-Up procedure (humidification on room temperature). Additionally, it was installed in preparation to usage of other gases (Methane) to prevent Carbon formation on the anode of Solid Oxide Fuel Cell.

Humidifying unit can be bypassed if desired to use dry gas in Fuel Cell.

## Power Supply


*Agilent N5763A Power Supply*

Agilent N5763A Power Supply (see Figure 4.2.9 above) is basic power supply source with single output and universal AC input. Control of output current and voltage is provided by analog/resistance. It's one medium size unit that can provide up to 1.5 kW of power that enables convenient way of supply power with following key specifications(Aligent technology):

| | | |
|---|---|---|
| **Output ratings** | Voltage<br>Current<br>Power | 12.5 V<br>120 A<br>1500 W |
| **Programming Accuracy** | Voltage<br>Current | 0,05% + 6.25 V<br>0,1% + 120 mA |
| **Ripple and Noise** | CV p-p<br>CV rms<br>CC rms | 60 mV<br>8 mV<br>240 mA |
| **Load Regulation**<br>**Load Effect**<br>**(from 10% to 90%)** | Voltage<br>Current | 3,25 mV<br>29 mA |
| **Load Transient** | Recovery Time | ≤1.5 ms |

*Key specifications for Agilent N5763A Power Supply Unit*(Aligent technology)

This device follows load in the circuit and as the main function increases Voltage collected from Fuel Cell by 3V, enabling measurement. This Voltage increase is later taken under consideration when data are processed.

## Electronic Load

*Aligent N3304A 300 W Electronic Load*

Aligent N3304A 300 W Electronic Load (see Figure 4.2.10 above) unit is located inside Aligent N3300A 1800 Watt DC Electronic Load Mainframe. It is fast device capable of maintaining constant programmed current, constant voltage or resistance and taking voltage, current and power measurements, with additional feature of digitize waveforms(Aligent technology). Key specification available :

| | | |
|---|---|---|
| **Input ratings** | Current | 0 – 60 A |
| | Voltage | 0 – 60 V |
| | Maximum Power @ 40°C | 300 W |
| | Typical Minimum Operating Voltage at Full Scale Current | 1.2 V |
| **Constant Current Mode** | Low Range / High Range | 6A/60A |
| | Regulation | 10 mA |
| | Low Range Accuracy | 0.1% + 7.5 mA |
| | High Range Accuracy | 0.1% + 15 mA |
| **Constant Voltage Mode** | Low Range / High Range | 6A/60A |
| | Regulation | 10 mA |
| | Low Range Accuracy | 0.1% + 3 mV |
| | High Range Accuracy | 0.1% + 8 mV |
| **Constant Resistance Mode** | Range 1 (I>10% of current rating) | 0.033-2 Ω |
| | Range 2 (I>1% of current rating) | 1.8-20 Ω |
| | Range 3 (I>0.1% of current rating) | 18-200 Ω |
| | Range 4 (I>0.01% of current rating) | 180-2000 Ω |

*Key specifications for N3304A 300 W Electronic Load Unit*(Aligent technology)

Electronic Load device is controlled remotely from PC unit and takes active role in measuring j-V curve. Changing of load applied to Fuel Cell

## Data Acquisition Unit


*Aligent 34980A Multifunction Switch/Measure*

Aligent 34980A Multifunction Switch/Measure Unit (see Figure 4.2.11 above) is a compact, one box device destined for medium to high density measure applications in design verification, automated test and data acquisition(Aligent technology). It's very multilateral device, which, with variety of different plug-ins can acquire possibility to switch DC to 20 GHz, being digital I/O, D/A convert and count/totalize. Other counted features include USB, Ethernet and GPIB in standard as a way to communicate with PC. Modules also possess standard sockets compatible with normal 50 and 70-pin shielded cables, and additional option for detachable terminal blocks and mass interconnect solutions. Ethernet connection allow for remote control from PC(Aligent technology). This device acquires data from:

- ➔ Two thermocouples located inside Oven (one detecting temperature of Oven and second one detecting temperature of Fuel Cell)
- ➔ Current collectors, giving Cell voltage

Above data are going via switch to PC unit, where are registered.

## Thermo regulator

This device collects data from thermocouple acquiring data of temperature in Oven and controls it, by controlling resistive wires. It's set manually and can be set to maintaining temperature or to increase/decrease temperature in steady pace. First option is used during tests of Fuel Cell, second have its use during start-up and cool-down. For example, heating speed during start-up is set to 27 °C/h.

*Thermo regulator*

## Pipes and instruments design

The pipes and instruments design system presented below show how gas pipes and main instruments are constructed and located. From the figure, it can be noticed:

- that each system for gas storing consists of main tank and backup tank,
- how air in the system is constructed - compressor , drier, filter and storage tanks,
- that methane supply line is equipped with evaporator – which is used when needed.

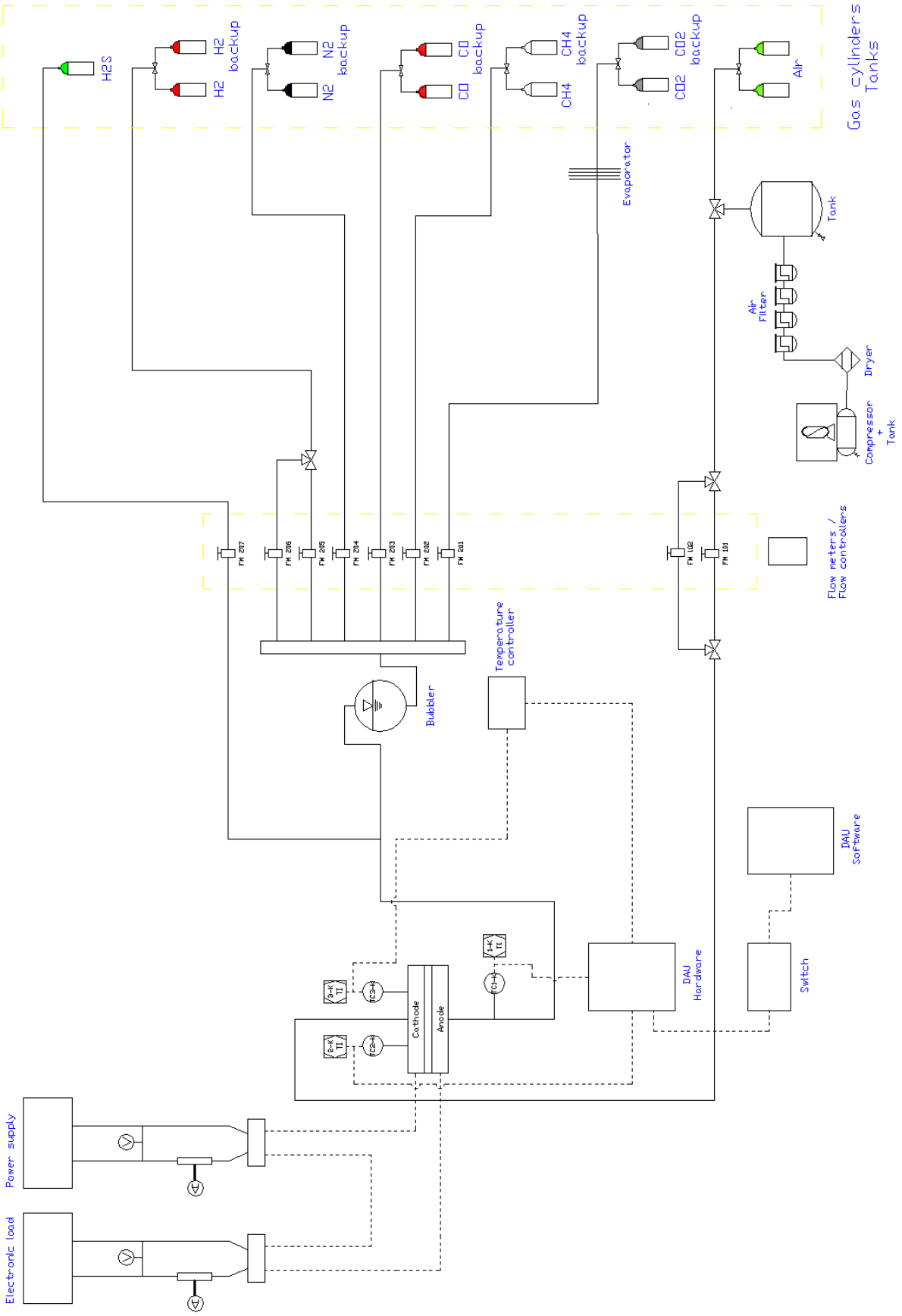


*Pipes and instruments design*

## Data acquisition system

The DAS system is used to measure electrical and physical phenomenon such as voltage, current, gas flow and temperature by using appropriate electrical conductors, thermocouples and flow meters - which can be named sensors. Analogical signal from such sensors in real time is transferred to appropriate devices, which convert them to digital signal and transmit to the central unit, which is used to collect and save the data. The system scheme with types of connections between sensors and devices which read/convert measured signals/data and central PC unit (with control program) is shown in figure below.

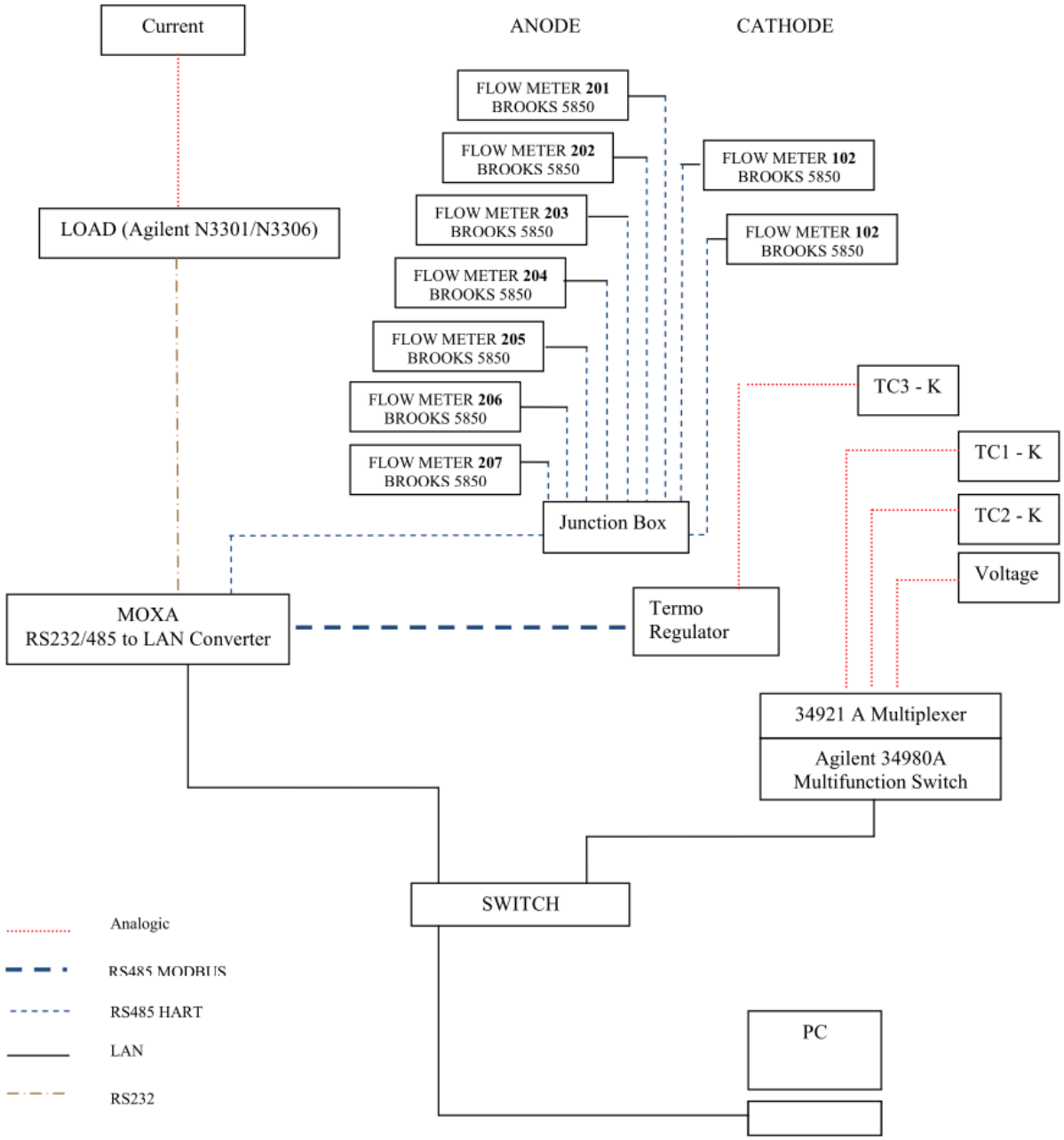


*Scheme of data acquisition system*

# APPENDIX C

File name: 01-LD Cell Performance and Endurance - H2

## SOFC light-duty cell performance and endurance with hydrogen

Procedure for evaluation of performance and endurance at light-duty operating conditions, of SOFC single cells operated with hydrogen.

Test input ..... Current density and temperature
Test output ..... Voltage

Class of test object..... Cell
Class of application..... Generic

Authors ..... Bert Rietveld, Arno Janssen
Revision date ..... 07-05-2010

**Revision history**

| Version | Change | Date | Status | Text / revision by |
|---|---|---|---|---|
| 1 | | 28-11-2006 | Draft | Bert Rietveld |
| 2 | | 07-05-2010 | Final | Arno Janssen |

# Table of Contents

**1 Objective and scope ..... 3**

**2 Terminology, definitions and symbols ..... 3**
2.1 Terminology and definitions ..... 3
2.2 Symbols ..... 3

**3 Test inputs ..... 3**
3.1 Variable test inputs ..... 3
3.2 Static test inputs for performance and endurance phase ..... 4
3.3 Static test inputs for polarisation measurement at start and end ..... 4

**4 Test outputs ..... 4**

**5 References, required documentation and provisions ..... 4**
5.1 References and required documentation ..... 4
5.2 Provisions ..... 4

**6 Test equipment and experimental set-up ..... 4**

**7 Test programme ..... 5**
7.1 Assembly and pre-conditioning of the cell ..... 5
7.2 Recording of the initial polarisation curves ..... 6
7.3 Steady-state operation for performance evaluation ..... 7
7.4 Recording of the second series of polarisation curves ..... 7
7.5 Steady-state operation for endurance evaluation ..... 7
7.6 Recording of the last series of polarisation curves ..... 7

**8 Presentation of results ..... 7**

Annex A Test report template

## 1 Objective and scope

Procedure for evaluation of performance and endurance at light-duty operating conditions, of SOFC single cells operated with hydrogen.

The operating conditions defined in this performance and endurance test are considered relatively mild compared to these envisaged for practical SOFC based systems.

This test is a general performance characterisation method for the research and development of SOFC cells.

## 2 Terminology, definitions and symbols

### *2.1 Terminology and definitions*

Terminology and definitions used in this document are according to the FCTESTnet Fuel Cells Glossary.
Additional terminology and definitions are:

*Cell area*

- The (effective) cell area is defined as the area of the zone in which all cell components, that is anode, electrolyte and cathode, and the anode and cathode current collectors overlap.

### *2.2 Symbols*

Symbols for physical quantities are defined in the Handbook of Chemistry and Physics, 69th Edition, CRC Press. Below additional symbols are defined.

| Symbol | Formula definition | Unit | Description |
|---|---|---|---|
| $A_{cell}$ | Cell area | $cm^2$ | Effective cell area |
| $X_{fuel}$ | | - | Volume composition of fuel |
| $X_{ox}$ | | - | Volume composition of oxidant |
| $q_{fuel}$ | $q_{v,fuel}$ / $A_{cell}$ | $ml.min^{-1}.cm^{-2}$ | Volume flow of fuel per unit cell area (STP) |
| $q_{ox}$ | $q_{v,ox}$ / $A_{cell}$ | $ml.min^{-1}.cm^{-2}$ | Volume flow of oxidant per unit cell area (STP) |

## 3 Test inputs

### *3.1 Variable test inputs*

Essentially all relevant operating parameters are constant. Only variable test inputs occur during the execution of the polarisation curve registration module. See there.

| Input | Description | Range | Tolerance |
|---|---|---|---|
| t | Operating time | 0 - 3000 hours | ± 1 hour |
| T | Operating temperature | 400 - (n x 50) - 1050°C | ± 4°C |

*3.2 Static test inputs for performance and endurance phase*

| Input | Description | Value | Tolerance |
|---|---|---|---|
| $X_{fuel}$ | Fuel composition | 17.5 $ml.min^{-1}.cm^{-2}$ $H_2$ | ± 5% (rel) |
| | | 0.54 $ml.min^{-1}.cm^{-2}$ $H_2O$ | ± 10% (rel) |
| $q_{fuel}$ | Fuel flow (STP) | 18.0 $ml.min^{-1}.cm^{-2}$ | ± 10% (rel) |
| $X_{ox}$ | Oxidant composition | 8.7 $ml.min^{-1}.cm^{-2}$ $O_2$ | ± 5% (rel) |
| | | 32.8 $ml.min^{-1}.cm^{-2}$ $N_2$ | ± 10% (rel) |
| $q_{ox}$ | Oxidant flow (STP) | 41.5 $ml.min^{-1}.cm^{-2}$ | ± 10% (rel) |
| J | Current density | 0.5 $A.cm^{-2}$ | ± 10 $mA.cm^{-2}$ |
| $T_{cell}$ | Inlet temperature | 400 - (n x 50) - 1050°C | ± 4°C |

*3.3 Static test inputs for polarisation measurement at start and end*

| Input | Description | Value | Tolerance |
|---|---|---|---|
| $X_{fuel}$ | Fuel composition | 10.7 $ml.min^{-1}.cm^{-2}$ $H_2$ | ± 5% (rel) |
| | | 0.3 $ml.min^{-1}.cm^{-2}$ $H_2O$ | ± 10% (rel) |
| $q_{fuel}$ | Fuel flow (STP) | 11.0 $ml.min^{-1}.cm^{-2}$ | ± 10% (rel) |
| $X_{ox}$ | Oxidant composition | 6.7 $ml.min^{-1}.cm^{-2}$ $O_2$ | ± 5% (rel) |
| | | 25.2 $ml.min^{-1}.cm^{-2}$ $N_2$ | ± 10% (rel) |
| $q_{ox}$ | Oxidant flow (STP) | 31.9 $ml.min^{-1}.cm^{-2}$ | ± 10% (rel) |
| $T_{cell}$ | Inlet temperature | 400 - (n x 50) - 1050°C | ± 4°C |

## 4 Test outputs

| Output | Description | Range | Accuracy | Sample Rate |
|---|---|---|---|---|
| V | Cell voltage | 0.3 - 1.50 V | ± 5 mV | > 1 $min^{-1}$ |

## 5 References, required documentation and provisions

*5.1 References and required documentation*

[1] FCTESTnet Fuel Cells Glossary
[2] Test module M01-SOFC cell polarisation curve

*5.2 Provisions*

Standard local safety precautions for working with the concerning gaseous fuels, electrical installations and chemicals contained by the SOFC have to be respected.

## 6 Test equipment and experimental set-up

This test procedure does not prescribe the geometry and size of the cell test housing.

The materials of the single cell test housing should be:

- an inert ceramic material (e.g. $Al_2O_3$) for the cell housing
- a platinum cathode current collector
- a nickel anode current collector.

The current collectors are directly contacting the electrodes of the cells. No intermediate contact layers are applied between the electrodes and the current collectors.

It is recommended to apply mesh type current collectors, preferably double grids at both the anode and the cathode side of the cell. The fine grid (e.g. wire diameter of 0.040 mm, 3600 meshes.cm$^{-2}$) directly contacts the cell. The coarser grid (e.g. wire diameter of 0.25 mm, 100 meshes.cm$^{-2}$), completely covers the finer grid. The current and voltage leads are attached to the coarser grid.

The thermocouple for measuring the cell temperature should be as close as possible to the gas inlet of the cell and the measuring point should be in the solid material of the cell housing (not in the gas flow). It is recommended to apply additional thermocouples for monitoring the temperature profile from gas inlet to outlet.

The test report describes the materials, types and sizes of the current collectors, and the geometry and dimensions of the cell and cell test housing.

## 7 Test programme

The test programme described here consists of three phases.

The first phase comprises the assembly and pre-conditioning of the cell. The degree of specification for this part is limited. Preferably the recommendations of the cell supplier are applied. This phase is concluded with one polarisation curve measurement, as described in a separate test module [2], at the selected nominal operating temperature of this test and at the gas conditions of *3.3*.

The second phase, the performance test, consists of a 20 hours period of galvanostatic controlled, steady-state operation. This phase is started and concluded with a series of polarisation curve measurements at three or five temperatures centred on the selected nominal operating temperature of this test. The polarisation curve measurement itself is described in a separate test module [2].

The third phase is the endurance test. The operating conditions are identical to those of the performance test. Recommended duration of the endurance test is minimum 3000 hours. At each 500 hours interval during the endurance test a single polarisation curve measurement is executed, that is only at the selected operating temperature.
The endurance test is concluded with a series of polarisation curve recordings at three or five temperatures, as described in a separate test module [2].

The test programme is concluded with one polarisation curve measurement, as described in a separate test module [2], at the selected nominal operating temperature of this test and at the gas conditions of *3.3*.

### *7.1 Assembly and pre-conditioning of the cell*

The applied mechanical clamping pressure of the cell is according to the recommendations of the cell manufacturer or according to common practice at the testing organisation.

The start-up of the cell occurs according to the procedure recommended by the cell supplier or by the procedure that is common practice at the testing organisation.

The stabilisation of the cell can be part of the start-up procedure. If this is not the case it is recommended to follow either:

a) The recommendation of the cell supplier
b) The common practice at the testing organisation

c) Galvanostatic operation of the cell at the selected operating temperature, at the gas conditions of *3.3*, for minimum 2 hours, at a current density of 0.3 A.cm$^{-2}$.

The actual testing temperature is an integer multiple of 50°C.

After the start-up and stabilisation of the cell one polarisation curve measurement, as described in a separate test module [2], at the selected nominal operating temperature of this test and at the gas conditions of *3.3* is performed.

A second stabilisation period of minimum 2 hours galvanostatic operation at the selected operating temperature, the gas conditions of *3.2* and a current density of 0.3 A.cm$^{-2}$ is applied before the next phase starts.

Applied conditions and procedure for start-up and stabilisation should be described in the report of the test result.

*7.2 Recording of the initial polarisation curves*

After the start-up and stabilisation phase of *7.1*, cell polarisation curves have to be recorded according to the Test Module M01-SOFC cell polarisation curve [2].

The gas conditions as prescribed in *3.2* are constant during all phases of the polarisation curve measurements.

It is recommended to perform polarisation curve measurements at minimum three operating temperatures, preferably five, each differing 50°C. In that case the first polarisation measurement is at the selected operating temperature.

After completion of the first polarisation curve measurement the cell is brought to the nearest lower temperature. The new temperature is reached if the actual registered cell temperature is within the interval ± 10°C of this new target temperature for 10 minutes. From that moment on, the performance stabilisation period starts.

At the new operating temperature, a performance stabilisation period of 2 hours at 0.3 A.cm$^{-2}$ and at the gas conditions of *3.2* is applied, after which the next procedure for recording the polarisation curve as described in [2] is executed.

The consecutive phases of stabilisation and polarisation curve measurement are repeated at the next 50°C lower temperature.

After the polarisation measurement has been performed at the lowest temperature in the range, the temperature is ramped up to a temperature 50°C higher compared to the one of the first polarisation curve measurement. After the prescribed stabilisation procedure the polarisation curve after [2] is recorded.

The next polarisation curve measurement will be at a 50°C higher temperature.

*Example*

Suppose the selected temperature for steady-state operation in this test is 750°C, then the temperature sequence at which the polarisation measurements are executed is:

- 750-700-650-800-850°C (in case of selecting five temperatures for polarisation measurements)

or

- 750-700-800°C (in case of selecting three temperatures for polarisation measurements).

*7.3 Steady-state operation for performance evaluation*

This test phase starts immediately after completion of the polarisation recordings described in *7.2*.

The performance test is under galvanostatic control at the selected operating temperature, and the gas conditions and current density of *3.2*.

The duration of the steady-state operation is 20 hours.

*7.4 Recording of the second series of polarisation curves*

This series of polarisation curves make-up the conclusion of the short-term performance test, and the start of the long-term endurance test.

The measurement procedure for recording the second series of polarisation curves is exactly identical to the initial series described in *7.2*.

*7.5 Steady-state operation for endurance evaluation*

This test phase starts immediately after completion of the polarisation recordings described in *7.4*.

The performance test is under galvanostatic control at the selected operating temperature, and the gas conditions and current density of *3.2*.

The duration of the steady-state operation is minimum 3000 hours.

Every 500 hours a single polarisation curve, only at the selected operating temperature, is recorded according to the procedure described in [2] and at the gas conditions prescribed by *3.2* in this procedure.

*7.6 Recording of the last series of polarisation curves*

This series of polarisation curves make-up the conclusion of the long-term endurance test.

The measurement procedure for recording the last series of polarisation curves is exactly identical to the initial series described in *7.2*.

A final stabilisation period of minimum 2 hours galvanostatic operation at the selected operating temperature, the gas conditions of *3.3* and a current density of 0.3 $A.cm^{-2}$ is applied before the programme is ended.

One final polarisation curve measurement, as described in a separate test module [2], at the selected nominal operating temperature of this test and at the gas conditions of *3.3* is performed.

## 8 Presentation of results

The presentation of the results should at least include:

- a description of the geometry and materials of the test housing: particularly the oxidant and fuel flow patterns
- a description of size and geometry of the cell
- the start-up procedure
- the stabilisation procedure
- the operating temperature of the test
- the statement that the test procedure described here has been applied and any intentional or accidental deviations from this test programme

or

- the actual test conditions: fuel composition and flow, oxidant composition and flow, current density.

The results of the short-term performance test should be presented by both:

- a graph representing the cell voltage versus the operating time
- a table representing the Open Circuit Voltage (OCV), the current density at 0.7 and 0.8 V and the Area Specific cell Resistance (ASR), as recorded by or calculated from all the polarisation curve measurements.

The degradation/endurance results should be presented by both:

- a graph representing the cell voltage versus the operating time
- a table representing the Open Circuit Voltage (OCV), the current density at 0.7 and 0.8 V and the Area Specific cell Resistance (ASR), as recorded by or calculated from all the polarisation curve measurements.

The definition and calculation of the ASR is described in [2].

The test report should include the results of the polarisation curve measurements yielded during this test. The presentation of the polarisation data is provided by [2].

A proposed test result report is presented in Annex A.

# Annex A Test report template

***General information***

| | | | |
|---|---|---|---|
| Test programme | | Test date | |
| Test version | | Company performing test | |
| Company requesting test | | Test location | |
| Test request nr | | Test cell/equipment | |

***Test object description***

| | | | |
|---|---|---|---|
| Object manufacturer | | Object weight [kg] | |
| Fuel cell technology | | Object dimensions Length×Width×Height ($cm^3$) | |
| Object type | | Object nominal power [W] | |
| Product number | | Object peak power [W] | |
| Test object identification nr | | Object voltage range [V] | |

***Test set-up***

| |
|---|
| *Sketch of test set-up, including sensor locations* |

***Cell test housing***

- Description of materials, grid types, geometry and sizes of the test housing.

***Pre-conditioning of the cell***

- Description of the start-up and stabilisation process.
- Applied mechanical clamping force.

***Test procedure***

- Reference to this test procedure.
- Any intentional or accidental deviations.

***Test results***

Performance test

- Graph representing the cell voltage versus the operating time
- Table representing the OCV, the current density at 0.7 V and the ASR recorded by or calculated from the polarisation curve measurements at all T and t.

Endurance test

- Graph representing the cell voltage versus the operating time
- Table representing the OCV, the current density at 0.7 V and the ASR recorded by or calculated from the polarisation curve measurements at all T and t.

Polarisation curves

- As described in [2]

# APPENDIX D



## SOFC cell polarisation curve

Test module for measurement of the voltage as function of the current density as a generic method for evaluating the performance of single SOFC cells.

Test input ..... Current density
Test output ..... Voltage

Class of test object..... Cell
Class of application..... Generic

Authors ..... Bert Rietveld, Arno Janssen
Revision date ..... 09-04-2010

**Revision history**

| Version | Change | Date | Status | Text / revision by |
|---|---|---|---|---|
| 1 | | 23-10-2006 | Draft | Bert Rietveld |
| 2 | | 10-10-2008 | Draft | Arno Janssen |
| 3 | | 08-05-2009 | Draft | Arno Janssen |
| 4 | | 09-04-2010 | Final | Arno Janssen |

# Table of Contents

**1 Objective and scope ..... 3**

**2 Terminology, definitions and symbols ..... 3**
2.1 Terminology and definitions ..... 3
2.2 Symbols ..... 3

**3 Test inputs ..... 3**
3.1 Variable test inputs ..... 3
3.2 Static test inputs ..... 4

**4 Test outputs ..... 4**

**5 References, required documentation and provisions ..... 4**
5.1 References and required documentation ..... 4
5.2 Provisions ..... 4

**6 Test equipment and experimental set-up ..... 4**

**7 Test procedure ..... 4**
7.1 Pre-conditioning the cell ..... 4
7.2 Recording of the polarisation curve ..... 4

**8 Presentation of results ..... 5**

## 1 Objective and scope

Test module for measurement of the voltage as function of the current density as a generic method for evaluating the performance of single SOFC cells.

This module is applied in combination with a test programme, which will describe the operating conditions of the cell.

## 2 Terminology, definitions and symbols

### *2.1 Terminology and definitions*

Terminology and definitions used in this document are according to the FCTESTnet Fuel Cells Glossary.

Additional terminology and definitions are:

*Cell area*

- The (effective) cell area is defined as the area of the zone in which all cell components, that is anode, electrolyte and cathode, and the anode and cathode current collectors overlap.

### *2.2 Symbols*

Symbols for physical quantities are defined in the Handbook of Chemistry and Physics, 69th Edition, CRC Press. Below additional symbols are defined.

| Symbol | Formula definition | Unit | Description |
|---|---|---|---|
| $A_{cell}$ | Cell area | $cm^2$ | Effective cell area |
| $X_{fuel}$ | | - | Volume composition of fuel |
| $X_{ox}$ | | - | Volume composition of oxidant |
| $q_{fuel}$ | $q_{v,fuel} / A_{cell}$ | $ml.min^{-1}.cm^{-2}$ | Volume flow of fuel per unit cell area (STP) |
| $q_{ox}$ | $q_{v,ox} / A_{cell}$ | $ml.min^{-1}.cm^{-2}$ | Volume flow of oxidant per unit cell area (STP) |

## 3 Test inputs

### *3.1 Variable test inputs*

| Input | Description | Range | Tolerance |
|---|---|---|---|
| J | Current density | 0 - n x 0.05 - 1.25 $A.cm^{-2}$ *) | ± 5 $mA.cm^{-2}$ |
| $t_{hold}$ | Hold time at current step | 10 seconds | ± 1 second |

*) Either this maximum current density or the limiting cell voltage of 0.6 V

*3.2 Static test inputs*

| Input | Description | Value | Tolerance |
|---|---|---|---|
| $X_{fuel}$ | Fuel composition | From test programme | - |
| $q_{fuel}$ | Fuel flow (STP) | From test programme | - |
| $X_{ox}$ | Oxidant composition | From test programme | - |
| $q_{ox}$ | Oxidant flow (STP) | From test programme | - |
| $T_{cell}$ | Inlet temperature (°C) | From test programme | - |

## 4 Test outputs

| Output | Description | Range | Accuracy | Sample Rate |
|---|---|---|---|---|
| V | Cell voltage | 0.3 - 1.50 V | ± 5 mV | > 1 $sec^{-1}$ |

## 5 References, required documentation and provisions

*5.1 References and required documentation*

[1] FCTESTnet Fuel Cells Glossary

[2] Test procedure (e.g. 05-HD Cell Performance and Endurance-H2 v2.doc)

*5.2 Provisions*

Standard local safety precautions for working with the concerning gaseous fuels, electrical installations and chemicals contained by the SOFC have to be respected.

## 6 Test equipment and experimental set-up

Test equipment and experimental set-up are determined by the test programme that invokes this module.

## 7 Test procedure

*7.1 Pre-conditioning the cell*

The start-up and pre-conditioning of the cell are determined by the test programme that invokes this module.

*7.2 Recording of the polarisation curve*

The recording of current-voltage (polarisation) curves is under galvanostatic control, starting at the open circuit voltage using a fixed current step size and holding time as prescribed in *3.1*. Gas compositions, flow rates and the temperature are constant during the measurement and are determined by the test programme that invokes this module.

At higher current densities considerable heating of the cell may occur. Therefore, it is recommended to monitor the cell temperature during the whole measurement procedure.

The characteristic value of the cell voltage at each current density step is taken as the average value over the last 5 seconds of each current step.

It is generally recommended not to allow cell voltages lower than 0.6 V. When this value is yielded before getting at the maximum current density the scan should be stopped.

Once the maximum current density of 1.25 A.cm$^{-2}$ or the limiting cell voltage of 0.6 V has been achieved the measurement is stopped, that is the operation parameters are set to the values prescribed by the test programme that invokes this module.

*Recommendation*
Instead of stopping the measurement at the maximum current density or the limiting cell voltage, the scan can be reversed applying the same step size and holding time. If the measurement is continued with a reversed scan, it should be started immediately after conclusion of the forward scan, i.e. immediately after the last hold of 10 seconds.

## 8 Presentation of results

The presentation of the results should at least include:

- the statement that the measurement procedure described here has been applied and any intentional or accidental deviations from this measurement procedure

or

- the actual parameters of the measurement, i.e. control mode (galvanostatic or potentiostatic), starting voltage, step size, hold time, et cetera.

The polarisation data should be presented by both:

- A two-dimensional graph with the current density on the abscissa (x-axis) and the cell voltage and the cell inlet temperature on the ordinate (y-axis). In case a reverse scan is done, the forward and backward scan should be plotted in the same graph.
- The following numeric data (see example table below):
  - The open circuit voltage (OCV), i.e. the cell voltage at a current density of zero.
  - The current density at 0.7 and 0.8 Volt.
  - The Area Specific cell Resistance (ASR) which is defined by dV/dJ at 0.8 V and is determined from the slope of the best fitting line over the measurement data within and including the interval 0.75 - 0.85 V.

| | |
|---|---|
| OCV [V] | |
| J @ 0.7 V [A.cm$^{-2}$] | |
| J @ 0.8 V [A.cm$^{-2}$] | |
| ASR @ 0.8 V [Ω.cm$^{2}$] | |

# APPENDIX E

## Reference state test plan

As it was briefly presented in the previous chapter, the reference state plan is focused on the fuel cell testing in accordance with the FCTESTNET procedures but also with specific volumetric fuel flows recommended by the FClab and the supplier A. This test plan is designed to verify the performance of the cell at these specific volumetric fuel flows and also at different temperatures.

In the table below is presented list of the polarizations which form the reference state plan.

*Reference state test plan*

| ASC 700 3-10 | | | | | | | | Cell active area: | | 50 $cm^2$ | |
|---|---|---|---|---|---|---|---|---|---|---|---|
| Name | | T | $H_2$ | | $N_2$ | | Air | | $H_2$ | $D_{N2}$ | λ | T |
| std. | Pn | °C | Nl/h | Nl/h cm2 | Nl/h | Nl/h cm2 | Nl/h | Nl/h cm2 | Nl/h cm2 | - | - | °C |
| FClab standard | **P1** | 750 | 48,5 | 0,97 | 0 | 0 | 112,5 | 2,25 | 0,97 | 0 | 0,97 | 800 |
| | **P2** | 750 | 48,5 | 0,97 | 0 | 0 | 112,5 | 2,25 | 0,97 | 0 | 0,97 | 800 |
| | **P3** | 750 | 48,5 | 0,97 | 0 | 0 | 112,5 | 2,25 | 0,97 | 0 | 0,97 | 800 |
| | **P4** | 700 | 48,5 | 0,97 | 0 | 0 | 112,5 | 2,25 | 0,97 | 0 | 0,97 | 750 |
| | **P5** | 700 | 48,5 | 0,97 | 0 | 0 | 112,5 | 2,25 | 0,97 | 0 | 0,97 | 750 |
| | **P6** | 700 | 48,5 | 0,97 | 0 | 0 | 112,5 | 2,25 | 0,97 | 0 | 0,97 | 750 |
| | **P7** | 800 | 48,5 | 0,97 | 0 | 0 | 112,5 | 2,25 | 0,97 | 0 | 0,97 | 700 |
| | **P8** | 800 | 48,5 | 0,97 | 0 | 0 | 112,5 | 2,25 | 0,97 | 0 | 0,97 | 700 |
| | **P9** | 800 | 48,5 | 0,97 | 0 | 0 | 112,5 | 2,25 | 0,97 | 0 | 0,97 | 700 |
| FCTESTNET standard | **P10** | 750 | 52,5 | 1,05 | 0 | 0 | 124,5 | 2,49 | 1,05 | 0 | 1,00 | 700 |
| | **P11** | 750 | 52,5 | 1,05 | 0 | 0 | 124,5 | 2,49 | 1,05 | 0 | 1,00 | 750 |
| | **P12** | 750 | 52,5 | 1,05 | 0 | 0 | 124,5 | 2,49 | 1,05 | 0 | 1,00 | 750 |
| | **P13** | 700 | 52,5 | 1,05 | 0 | 0 | 124,5 | 2,49 | 1,05 | 0 | 1,00 | 700 |
| | **P14** | 700 | 52,5 | 1,05 | 0 | 0 | 124,5 | 2,49 | 1,05 | 0 | 1,00 | 700 |
| | **P15** | 700 | 52,5 | 1,05 | 0 | 0 | 124,5 | 2,49 | 1,05 | 0 | 1,00 | 800 |
| | **P16** | 800 | 52,5 | 1,05 | 0 | 0 | 124,5 | 2,49 | 1,05 | 0 | 1,00 | 800 |
| | **P17** | 800 | 52,5 | 1,05 | 0 | 0 | 124,5 | 2,49 | 1,05 | 0 | 1,00 | 800 |
| | **P18** | 800 | 52,5 | 1,05 | 0 | 0 | 124,5 | 2,49 | 1,05 | 0 | 1,00 | 800 |
| Supplier A standard | **P19** | 750 | 24 | 0,48 | 0 | 0 | 60 | 1,2 | 4,5 | 0 | 1,05 | 800 |
| | **P20** | 750 | 24 | 0,48 | 0 | 0 | 60 | 1,2 | 4,5 | 0 | 1,05 | 800 |
| | **P21** | 750 | 24 | 0,48 | 0 | 0 | 60 | 1,2 | 4,5 | 0 | 1,05 | 800 |
| | **P22** | 700 | 24 | 0,48 | 0 | 0 | 60 | 1,2 | 4,5 | 0 | 1,05 | 750 |
| | **P23** | 700 | 24 | 0,48 | 0 | 0 | 60 | 1,2 | 4,5 | 0 | 1,05 | 750 |
| | **P24** | 700 | 24 | 0,48 | 0 | 0 | 60 | 1,2 | 4,5 | 0 | 1,05 | 750 |
| | **P25** | 800 | 24 | 0,48 | 0 | 0 | 60 | 1,2 | 4,5 | 0 | 1,05 | 700 |
| | **P26** | 800 | 24 | 0,48 | 0 | 0 | 60 | 1,2 | 4,5 | 0 | 1,05 | 700 |
| | **P27** | 800 | 24 | 0,48 | 0 | 0 | 60 | 1,2 | 4,5 | 0 | 1,05 | 700 |
| | | | anode | | | | cathode | | anode | | cathode | |

Presented above test plan consist of twenty seven polarizations. Each single polarization contains all required test input information - cell temperature, volumetric flow and specific volumetric flow volumetric for all input gasses. The plan contains also expected test outputs ($q_{H2,}$ $D_{N2,}$ $\lambda$ and T) which are dependent on the inputs – what was discussed in the third chapter. Moreover it should be noticed, that the polarizations are divided based on the standards - according to which they are developed. The table above consists also division on the anode input gases and cathode input gases (in the test input part). The similar division is applied in the part named expected test outputs – what helps in fast identification of the conditions of the test.

## Reference state test elaborating

The results obtained from performed reference state polarizations were elaborated into the three reports using Microsoft Office Excel software. The reports are named A, B and C report from performed as the first, second and third report, respectively. Report A is focused on all single performed polarization. Example of one of this report is presented below.

**POLARIZATION P5** **ASC700 3-10** **Active area 50 cm2**

| Name | Date | T | $H_2$ | | $N_2$ | | Air | | $H_2O$ | λ | $DN_2$ |
|---|---|---|---|---|---|---|---|---|---|---|---|
| PN | - | °C | Nl/h | Nl/hcm$^2$ | Nl/h | Nl/hcm$^2$ | Nl/hcm$^2$ | Nl/h | Nl/h | - | - |
| **P5** | **23.11.2010** | **754,68** | **48,47** | **0,97** | **0,00** | **0,00** | **113,00** | **2,26** | **RT** | **0,98** | **0** |

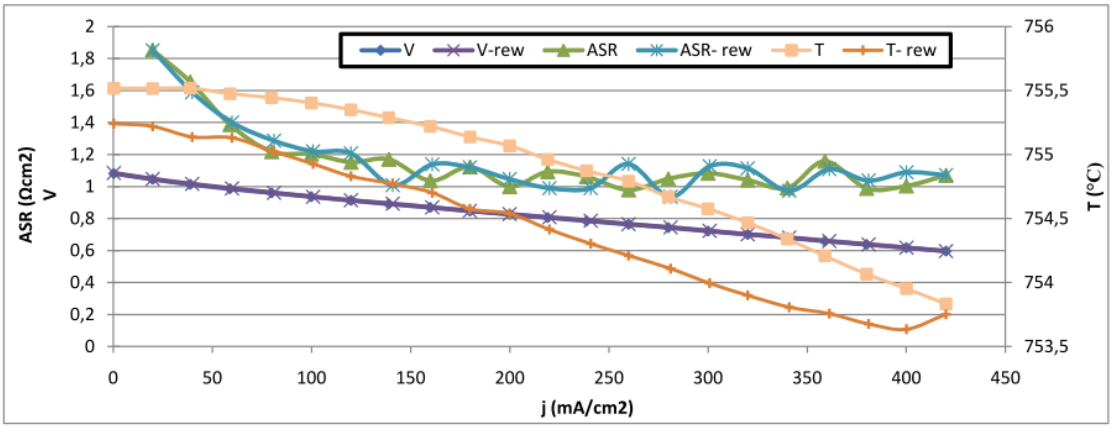


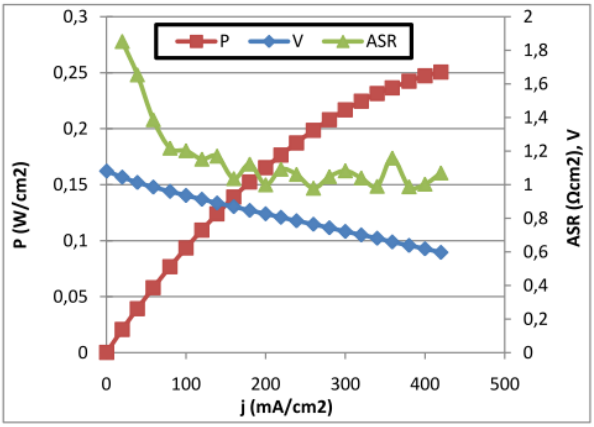


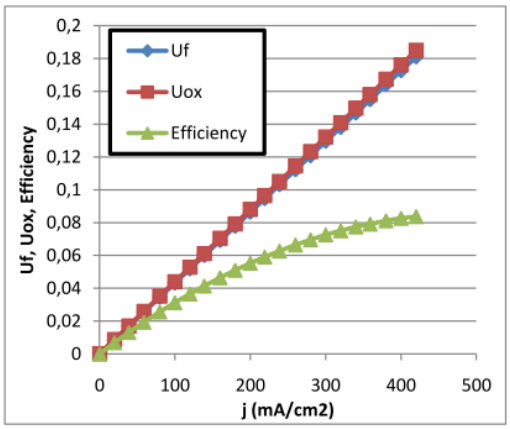


| Control mode | galvanostatic | Step size (A) | 1 |
|---|---|---|---|
| Starting voltage (V) | - | Hold time (s) | 19 |
| ASR @ 0,8 V | 1,027 | | Ωcm$^2$ |
| ASR @ 0,7 V | 1,073 | | Ωcm$^2$ |
| OCV | 1,083 | | V |
| J max | 420,04 | | mA/cm$^2$ |
| P max | 0,25 | | W/cm$^2$ |
| J @ 0,8 V | 219,52 | | mA/cm$^2$ |
| J @ 0,7 V | 319,98 | | mA/cm$^2$ |

*Example of reference state test report A*

Report above contains all information about the test conditions and also the test results. From the top left to top right part of this report, there are placed

- the polarization number - POLARIZATION P5,
- the cell model and its number - ASC700 3-10,

and also the cell active area which amounts of 50 cm$^2$.

Below in a table there are placed the polarization number and the date of the test – P5 and 23.11.2010, respectively. Next in the same table there are listed the test conditions:

- temperature - 754,65 °C,
- volumetric flow and specific volumetric flow of hydrogen - 48,47 Nl/h and 0,97 Nl/h $cm^2$, respectively,
- volumetric flow and specific volumetric flow of nitrogen - 0 Nl/h and 0 Nl/h $cm^2$,
- and also volumetric flow and specific volumetric flow of air 113 Nl/h and 2,26 Nl/h $cm^2$, respectively,
- water volumetric flow – water content in the fuel flow mixture at reference conditions (25 °C and 1 bar).

For these conditions the volumetric flow of water always is equal of three percent of the total volumetric flow of the fuel mixture. At the end of this table, there can be found calculated values of $\lambda$ and $D_{N2}$ parameters – 0,98 and 0 respectively.

In the main chart below are shown forward and backward voltage, area specific resistance and temperature as a function of current density, during the polarization test.

In the next two charts below, there are presented the forward specific power, area specific resistance and voltage versus current density (chart on the right), and also forward fuel utilization coefficient, oxidant utilization coefficient and efficiency as a function of current density (chart on the left).

All presented in the thesis polarizations were performed as a reversible scan, what means that each single test consist one forward and backward polarization.

At the bottom of this report (in the table) can be found following information:

- control mode - galvanostatic (in all performed tests),
- starting voltage -
- step size – 1A (also the same in all performed tests - what gives 0,05A/$cm^2$),
- hold time – 19 s (the time of measurements at single step),
- ASR at 0,8V – 1,027 $\Omega cm^2$,
- ASR at 0,7 V – 1,073 $\Omega cm^2$,
- OCV – 1,083 V,
- Jmax – 420,04 mA/$cm^2$,
- Pmax – 0,25 W/$cm^2$,
- J at 0,8 V – 219,52 mA/$cm^2$,
- J at 0,7 V - 319,98 mA/$cm^2$.

Presented above example as well as the all rest performed measurements and reports are applied to the FCTESTNET procedures – which are included in the appendix C and D. At this point it should be also noted that the hold time ($t_{hold}$) recommended by the reference procedures is 10 s. In all performed and presented in this thesis tests this time is longer and amounts around 20 s. This fact is due to the internal FClab procedures which were developed during test activity – longer time at the given step gives more measured points what in turn results in more precise measurement output value.

The table with performed reference state polarizations is presented below.

*List of reference state test reports A*

| ASC700 3-10 | | | | | | | | Cell active area: | | 50 cm$^2$ | | |
|---|---|---|---|---|---|---|---|---|---|---|---|---|
| **Name** | | **Date** | **T** | **$H_2$** | **$N_2$** | **Air** | **$H_2O$** | **λ** | **$D_{N2}$** | **ASR at 0,8 V** | **ASR at 0,7 V** | **OCV** |
| *std.* | *Pn* | - | *°C* | *Nl/hcm$^2$* | *Nl/hcm$^2$* | *Nl/hcm$^2$* | *Nl/h* | - | - | *Ωcm2* | *Ωcm2* | *V* |
| **Fclab standard** | **P1** | 19.11.2010 | 804,4 | 0,97 | 0 | 2,26 | RT | 0,98 | 0 | 0,66 | 0,69 | 1,07 |
| | **P2** | 22.11.2010 | 804,6 | 0,97 | 0 | 2,26 | RT | 0,98 | 0 | 0,67 | 0,71 | 1,07 |
| | **P3** | 22.11.2010 | 804,6 | 0,97 | 0 | 2,26 | RT | 0,98 | 0 | 0,67 | 0,71 | 1,06 |
| | **P4** | 23.11.2010 | 754,6 | 0,97 | 0 | 2,26 | RT | 0,98 | 0 | 1,05 | 1,05 | 1,08 |
| | **P5** | 23.11.2010 | 754,7 | 0,97 | 0 | 2,26 | RT | 0,98 | 0 | 1,03 | 1,07 | 1,08 |
| | **P6** | 23.11.2010 | 755,0 | 0,97 | 0 | 2,26 | RT | 0,98 | 0 | 1,04 | 1,04 | 1,08 |
| | **P6a** | 23.11.2010 | 755,1 | 0,97 | 0 | 2,26 | RT | 0,98 | 0 | 1,03 | 1,03 | 1,08 |
| | **P7** | 24.11.2010 | 704,5 | 0,97 | 0 | 2,26 | RT | 0,98 | 0 | 1,64 | 1,59 | 1,10 |
| | **P8** | 24.11.2010 | 704,4 | 0,97 | 0 | 2,26 | RT | 0,98 | 0 | 1,64 | 1,52 | 1,10 |
| | **P9** | 24.11.2010 | 704,5 | 0,97 | 0 | 2,26 | RT | 0,98 | 0 | 1,57 | 1,58 | 1,10 |
| **FCTESTNET standard** | **P10** | 29.11.2010 | 755,3 | 1,1 | 0 | 2,5 | RT | 1,0 | 0 | 1,08 | 1,11 | 1,09 |
| | **P11** | 29.11.2010 | 755,2 | 1,0 | 0 | 2,5 | RT | 1,0 | 0 | 1,07 | 1,08 | 1,09 |
| | **P12** | 29.11.2010 | 755,2 | 1,0 | 0 | 2,5 | RT | 1,0 | 0 | 1,07 | 1,08 | 1,09 |
| | **P13** | 29.11.2010 | 755,2 | 1,0 | 0 | 2,5 | RT | 1,0 | 0 | 1,08 | 1,08 | 1,09 |
| | **P14** | 30.11.2010 | 704,9 | 1,1 | 0 | 2,5 | RT | 1,0 | 0 | 1,68 | 1,63 | 1,11 |
| | **P15** | 30.11.2010 | 704,8 | 1,1 | 0 | 2,5 | RT | 1,0 | 0 | 1,66 | 1,64 | 1,10 |
| | **P16** | 30.11.2010 | 704,8 | 1,1 | 0 | 2,5 | RT | 1,0 | 0 | 1,66 | 1,60 | 1,10 |
| | **P17** | 3.12.2010 | 805,5 | 1,1 | 0 | 2,5 | RT | 1,0 | 0 | 0,74 | 0,83 | 1,08 |
| | **P18** | 3.12.2010 | 805,4 | 1,1 | 0 | 2,5 | RT | 1,0 | 0 | 0,72 | 0,79 | 1,08 |
| | **P19** | 6.12.2010 | 805,3 | 1,1 | 0 | 2,5 | RT | 1,0 | 0 | 0,81 | 0,85 | 1,08 |
| **Supplier A standard** | **P20** | 2.12.2010 | 804,0 | 0,48 | 0 | 1,2 | RT | 1,05 | 0,0 | 0,8 | 0,9 | 1,04 |
| | **P21** | 2.12.2010 | 803,7 | 0,48 | 0 | 1,2 | RT | 1,05 | 0,0 | 0,8 | 0,9 | 1,04 |
| | **P22** | 6.12.2010 | 803,8 | 0,48 | 0 | 1,2 | RT | 1,05 | 0,0 | 0,9 | 1,0 | 1,04 |
| | **P23** | 6.12.2010 | 753,8 | 0,48 | 0 | 1,2 | RT | 1,05 | 0,0 | 1,3 | 1,3 | 1,05 |
| | **P24** | 6.12.2010 | 753,7 | 0,48 | 0 | 1,2 | RT | 1,05 | 0,0 | 1,3 | 1,3 | 1,05 |
| | **P25** | 6.12.2010 | 753,8 | 0,48 | 0 | 1,2 | RT | 1,05 | 0,0 | 1,3 | 1,3 | 1,05 |
| | **P26** | 7.12.2010 | 703,6 | 0,48 | 0 | 1,2 | RT | 1,05 | 0,0 | 2,0 | 2,0 | 1,07 |
| | **P27** | 7.12.2010 | 703,5 | 0,48 | 0 | 1,2 | RT | 1,05 | 0,0 | 2,1 | 2,0 | 1,07 |
| | **P28** | 7.12.2010 | 703,6 | 0,48 | 0 | 1,2 | RT | 1,05 | 0,0 | 2,1 | 2,0 | 1,07 |

Next step in elaborating data is to calculate the average output values for performed at the same conditions polarizations. For this purpose presented above polarizations were grouped and elaborated according to the standard and the temperature at which they were performed/tested. The tests grouped in such a way are the inputs for reports B. One of these reports based on polarizations P17, P18 and P19 is shown below.

**RREPORT B** ***FClab standard***

**ASC700 3-10** **Active area** **50 cm2**

| Name | Date | T | $H_2$ | $N_2$ | Air | $H_2O$ | λ | $DN_2$ |
|---|---|---|---|---|---|---|---|---|
| PN | - | °C | Nl/hcm$^2$ | Nl/hcm$^2$ | Nl/hcm$^2$ | Nl/h | - | - |
| **P17** | **3.12.2010** | **805,49** | **1,05** | **0,00** | **2,49** | **RT** | **1,00** | **0,00** |
| **P18** | **3.12.2010** | **805,41** | **1,05** | **0,00** | **2,49** | **RT** | **1,00** | **0,00** |
| **P19** | **6.12.2010** | **805,35** | **1,05** | **0,00** | **2,49** | **RT** | **1,00** | **0,00** |

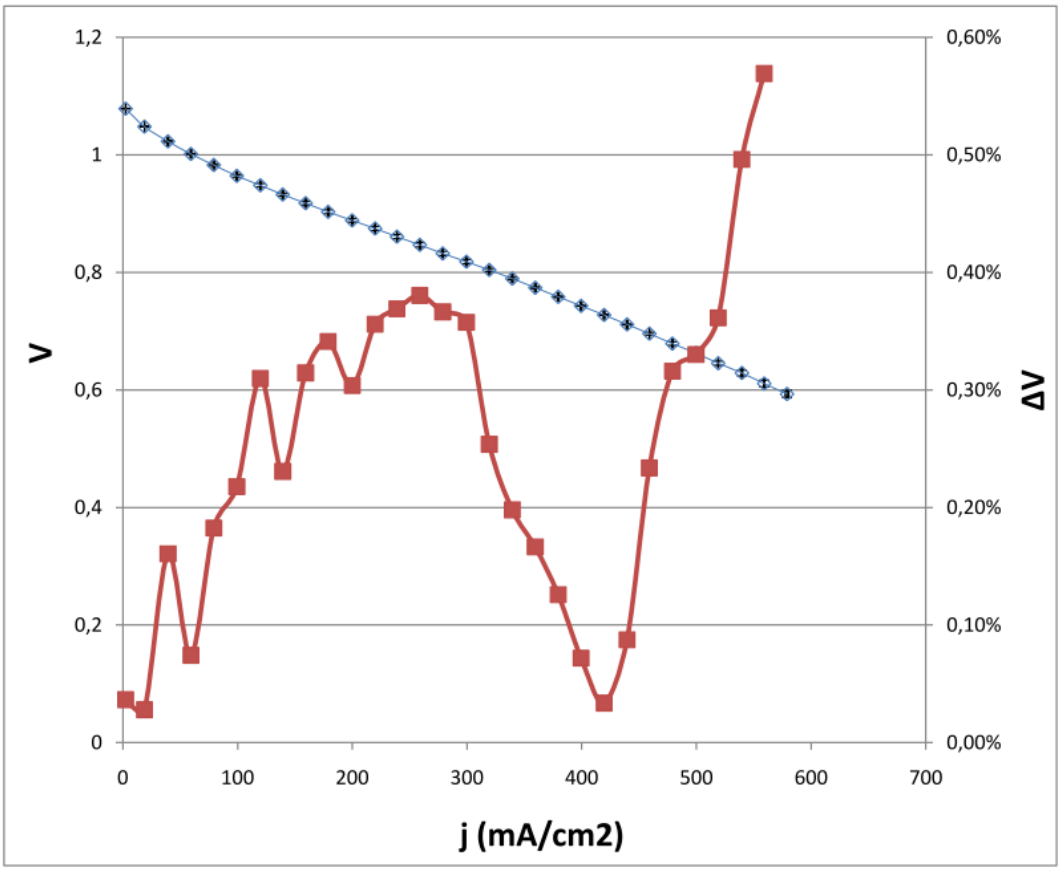


| Name | T | $H_2$ | λ | $DN_2$ | OCV | ASR at 0,8V | ASR at 0,7V |
|---|---|---|---|---|---|---|---|
| Pn-n | °C | Nl/hcm$^2$ | - | - | V | Ωcm$^2$ | Ωcm$^2$ |
| **P17-19** | **805,4** | **1,05** | **1,00** | **0** | **1,08** | **0,73** | **0,81** |

*Example of reference state test report B*

Example of report B presented above contains information about all polarizations based on which it is elaborated (in this case P17, P18, P19). These polarizations were performed according to the FClab standard (the same gas flows conditions - $D_{N2}$, λ, $q_{H2}$) and also all of them were performed at the same temperature of around 805,4 °C.

The output of this report is the average polarization within three or more polarizations performed at the same conditions. It should be noted, that the polarization result (presented in

the report chart) is the average of the polarizations performed (report A) with a deviation for each point (voltage) smaller than 5% - also shown in the chart. The output of this report is not only polarization but also the ASR and the OCV values. The main purpose of these reports is to evaluate the repeatability of the tests.

List of all performed reference state reports B is presented below.

*List of reference state test reports B*

| Name | | T | $H_2$ | λ | $DN_2$ | OCV | ASR at 0,8V | ASR at 0,7V |
|---|---|---|---|---|---|---|---|---|
| std. | Pn-n | °C | Nl/hcm$^2$ | - | - | V | Ωcm$^2$ | Ωcm$^2$ |
| **FClab** | **P1-3** | 804,53 | 0,97 | 0,98 | 0 | 1,07 | 0,67 | 0,70 |
| | **P4-6a** | 754,87 | 0,97 | 0,98 | 0 | 1,08 | 1,04 | 1,05 |
| | **P7-9** | 704,50 | 0,97 | 0,98 | 0 | 1,10 | 1,62 | 1,56 |
| **FCTEST NET** | **P10-13** | 755,2 | 1,05 | 1,00 | 0 | 1,09 | 1,07 | 1,09 |
| | **P14-16** | 704,8 | 1,05 | 1,00 | 0 | 1,10 | 1,67 | 1,63 |
| | **P17-19** | 805,4 | 1,05 | 1,00 | 0 | 1,08 | 0,73 | 0,81 |
| **Supplier A** | **P20-22** | 803,8 | 0,48 | 1,05 | 0 | 1,04 | 0,81 | 0,91 |
| | **P23-25** | 753,8 | 0,48 | 1,05 | 0 | 1,05 | 1,29 | 1,27 |
| | **P26-28** | 703,6 | 0,48 | 1,05 | 0 | 1,07 | 2,06 | 2,02 |

Finally based on reports all B reports presented in the table above report C was elaborated. The output of report C is the sensitive analysis of ASR varying with one or more parameters and keeping constant all the others. In fact the report is the result of sensitivity to one or more parameters.

In the case of tests performed at reference state conditions, the varying parameter is temperature, whereas constant values are λ, $D_{N2}$ and $q_{H2.}$ Below is presented final report for all reference state performed test.

The output of the repot C are two charts, where in the first one is presented ASR sensitivity and in the second one OCV sensitivity as a function of temperature for both of them. In the following chapter conclusions and further results applied in the thesis are discussed.

What more should be noted is that the all files (reports A, reports B, final report C and others) with presented so far results as well as for these ones presented in the following chapters are included in appendix H (CD).

This appendix contains CD with all performed polarizations, reports and other used in the thesis files and documents.

## APPENDIX F

## Reference state variation test plan

As it was previously discussed, the next test plan is based on the modifications in the reference state test procedure. The main aim of the test activity is constancy the same – evaluation of the performance parameters. However, in this case, the main goal of the reference state variation plan is to define how the investigated parameters depend on the fuel quality and air quantity - DN2 and λ, respectively. For this purpose, the reference state variation test plan presented in table below was developed.

*Reference state variation test plan*

| ASC 700 3-10 | | | | | Cell active area | | | | 50 | cm$^2$ | | |
|---|---|---|---|---|---|---|---|---|---|---|---|---|
| Name | | T | H2 | | N2 | | Air | | $q_{H2}$ | $D_{N2}$ | λ | T |
| std. | Pn | °C | Nl/h | Nl/h cm$^2$ | Nl/h | Nl/h cm$^2$ | Nl/h | Nl/h cm$^2$ | Nl/h cm$^2$ | - | - | °C |
| FCTEST NET | p1 | 750 | 52,5 | 1,05 | 0 | 0 | 124,5 | 2,49 | 1,05 | 0 | 1,00 | 750 |
| | p2 | 750 | 52,5 | 1,05 | 0 | 0 | 124,5 | 2,49 | 1,05 | 0 | 1,00 | 750 |
| *λ variations* | p3 | 750 | 52,5 | 1,05 | 0 | 0 | 84,5 | 1,7 | 1,05 | 0 | 0,7 | 750 |
| | p4 | 750 | 52,5 | 1,05 | 0 | 0 | 84,5 | 1,7 | 1,05 | 0 | 0,7 | 750 |
| | p5 | 750 | 52,5 | 1,05 | 0 | 0 | 84,5 | 1,7 | 1,05 | 0 | 0,7 | 750 |
| | p6 | 750 | 52,5 | 1,05 | 0 | 0 | 54,5 | 1,1 | 1,05 | 0 | 0,4 | 750 |
| | p7 | 750 | 52,5 | 1,05 | 0 | 0 | 54,5 | 1,1 | 1,05 | 0 | 0,4 | 750 |
| | p8 | 750 | 52,5 | 1,05 | 0 | 0 | 54,5 | 1,1 | 1,05 | 0 | 0,4 | 750 |
| | p9 | 750 | 52,5 | 1,05 | 0 | 0 | 24,5 | 0,5 | 1,05 | 0 | 0,2 | 750 |
| | p10 | 750 | 52,5 | 1,05 | 0 | 0 | 24,5 | 0,5 | 1,05 | 0 | 0,2 | 750 |
| | p11 | 750 | 52,5 | 1,05 | 0 | 0 | 24,5 | 0,5 | 1,05 | 0 | 0,2 | 750 |
| FCTEST NET | p12 | 750 | 52,5 | 1,05 | 0 | 0 | 124,5 | 2,49 | 1,05 | 0 | 1,00 | 750 |
| | p13 | 750 | 52,5 | 1,05 | 0 | 0 | 124,5 | 2,49 | 1,05 | 0 | 1,00 | 750 |
| *$D_{N2}$ variations* | p14 | 750 | 52,5 | 1,05 | 15 | 0,3 | 124,5 | 2,49 | 1,05 | 0,22 | 1,00 | 750 |
| | p15 | 750 | 52,5 | 1,05 | 15 | 0,3 | 124,5 | 2,49 | 1,05 | 0,22 | 1,00 | 750 |
| | p16 | 750 | 52,5 | 1,05 | 15 | 0,3 | 124,5 | 2,49 | 1,05 | 0,22 | 1,00 | 750 |
| | p17 | 750 | 52,5 | 1,05 | 37,5 | 0,75 | 124,5 | 2,49 | 1,05 | 0,42 | 1,00 | 750 |
| | p18 | 750 | 52,5 | 1,05 | 37,5 | 0,75 | 124,5 | 2,49 | 1,05 | 0,42 | 1,00 | 750 |
| | p19 | 750 | 52,5 | 1,05 | 37,5 | 0,75 | 124,5 | 2,49 | 1,05 | 0,42 | 1,00 | 750 |
| | p20 | 750 | 52,5 | 1,05 | 50 | 1 | 124,5 | 2,49 | 1,05 | 0,49 | 1,00 | 750 |
| | p21 | 750 | 52,5 | 1,05 | 50 | 1 | 124,5 | 2,49 | 1,05 | 0,49 | 1,00 | 750 |
| | p22 | 750 | 52,5 | 1,05 | 50 | 1 | 124,5 | 2,49 | 1,05 | 0,49 | 1,00 | 750 |

It should be noted that also some reference state tests are included in the plan. These tests allowed for checking whether the cell performances are comparable with these ones performed at the beginning of the test activity, or not. This issue is discussed in the following parts of the study.

## Reference state variation test elaborating

As in the previous chapter, the results obtained from performed reference variation state polarizations were elaborated into the three reports – also named A, B and C. Single examples for λ and DN2 variations, like also list of all reports A are presented below in figures and in table below, respectively.

**POLARIZATION p7** **ASC700 3-10** **Active area** **50 cm2**

| Name | Date | T | $H_2$ | | $N_2$ | | Air | | $H_2O$ | λ | $DN_2$ |
|---|---|---|---|---|---|---|---|---|---|---|---|
| PN | - | °C | Nl/h | Nl/hcm$^2$ | Nl/h | Nl/hcm$^2$ | Nl/hcm$^2$ | Nl/h | Nl/h | - | - |
| **p7** | **18.1.2011** | **756,15** | **52,45** | **1,05** | **0,00** | **0,00** | **54,50** | **1,09** | **RT** | **0,44** | **0,0** |

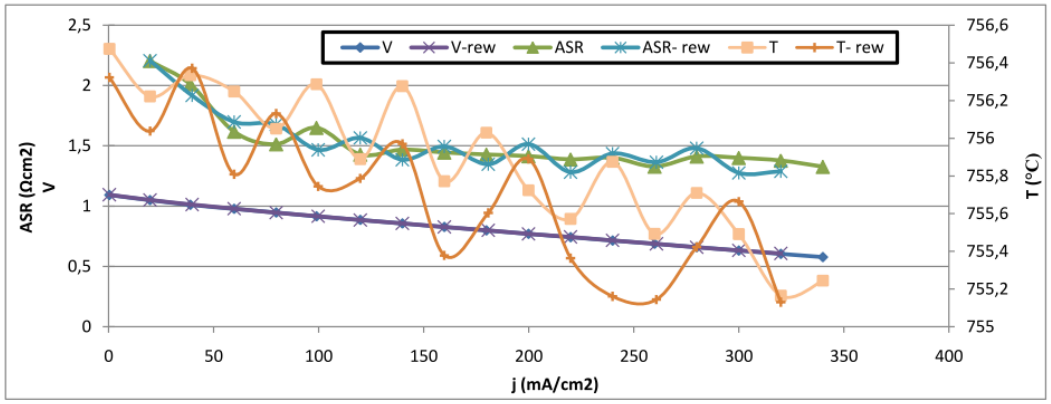


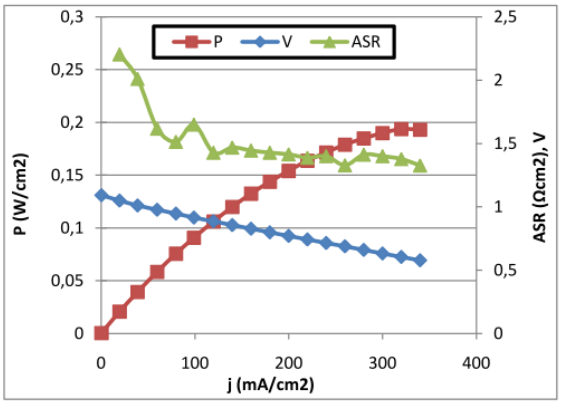


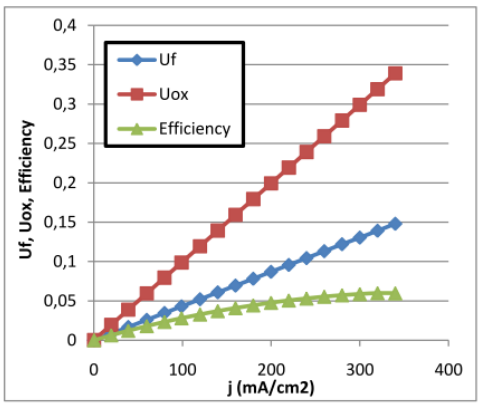


| Control mode | galvanostatic | Step size (A) | 1 |
|---|---|---|---|
| Starting voltage (V) | - | Hold time (s) | 23 |
| ASR @ 0,8 V | 1,413 | | Ωcm2 |
| ASR @ 0,7 V | 1,403 | | Ωcm2 |
| OCV | 1,093 | | V |
| J max | 339,97 | | mA/cm2 |
| P max | 0,19 | | W/cm2 |
| J @ 0,8 V | 180,27 | | mA/cm2 |
| J @ 0,7 V | 250,34 | | mA/cm2 |

*Example of reference state λ variation test report A.*

**POLARIZATION p18** **ASC700 3-10** **Active area** **50 cm2**

| Name | Date | T | $H_2$ | | $N_2$ | | Air | | $H_2O$ | λ | $DN_2$ |
|---|---|---|---|---|---|---|---|---|---|---|---|
| PN | - | °C | Nl/h | Nl/hcm$^2$ | Nl/h | Nl/hcm$^2$ | Nl/hcm$^2$ | Nl/h | Nl/h | - | - |
| p18 | 19.1.2011 | 756,99 | 52,47 | 1,05 | 37,51 | 0,75 | 124,50 | 2,49 | RT | 1,00 | 0,42 |

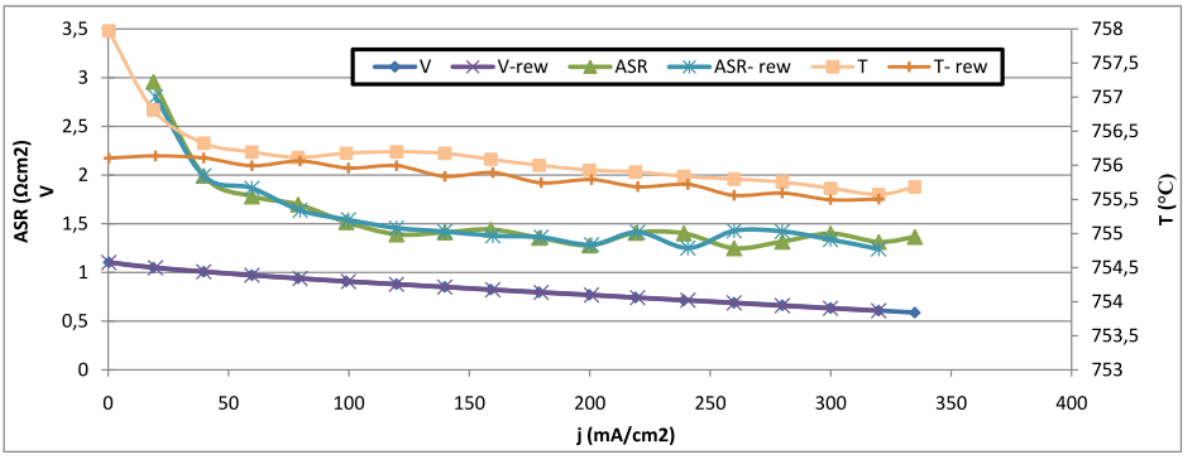


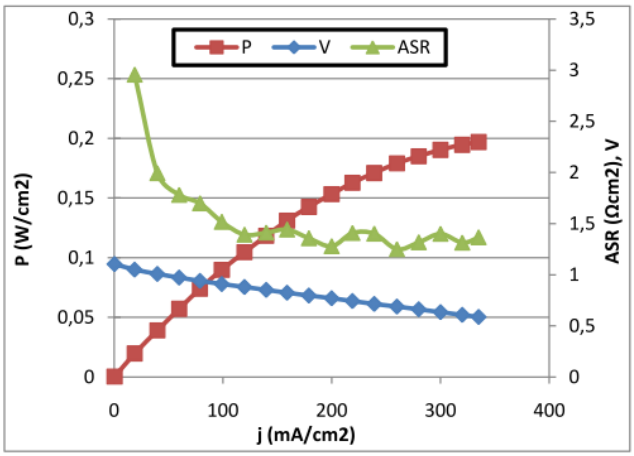


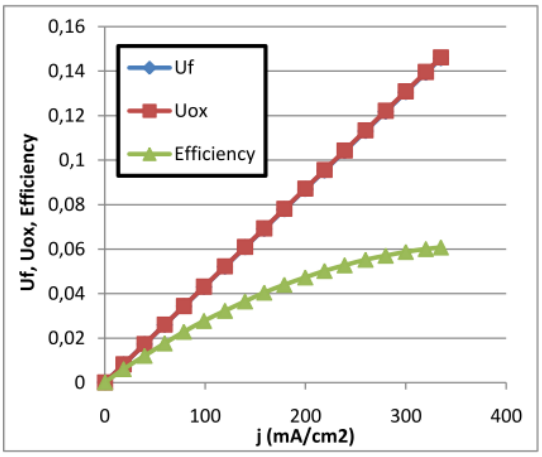


| Control mode | galvanostatic | Step size (A) | 1 |
|---|---|---|---|
| Starting voltage (V) | - | Hold time (s) | 23 |
| ASR @ 0,8 V | 1,364 | | Ωcm2 |
| ASR @ 0,7 V | 1,353 | | Ωcm2 |
| OCV | 1,103 | | V |
| J max | 334,97 | | mA/cm2 |
| P max | 0,20 | | W/cm2 |
| J @ 0,8 V | 179,39 | | mA/cm2 |
| J @ 0,7 V | 259,90 | | mA/cm2 |

*Example of reference state DN2 variation test report A.*

*List of reference state variation tests reports A*

| ASC700 3-10 | | | | | | | | | | Cell active area: | | 50 cm$^2$ |
|---|---|---|---|---|---|---|---|---|---|---|---|---|
| **Name** | | **Date** | **T** | **$H_2$** | **$N_2$** | **Air** | **$H_2O$** | **λ** | **$D_{N2}$** | **ASR at 0,8 V** | **ASR at 0,7 V** | **OCV** |
| **std.** | **Pn** | **-** | **°C** | **Nl/hcm$^2$** | **Nl/hcm$^2$** | **Nl/hcm$^2$** | **Nl/h** | **-** | **-** | **Ωcm2** | **Ωcm2** | **V** |
| FCTEST NET | **p1** | 18.1.2011 | 755 | 1,05 | 0 | 2,5 | RT | 1 | 0 | 1,29 | 1,23 | 1,09 |
| | **p2** | 18.1.2011 | 755 | 1,05 | 0 | 2,5 | RT | 1 | 0 | 1,25 | 1,24 | 1,09 |
| ***λ variations*** | **p3** | 18.1.2011 | 755 | 1,05 | 0 | 1,7 | RT | 0,68 | 0 | 1,39 | 1,34 | 1,09 |
| | **p4** | 18.1.2011 | 755 | 1,05 | 0 | 1,7 | RT | 0,68 | 0 | 1,37 | 1,31 | 1,09 |
| | **p5** | 18.1.2011 | 755 | 1,05 | 0 | 1,7 | RT | 0,68 | 0 | 1,36 | 1,32 | 1,09 |
| | **p6** | 18.1.2011 | 756 | 1,05 | 0 | 1,1 | RT | 0,44 | 0 | 1,40 | 1,38 | 1,09 |
| | **p7** | 18.1.2011 | 756 | 1,05 | 0 | 1,1 | RT | 0,44 | 0 | 1,41 | 1,40 | 1,09 |
| | **p8** | 18.1.2011 | 756 | 1,05 | 0 | 1,1 | RT | 0,44 | 0 | 1,41 | 1,39 | 1,09 |
| | **p9** | 18.1.2011 | 756 | 1,05 | 0 | 0,5 | RT | 0,2 | 0 | 2,40 | 2,94 | 1,09 |
| | **p10** | 18.1.2011 | 756 | 1,05 | 0 | 0,5 | RT | 0,2 | 0 | 2,45 | 2,93 | 1,09 |
| | **p11** | 18.1.2011 | 755 | 1,05 | 0 | 0,5 | RT | 0,2 | 0 | 2,56 | 2,86 | 1,09 |
| FCTEST NET | **p12** | 18.1.2011 | 755 | 1,05 | 0 | 2,5 | RT | 1 | 0 | 1,34 | 1,32 | 1,09 |
| | **p13** | 18.1.2011 | 755 | 1,05 | 0 | 2,5 | RT | 1 | 0 | 1,29 | 1,27 | 1,09 |
| ***$D_{N2}$ variations*** | **p14** | 18.1.2011 | 756 | 1,05 | 0,3 | 2,5 | RT | 1 | 0,22 | 1,28 | 1,24 | 1,10 |
| | **p15** | 18.1.2011 | 755 | 1,05 | 0,3 | 2,5 | RT | 1 | 0,22 | 1,28 | 1,28 | 1,10 |
| | **p16** | 18.1.2011 | 755 | 1,05 | 0,3 | 2,5 | RT | 1 | 0,22 | 1,28 | 1,27 | 1,10 |
| | **p17** | 18.1.2011 | 756 | 1,05 | 0,75 | 2,5 | RT | 1 | 0,42 | 1,30 | 1,30 | 1,10 |
| | **p18** | 19.1.2011 | 756 | 1,05 | 0,75 | 2,5 | RT | 1 | 0,42 | 1,36 | 1,35 | 1,10 |
| | **p19** | 19.1.2011 | 757 | 1,05 | 0,75 | 2,5 | RT | 1 | 0,42 | 1,37 | 1,36 | 1,10 |
| | **p20** | 19.1.2011 | 758 | 1,05 | 1,0 | 2,5 | RT | 1 | 0,49 | 1,41 | 1,40 | 1,10 |
| | **p21** | - | - | - | - | - | - | - | - | - | - | - |
| | **p22** | - | - | - | - | - | - | - | - | - | - | - |

The tests outputs listed in the table above are grouped by the type of the applied modification. It should be noted, that there is no data for polarizations 21 and 22 because of technical problems during the test activity. However, 20$^{th}$ polarization with the same planed test conditions as in the case of p21 and p22 (what can be noticed from the discussed in this part plan) is completed and used for the further analysis.

Next, the reports B were elaborated. The example of this report and list of all reports B is presented in figure and table below, respectively.

**RREPORT B** ***λ variation - FCtestNET***

**ASC700 3-10** **Active area** **50** **cm2**

| Name | Date | T | $H_2$ | $N_2$ | Air | $H_2O$ | λ | $DN_2$ |
|---|---|---|---|---|---|---|---|---|
| pN | - | °C | Nl/hcm$^2$ | Nl/hcm$^2$ | Nl/hcm$^2$ | Nl/h | - | - |
| **p9** | **18.1.2011** | **756,2** | **1,05** | **0,00** | **0,49** | **RT** | **0,20** | **0,0** |
| **p10** | **18.1.2011** | **756,1** | **1,05** | **0,00** | **0,49** | **RT** | **0,20** | **0,0** |
| **p11** | **18.1.2011** | **756,0** | **1,05** | **0,00** | **0,49** | **RT** | **0,20** | **0,0** |

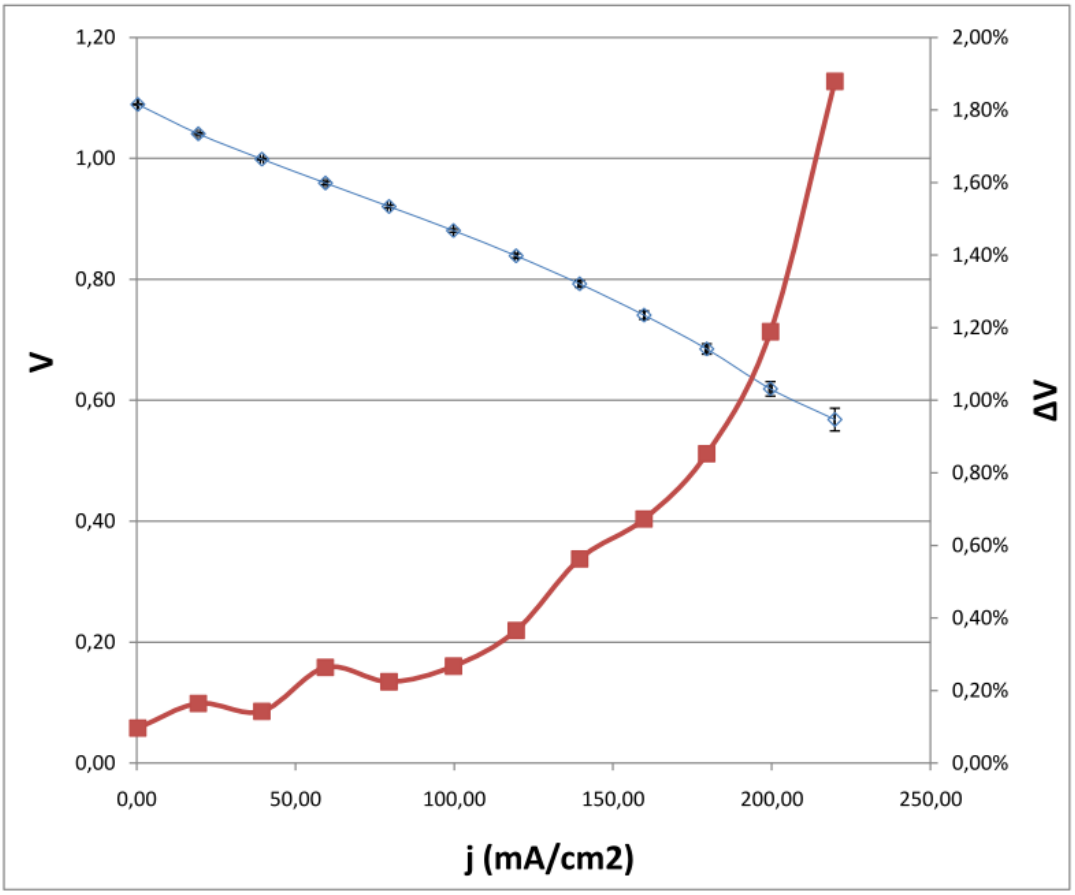


| Name | T | $H_2$ | λ | $DN_2$ | OCV | ASR at 0,8V | ASR at 0,7V |
|---|---|---|---|---|---|---|---|
| Pn-n | °C | Nl/hcm$^2$ | - | - | V | Ωcm$^2$ | Ωcm$^2$ |
| **p9-11** | **756,1** | **1,05** | **0,20** | **0** | **1,09** | **2,47** | **2,91** |

*Example of reference state variation test reports B*

*List of reference state variation test reports B*

| Name | | T | $H_2$ | λ | $DN_2$ | OCV | ASR at 0,8V | ASR at 0,7V |
|---|---|---|---|---|---|---|---|---|
| std. | Pn-n | °C | Nl/hcm² | - | - | V | Ωcm² | Ωcm² |
| **FCTESTNET** | **P1;2-12;13** | **755,61** | **1,05** | **1,00** | **0,00** | **1,09** | **1,29** | **1,26** |
| **λ variations** | **p3-5** | **755,76** | **1,05** | **0,68** | **0,00** | **1,09** | **1,37** | **1,33** |
| | **p6-8** | **756,19** | **1,05** | **0,44** | **0,00** | **1,09** | **1,41** | **1,39** |
| | **p9-11** | **756,10** | **1,05** | **0,20** | **0,00** | **1,09** | **2,47** | **2,91** |
| **$D_{N2}$ variations** | **p14-16** | **755,95** | **1,05** | **1,00** | **0,22** | **1,10** | **1,28** | **1,26** |
| | **p17-19** | **756,97** | **1,05** | **1,00** | **0,42** | **1,10** | **1,35** | **1,34** |
| | **p20** | **758,63** | **1,05** | **1,00** | **0,49** | **1,10** | **1,41** | **1,40** |

Finally, presented below reports C for λ and $D_{N2}$ were developed.

# APPENDIX G

## New reference state variation test plan

The new reference state variation test plan is the same in the base assumption as the previous one. The difference between these two activities is to check that the others (reduced) total gas flows have the same influence on ASR and OCV parameters. For this purpose, new reference state variation test plan was developed as it is shown in table below.

At first, new reference state test plan was developed for eleven polarizations – gray highlighted. However, it was modified due to big differences in the results which come from short stabilization time between each test. The upgraded plan included polarizations named with *a* and *b* index at the end.

Moreover, polarizations 12a, 12b together with 11a, 11b are planned to be performed at the end of this plan. This is because of poor gas conditions and in the result of probability of damaging the cell during these tests.

The additional assumption of this plan is to check how the performance parameters are when higher and lower values for DN2 and λ, respectively are applied. Presented previously plan could not apply these changes because of the test system limitations; maximum nitrogen flow for the nitrogen flow meter is 50NL/h. The goal for this test plan is to performed tests at λmax=0,2 and DN2=0,65.

*New reference state test plan*

| ASC 700 3-10 | | Cell acive area | | | | | | | 50 | cm² | | |
|---|---|---|---|---|---|---|---|---|---|---|---|---|
| Name | | T | $H_2$ | | $N_2$ | | Air | | $H_2$ | $D_{N2}$ | λ | T |
| **std.** | **Sn** | **°C** | **Nl/h** | **Nl/h cm²** | **Nl/h** | **Nl/h cm²** | **Nl/h** | **Nl/h cm²** | **Nl/h cm²** | **-** | **-** | **°C** |
| **Ref.** | **S1** | 750 | 26,25 | 0,53 | 0 | 0 | 62,25 | 1,25 | 0 | 1,00 | 0,53 | 750 |
| **λ variations** | **S2** | 750 | 26,25 | 0,53 | 0 | 0 | 42,3 | 0,85 | 0,53 | 0 | 0,68 | 750 |
| | **S2a** | 750 | 26,25 | 0,53 | 0 | 0 | 42,3 | 0,85 | 0,53 | 0 | 0,68 | 750 |
| | **S2b** | 750 | 26,25 | 0,53 | 0 | 0 | 42,3 | 0,85 | 0,53 | 0 | 0,68 | 750 |
| | **S3** | 750 | 26,25 | 0,53 | 0 | 0 | 22,3 | 0,45 | 0,53 | 0 | 0,36 | 750 |
| | **S3a** | 750 | 26,25 | 0,53 | 0 | 0 | 22,3 | 0,45 | 0,53 | 0 | 0,36 | 750 |
| | **S3b** | 750 | 26,25 | 0,53 | 0 | 0 | 22,3 | 0,45 | 0,53 | 0 | 0,36 | 750 |
| | **S12** | 750 | 26,25 | 0,53 | 0 | 0 | 7,25 | 0,15 | 0,53 | 0 | 0,12 | 750 |
| | **S12a** | 750 | 26,25 | 0,53 | 0 | 0 | 7,3 | 0,15 | 0,53 | 0 | 0,12 | 750 |
| | **S12b** | 750 | 26,25 | 0,53 | 0 | 0 | 7,3 | 0,15 | 0,53 | 0 | 0,12 | 750 |
| **Ref.** | **S4** | 750 | 26,25 | 0,53 | 0 | 0 | 62,25 | 1,25 | 0,53 | 0 | 1 | 750 |
| | **S4a** | 750 | 26,25 | 0,53 | 0 | 0 | 62,25 | 1,25 | 0,53 | 0 | 1 | 750 |
| | **S4b** | 750 | 26,25 | 0,53 | 0 | 0 | 62,25 | 1,25 | 0,53 | 0 | 1 | 750 |
| **$D_{N2}$ variations** | **S5** | 750 | 26,25 | 0,53 | 6,5 | 0,13 | 62,25 | 2,49 | 0,53 | 0,20 | 1 | 750 |
| | **S5a** | 750 | 26,25 | 0,53 | 6,5 | 0,13 | 62,25 | 2,49 | 0,53 | 0,20 | 1 | 750 |
| | **S5b** | 750 | 26,25 | 0,53 | 6,5 | 0,13 | 62,25 | 2,49 | 0,53 | 0,20 | 1 | 750 |
| | **S6** | 750 | 26,25 | 0,53 | 24 | 0,48 | 62,25 | 2,49 | 0,53 | 0,48 | 1 | 750 |
| | **S6a** | 750 | 26,25 | 0,53 | 24 | 0,48 | 62,25 | 2,49 | 0,53 | 0,48 | 1 | 750 |
| | **S6b** | 750 | 26,25 | 0,53 | 24 | 0,48 | 62,25 | 2,49 | 0,53 | 0,48 | 1 | 750 |
| | **S7** | 750 | 26,25 | 0,53 | 49 | 0,98 | 62,25 | 2,49 | 0,53 | 0,65 | 1 | 750 |
| | **S7a** | 750 | 26,25 | 0,53 | 49 | 0,98 | 62,25 | 2,49 | 0,53 | 0,65 | 1 | 750 |
| | **S7b** | 750 | 26,25 | 0,53 | 49 | 0,98 | 62,25 | 2,49 | 0,53 | 0,65 | 1 | 750 |
| **Ref.** | **S8** | 750 | 26,25 | 0,53 | 0 | 0 | 62,25 | 1,25 | 0,53 | 0 | 1 | 750 |
| | **S8a** | 750 | 26,25 | 0,53 | 0 | 0 | 62,25 | 1,25 | 0,53 | 0 | 1 | 750 |
| | **S8b** | 750 | 26,25 | 0,53 | 0 | 0 | 62,25 | 1,25 | 0,53 | 0 | 1 | 750 |
| **$D_{N2}$ & λ variations** | **S9** | 750 | 26,25 | 0,53 | 6,5 | 0,13 | 42,3 | 0,85 | 0,53 | 0,2 | 0,68 | 750 |
| | **S9a** | 750 | 26,25 | 0,53 | 6,5 | 0,13 | 42,3 | 0,85 | 0,53 | 0,2 | 0,68 | 750 |
| | **S9b** | 750 | 26,25 | 0,53 | 6,5 | 0,13 | 22,3 | 0,45 | 0,53 | 0,2 | 0,36 | 750 |
| | **S10** | 750 | 26,25 | 0,53 | 24 | 0,48 | 22,3 | 0,45 | 0,53 | 0,48 | 0,36 | 750 |
| | **S10a** | 750 | 26,25 | 0,53 | 24 | 0,48 | 22,3 | 0,45 | 0,53 | 0,48 | 0,36 | 750 |
| | **S10b** | 750 | 26,25 | 0,53 | 24 | 0,48 | 22,3 | 0,45 | 0,53 | 0,48 | 0,36 | 750 |
| | **S11** | 750 | 26,25 | 0,53 | 49 | 0,98 | 7,3 | 0,15 | 0,53 | 0,65 | 0,12 | 750 |
| | **S11a** | 750 | 26,25 | 0,53 | 49 | 0,98 | 7,3 | 0,15 | 0,53 | 0,65 | 0,12 | 750 |
| | **S11b** | 750 | 26,25 | 0,53 | 49 | 0,98 | 7,3 | 0,15 | 0,53 | 0,65 | 0,12 | 750 |

## New reference state variation test elaborating

The same methodology of elaborating the test output data is used as presented in the previous chapters. From the beginning of this chapter, there are presented examples of reports A, list of reports A, example of report B, list of reports B, and finally both reports C, respectively.

**POLARIZATION S4b** **ASC700 3-10** **Active area** **50 cm2**

| Name | Date | T | $H_2$ | | $N_2$ | | Air | | $H_2O$ | λ | $DN_2$ |
|---|---|---|---|---|---|---|---|---|---|---|---|
| PN | - | °C | Nl/h | Nl/hcm$^2$ | Nl/h | Nl/hcm$^2$ | Nl/hcm$^2$ | Nl/h | Nl/h | - | - |
| S4b | 17.1.2011 | 754,54 | 26,21 | 0,52 | 0,00 | 0,00 | 62,27 | 1,25 | RT | 1,00 | 0 |

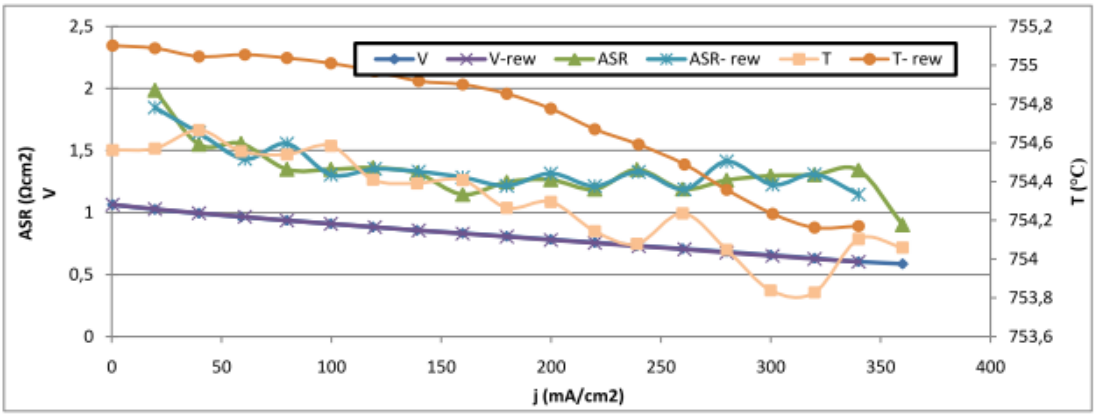


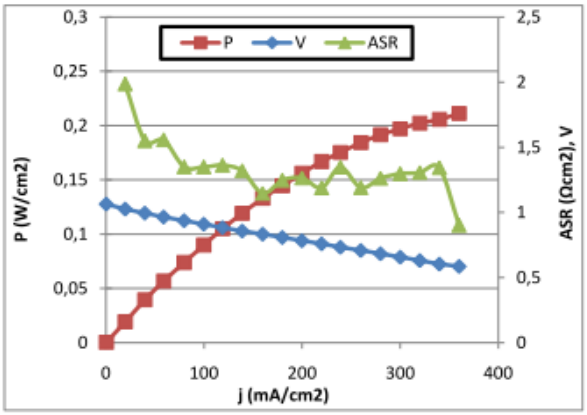


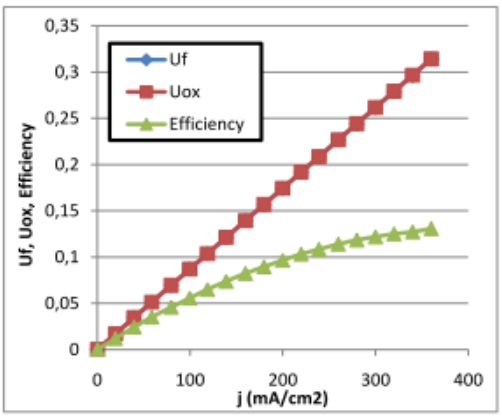


| Control mode | galvanostatic | Step size (A) | 1 |
|---|---|---|---|
| Starting voltage (V) | - | Hold time (s) | 23 |
| ASR @ 0,8 V | 1,235 | | Ωcm2 |
| ASR @ 0,7 V | 1,279 | | Ωcm2 |
| OCV | 1,064 | | V |
| J max | 360,02 | | mA/cm2 |
| P max | 0,21 | | W/cm2 |
| J @ 0,8 V | 179,80 | | mA/cm2 |
| J @ 0,7 V | 260,32 | | mA/cm2 |

*Example of new reference state variation test report A*

**POLARIZATION S3b** **ASC700 3-10** **Active area** **50 cm2**

| Name | Date | T | $H_2$ | | $N_2$ | | Air | | $H_2O$ | λ | $DN_2$ |
|---|---|---|---|---|---|---|---|---|---|---|---|
| PN | - | °C | Nl/h | Nl/hcm$^2$ | Nl/h | Nl/hcm$^2$ | Nl/hcm$^2$ | Nl/h | Nl/h | - | - |
| **S3b** | **17.1.2011** | **753,96** | **26,25** | **0,52** | **0,00** | **0,00** | **22,30** | **0,45** | **RT** | **0,36** | **0,0** |

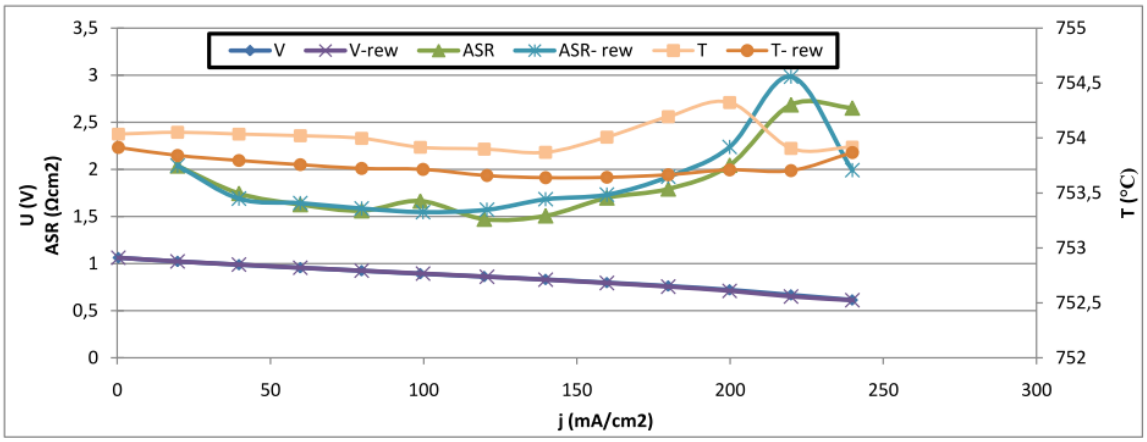


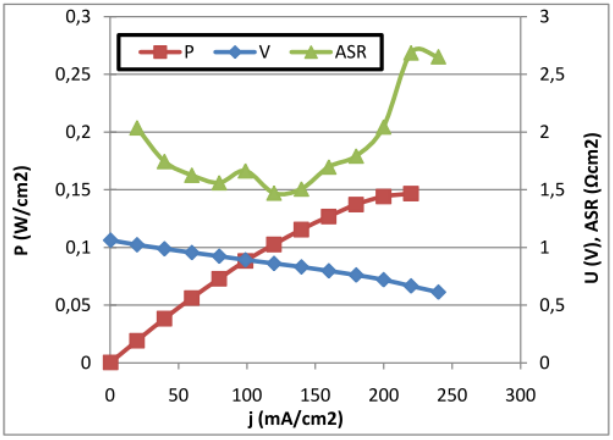


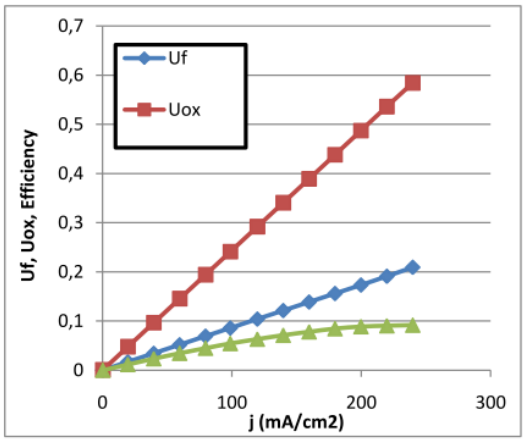


| Control mode | galvanostatic | Step size (A) | 1 |
|---|---|---|---|
| Starting voltage (V) | - | Hold time (s) | 21 |
| ASR @ 0,8 V | 1,723 | | Ωcm2 |
| ASR @ 0,7 V | 2,488 | | Ωcm2 |
| OCV | 1,063 | | V |
| J max | 239,89 | | mA/cm2 |
| P max | 0,15 | | W/cm2 |
| J @ 0,8 V | 159,79 | | mA/cm2 |
| J @ 0,7 V | 199,86 | | mA/cm2 |

*Example of new reference state λ variation test report A*

**POLARIZATION S7a** **ASC700 3-10** **Active area** **50 cm2**

| Name | Date | T | $H_2$ | | $N_2$ | | Air | | $H_2O$ | λ | $DN_2$ |
|---|---|---|---|---|---|---|---|---|---|---|---|
| PN | - | °C | Nl/h | Nl/hcm$^2$ | Nl/h | Nl/hcm$^2$ | Nl/hcm$^2$ | Nl/h | Nl/h | - | - |
| **S7a** | **17.1.2011** | **755,25** | **26,22** | **0,52** | **48,99** | **0,98** | **62,29** | **1,25** | **RT** | **1,00** | **0,65** |

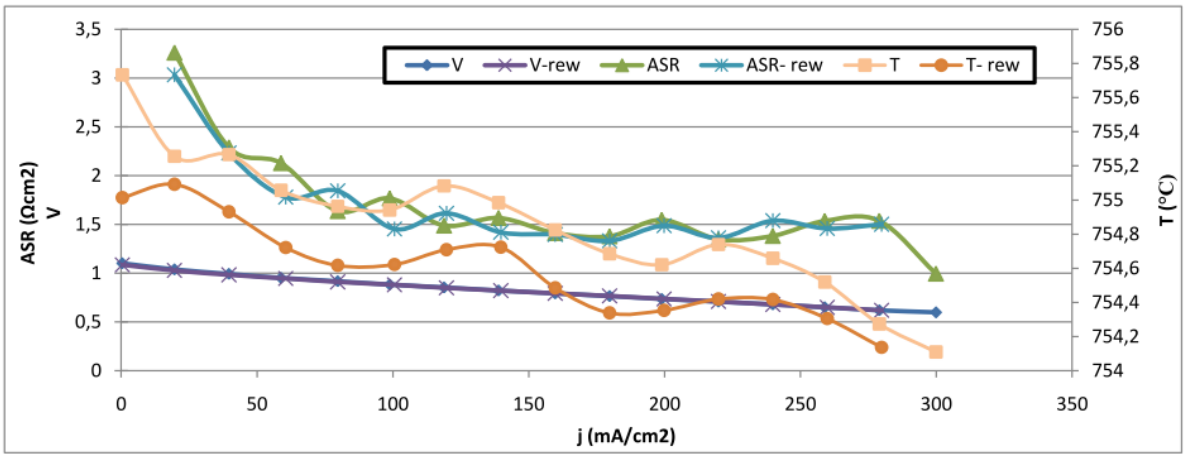


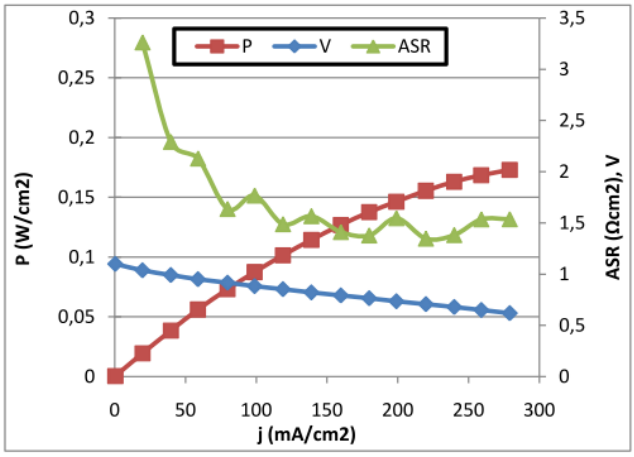


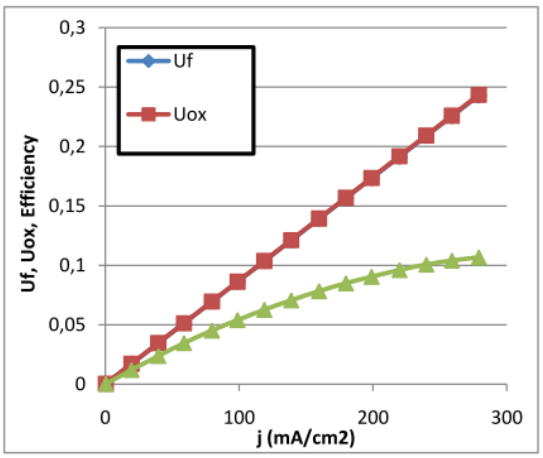


| Control mode | galvanostatic | Step size (A) | 1 |
|---|---|---|---|
| Starting voltage (V) | - | Hold time (s) | 23 |
| ASR @ 0,8 V | 1,418 | | Ωcm2 |
| ASR @ 0,7 V | 1,456 | | Ωcm2 |
| OCV | 1,093 | | V |
| J max | 299,95 | | mA/cm2 |
| P max | 0,18 | | W/cm2 |
| J @ 0,8 V | 159,75 | | mA/cm2 |
| J @ 0,7 V | 219,85 | | mA/cm2 |

*Example of new reference state $D_f$ variation test report A*

**POLARIZATION S10b** **ASC700 2-10** **Active area** **50 cm2**

| Name | Date | T | $H_2$ | | $N_2$ | | Air | | $H_2O$ | λ | $DN_2$ |
|---|---|---|---|---|---|---|---|---|---|---|---|
| PN | - | °C | Nl/h | Nl/hcm$^2$ | Nl/h | Nl/hcm$^2$ | Nl/hcm$^2$ | Nl/h | Nl/h | - | - |
| **S10b** | **18.1.2011** | **754,79** | **26,25** | **0,52** | **24,00** | **0,48** | **22,32** | **0,45** | **RT** | **0,36** | **0,48** |

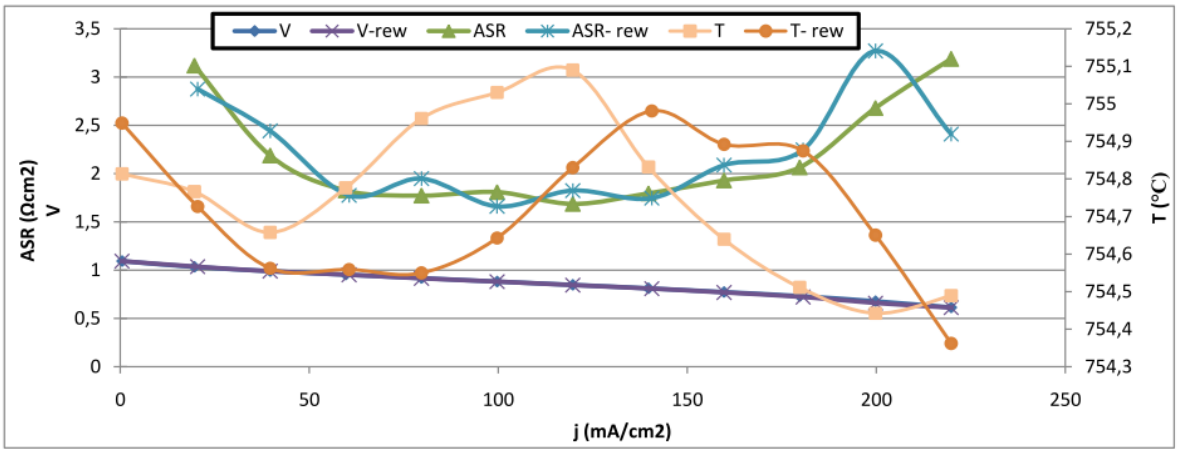


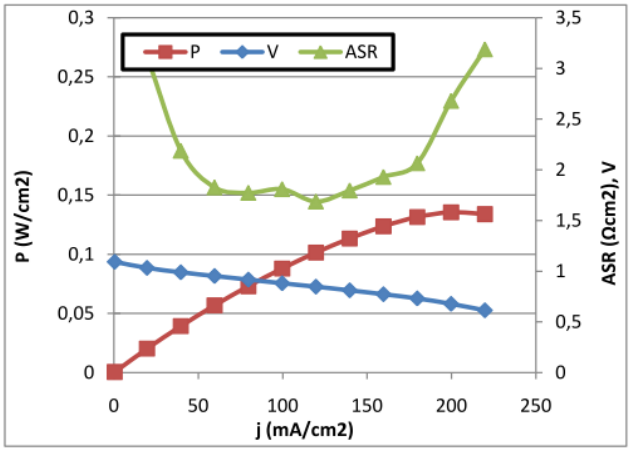


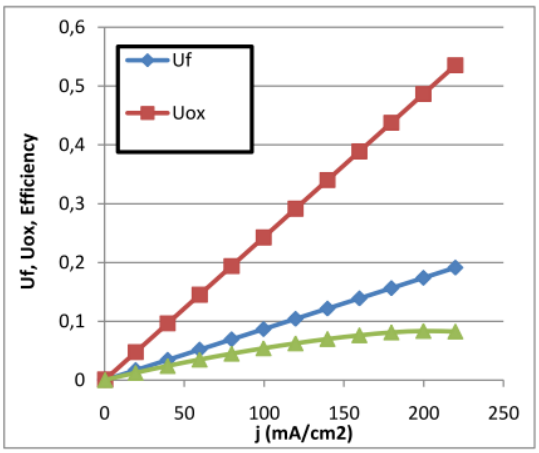


| Control mode | galvanostatic | Step size (A) | 1 |
|---|---|---|---|
| Starting voltage (V) | - | Hold time (s) | 22 |
| ASR @ 0,8 V | 1,920 | | Ωcm2 |
| ASR @ 0,7 V | 2,333 | | Ωcm2 |
| OCV | 1,093 | | V |
| J max | 219,84 | | mA/cm2 |
| P max | 0,14 | | W/cm2 |
| J @ 0,8 V | 140,17 | | mA/cm2 |
| J @ 0,7 V | 190,22 | | mA/cm2 |

*Example of new reference state λ and DN2 variation test report A*

In the report above, there are presented cumulative effects of λ and $D_f$ – discussed in the following chapter.

*List of new reference state variation test report A*

| ASC700 3-10 | | | | | | | | | | Cell active area: 50 $cm^2$ | | |
|---|---|---|---|---|---|---|---|---|---|---|---|---|
| Name | | Date | T | $H_2$ | $N_2$ | Air | $H_2O$ | λ | $D_f$ | ASR at 0,8 V | ASR at 0,7 V | OCV |
| std. | Sn | - | °C | Nl/$hcm^2$ | Nl/$hcm^2$ | Nl/$hcm^2$ | Nl/h | - | - | Ωcm² | Ωcm² | V |
| ref. | S1 | 14.1.2011 | 754 | 0,52 | 0 | 1,24 | RT | 0,99 | 0 | 1,41 | 1,41 | 1,06 |
| λ variations | S2 | 14.1.2011 | 754 | 0,52 | 0 | 0,85 | RT | 0,68 | 0 | 1,43 | 1,46 | 1,06 |
| | S2a | 17.1.2011 | 755 | 0,52 | 0 | 0,85 | RT | 0,68 | 0 | 1,32 | 1,34 | 1,06 |
| | S2b | 17.1.2011 | 754 | 0,52 | 0 | 0,85 | RT | 0,68 | 0 | 1,34 | 1,40 | 1,06 |
| | S3 | 14.1.2011 | 754 | 0,52 | 0 | 0,45 | RT | 0,36 | 0 | 1,78 | 2,46 | 1,06 |
| | S3a | 17.1.2011 | 754 | 0,52 | 0 | 0,45 | RT | 0,36 | 0 | 1,66 | 2,42 | 1,06 |
| | S3b | 17.1.2011 | 754 | 0,52 | 0 | 0,45 | RT | 0,36 | 0 | 1,72 | 2,49 | 1,06 |
| | S12 | 14.1.2011 | 754 | 0,52 | 0 | 0,15 | RT | 0,12 | 0 | 4,14 | 6,53 | 1,05 |
| | S12a | 18.1.2011 | 754 | 0,53 | 0 | 0,15 | RT | 0,12 | 0 | 4,40 | 6,39 | 1,05 |
| | S12b | - | - | - | - | - | - | - | - | - | - | - |
| ref. | S4 | 14.1.2011 | 754 | 0,52 | 0 | 1,25 | RT | 1 | 0 | 1,31 | 1,34 | 1,06 |
| | S4a | 17.1.2011 | 754 | 0,52 | 0 | 1,25 | RT | 1 | 0 | 1,24 | 1,27 | 1,06 |
| | S4b | 17.1.2011 | 755 | 0,52 | 0 | 1,25 | RT | 1 | 0 | 1,23 | 1,28 | 1,06 |
| $D_{N2}$ variations | S5 | 14.1.2011 | 755 | 0,52 | 0,13 | 1,25 | RT | 1 | 0,2 | 1,33 | 1,33 | 1,08 |
| | S5a | 17.1.2011 | 755 | 0,52 | 0,13 | 1,25 | RT | 1 | 0,2 | 1,29 | 1,26 | 1,08 |
| | S5b | 17.1.2011 | 755 | 0,52 | 0,13 | 1,25 | RT | 1 | 0,2 | 1,27 | 1,28 | 1,08 |
| | S6 | 14.1.2011 | 755 | 0,52 | 0,48 | 1,25 | RT | 1 | 0,48 | 1,40 | 1,34 | 1,09 |
| | S6a | 17.1.2011 | 755 | 0,52 | 0,48 | 1,25 | RT | 1 | 0,48 | 1,33 | 1,36 | 1,09 |
| | S6b | 17.1.2011 | 755 | 0,52 | 0,48 | 1,25 | RT | 1 | 0,48 | 1,37 | 1,41 | 1,09 |
| | S7 | 14.1.2011 | 755 | 0,53 | 0,98 | 1,25 | RT | 1 | 0,65 | 1,42 | 1,44 | 1,08 |
| | S7a | 17.1.2011 | 755 | 0,52 | 0,98 | 1,25 | RT | 1 | 0,65 | 1,42 | 1,46 | 1,09 |
| | S7b | 17.1.2011 | 755 | 0,52 | 0,98 | 1,25 | RT | 1 | 0,65 | 1,51 | 1,57 | 1,09 |
| ref. | S8 | 14.1.2011 | 754 | 0,52 | 0 | 1,25 | RT | 1 | 0 | 1,39 | 1,45 | 1,06 |
| | S8a | 18.1.2011 | 754 | 0,52 | 0 | 1,25 | RT | 1 | 0 | 1,42 | 1,43 | 1,07 |
| | S8b | 18.1.2011 | 754 | 0,52 | 0 | 1,25 | RT | 1 | 0 | 1,33 | 1,33 | 1,07 |
| $D_{N2}$ & λ variations | S9 | 14.1.2011 | 754 | 0,53 | 0,13 | 0,85 | RT | 0,68 | 0,2 | 1,51 | 1,55 | 1,08 |
| | S9a | 18.1.2011 | 755 | 0,52 | 0,13 | 0,85 | RT | 0,68 | 0,2 | 1,4 | 1,43 | 1,08 |
| | 9b | - | - | - | - | - | - | - | - | - | - | - |
| | S10 | 14.1.2011 | 755 | 0,53 | 0,48 | 0,45 | RT | 0,36 | 0,48 | 1,88 | 2,57 | 1,08 |
| | S10a | 18.1.2011 | 755 | 0,52 | 0,48 | 0,45 | RT | 0,36 | 0,48 | 1,91 | 2,55 | 1,09 |
| | S10b | 18.1.2011 | 755 | 0,52 | 0,48 | 0,45 | RT | 0,36 | 0,48 | 1,92 | 2,33 | 1,09 |
| | S11 | 14.1.2011 | 756 | 0,52 | 0,98 | 0,15 | RT | 0,12 | 0,65 | 6,75 | - | 1,01 |
| | S11a | 18.1.2011 | 755 | 0,52 | 0,98 | 0,15 | RT | 0,12 | 0,65 | ~6 | ~7 | 1,07 |
| | S11b | 18.1.2011 | 755 | 0,52 | 0,98 | 0,15 | RT | 0,12 | 0,65 | ~6 | ~7 | 1,07 |

From the table above, it can be noticed that polarizations S12b and S9b are not performed due to technical problems during the test activity. Moreover, the ASR values for S11a and S11b polarizations are calculated based on very imprecisely output data (due to poor gas conditions) and should not be treatment as the precise results.

**RREPORT B** ***D $_{N2}$ variations - New ref. state***

**ASC700 3-10** **Active area** **50 cm2**

| Name | Date | T | $H_2$ | $N_2$ | Air | $H_2O$ | λ | $DN_2$ |
|---|---|---|---|---|---|---|---|---|
| PN | - | °C | Nl/hcm$^2$ | Nl/hcm$^2$ | Nl/hcm$^2$ | Nl/h | - | - |
| **S7a** | **17.1.2011** | **755,25** | **0,52** | **0,98** | **1,25** | **RT** | **1,00** | **0,65** |
| **S7b** | **17.1.2011** | **754,85** | **0,52** | **0,98** | **1,25** | **RT** | **1,00** | **0,65** |

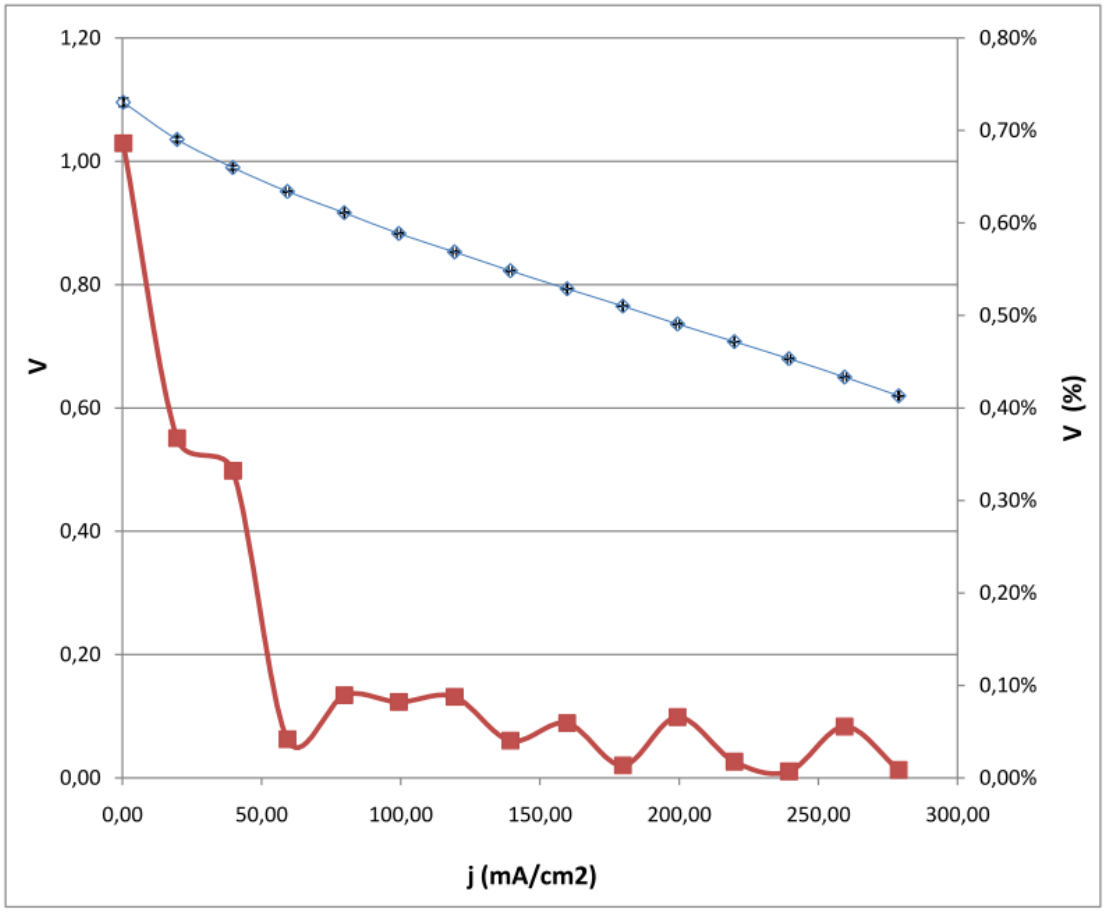


| Name | T | $H_2$ | λ | $D_{N2}$ | OCV | ASR at 0,8V | ASR at 0,7V |
|---|---|---|---|---|---|---|---|
| PN | °C | Nl/hcm$^2$ | - | - | V | Ωcm$^2$ | Ωcm$^2$ |
| **S7ab** | **755,0** | **0,52** | **0,998** | **0,65** | **1,09** | **1,42** | **1,45** |

*Example of new reference state DN2 variation test report B*

*List of new reference state variation test reports B*

| Name | | T | $H_2$ | λ | $D_{N2}$ | OCV | ASR at 0,8V | ASR at 0,7V |
|---|---|---|---|---|---|---|---|---|
| PN | | °C | Nl/hcm² | - | - | V | Ωcm² | Ωcm² |
| **λ variations** | **S2ab** | 754,7 | 0,52 | 0,68 | 0,0 | 1,06 | 1,33 | 1,37 |
| | **S3ab** | 754,1 | 0,52 | 0,36 | 0,0 | 1,06 | 1,69 | 2,47 |
| | **S12a** | 754,4 | 0,52 | 0,12 | 0,0 | 1,05 | 4,40 | 6,39 |
| **$D_{N2}$ variations** | **S5ab** | 754,7 | 0,52 | 1,00 | 0,2 | 1,08 | 1,28 | 1,27 |
| | **S6ab** | 754,9 | 0,52 | 1,00 | 0,48 | 1,09 | 1,35 | 1,38 |
| | **S7ab** | 755,0 | 0,52 | 1,00 | 0,65 | 1,09 | 1,42 | 1,45 |
| **λ & $D_{N2}$ variations** | **S9a** | 754,7 | 0,52 | 0,68 | 0,2 | 1,1 | 1,4 | 1,4 |
| | **S10ab** | 754,9 | 0,52 | 0,36 | 0,48 | 1,1 | 1,9 | 2,4 |
| | **S11ab** | 754,9 | 0,52 | 0,12 | 0,65 | 1,1 | ~6 | ~7 |
| **New ref. state** | **S4ab** | 754,4 | 0,52 | 1,0 | 0,0 | 1,06 | 1,24 | 1,28 |
| | **S8ab** | 754,3 | 0,52 | 1,0 | 0,0 | 1,07 | 1,37 | 1,38 |

## APPENDIX H